



Università della Calabria

Facoltà di Farmacia e Scienze della Nutrizione e della Salute

Dipartimento di Scienze Farmaceutiche

Scuola di Dottorato Bernardino Telesio – Scuola di Scienza e Tecnica

Bernardino Telesio – School of Science and Technique

*Doctorate Course:*

**“Organic Molecules of Pharmacological Interest”**

**(OMPI, cycle XXV CHIM/09)**

**Doctoral Thesis**

**Synthesis and characterization of novel**

**biopolymer for biomedical applications**

*PhD Student*

**Ilaria ALTIMARI**

*Supervisor*

**Prof.ssa Francesca IEMMA**

*Coordinator*

**Prof. Bartolo GABRIELE**

*School Director*

**Prof. Roberto BARTOLINO**

Anno accademico 2011/2012



## ABSTRACT

Attualmente le innovazioni nel settore biomedicale possono contare sull'impiego di numerosi sistemi polimerici per la realizzazione di nuovi materiali funzionali per applicazioni specifiche in campo biologico, farmaceutico, cosmetico e nutraceutico. Diversi sistemi polimerici vengono impiegati con successo in diverse aree biomedicali, come ad esempio:

- *nel campo farmaceutico* , nella preparazione di innovativi dispositivi per la somministrazione di farmaci come, ad esempio, idrogel come sistemi di rilascio biodegradabili;
- *in chirurgia*, in una vasta gamma di applicazioni impiantabili, quali: lenti intraoculari, sistemi ortopedici degradabili, cateteri, materiali che devono presentare importanti proprietà come una buona prestazione e resistenza meccanica, nonché buone proprietà di permeabilità.
- *nell'ingegneria tissutale*, come sostituti biologici per ristabilire, mantenere o migliorare la funzione di un tessuto, o nella realizzazione di organi artificiali. I materiali polimerici impiegati per questi scopi devono naturalmente presentare proprietà di biocompatibilità, biodegradabilità e totale assenza di tossicità, nonché buone proprietà meccaniche, durante l'intero processo di rigenerazione.

In tutti questi contesti, in realtà, è necessario che i materiali impiegati presentino ottime proprietà di biocompatibilità, biodegradabilità e atossicità, evitando qualsiasi reazione indesiderata all'interno dell'organismo umano.

La realizzazione di sistemi polimerici ibridi , cioè a base di polimeri naturali e sintetici, risulta un percorso interessante per produrre polimeri funzionali con possibili applicazioni nella biomedicina. Infatti, l'introduzione di funzioni chimiche reattive, derivanti da polimeri sintetici, all'interno o lungo catene polimeriche naturali, come polisaccaridi e proteine, porta ad una serie di risultati positivi in quanto la presenza di gruppi derivanti dai polimeri naturali garantiscono proprietà importanti dal punto di vista della biocompatibilità, biodegradabilità e bio-funzionalità, mentre i polimeri di origine sintetica sono in grado di migliorare le proprietà fisiche e meccaniche di questi sistemi ibridi.

Sulla base di tutte queste considerazioni, gli obiettivi generali della mia tesi di dottorato sono stati la sintesi e la caratterizzazione di nuovi materiali funzionali a base di biopolimeri, come polisaccaridi e proteine, con possibili applicazioni in campo biomedico. Il progetto di ricerca si è focalizzata su tre tematiche principali che verranno descritte in tre sezioni distinte, e in particolar modo:

- I. La prima sezione descrive la realizzazione e la caratterizzazione di nuovi idrogel pH- e temperatura-sensibili, come potenziali sistemi di rilascio di farmaci. In particolar modo, in primo luogo è stata posta l'attenzione sulla realizzazione di idrogel pH-sensibili a base di gelatina, come carrier di farmaci per uso orale. Successivamente è stato realizzato un potenziale sistema di rilascio a base di chitosano ,sensibile alla temperatura, in

grado di modulare il rilascio di farmaci in relazione alle variazioni di temperatura.

II. La seconda sezione pone l'attenzione sulla sintesi di coniugati a base di biopolimeri e antiossidanti come potenziali ingredienti per formulazioni farmaceutiche, cosmetiche e nutraceutiche. La possibilità di promuovere la coniugazione tra molecole biopolimeriche e gli antiossidanti risulta molto interessante dal punto di vista biomedico perché il sistema risultante presenta proprietà del biopolimero di partenza, come biocompatibilità, biodegradabilità e atossicità e l'attività delle molecole antiossidanti coniugate, come una maggiore stabilità e una minore velocità di degradazione.

III. L'ultima sezione descrive il lavoro che ho svolto durante il mio periodo di ricerca all'estero presso il Laboratorio di Medicina Rigenerativa e Farmacobiologia del Politecnico Federale di Losanna (EPFL, École Polytechnique Fédérale de Lausanne ). L'obiettivo principale di questo lavoro è stato la realizzazione di un nuovo sistema a base di PEG eterobifunzionale come potenziale biomateriale impiegabile nel processo della microincapsulazione cellulare. La scelta di un materiale adatto a preservare la vitalità e la funzione delle cellule incorporate all'interno del sistema realizzato diventa fondamentale se il materiale è destinato ad uno scopo terapeutico.



# CONTENTS

<b>PREFACE</b>	1
----------------	---

## SECTION I

### STIMULI RESPONSIVE HYDROGELS AS DRUG DELIVERY DEVICES

<b>INTRODUCTION</b>	6
---------------------	---

#### CHAPTER 1

##### pH-SENSITIVE DRUG DELIVERY SYSTEMS BY RADICAL POLYMERIZATION OF GELATIN DERIVATIVES

<b>1. Introduction</b>	21
<b>2. Experimental section</b>	23
2.1 <i>Materials</i>	23
2.2 <i>Synthesis of methacrylated gelatin hydrolyzate (HGL-MA)</i>	24
2.3 <i>Microspheres preparation</i>	24
2.4 <i>Characterization of pH-responsive microspheres</i>	25
2.5 <i>Incorporation of Drug into Preformed Microspheres</i>	27
2.6 <i>Differential Scanning Calorimetry analyses</i>	28
2.7 <i>Drug stability</i>	28
2.8 <i>In vitro</i> release studies	29
<b>3. Results and discussion</b>	29
3.1 <i>Synthesis of microspheres based on hydrolyzed gelatin</i>	29
3.2 <i>Characterization of gelatin microspheres</i>	31
3.3 <i>In vitro</i> release studies	34
<b>4. Conclusions</b>	39

## CHAPTER 2

### GRAFTED GELATIN MICROSPHERES AS POTENTIAL pH-RESPONSIVE DEVICES

<b>1. Introduction</b>	40
<b>2. Experimental section</b>	41
2.1 <i>Materials</i>	41
2.2 <i>Microspheres preparation</i>	42
2.3 <i>Characterization of pH-responsive microspheres</i>	43
2.4 <i>Drug stability</i>	45
2.5 <i>Drug loading by soaking procedure</i>	46
2.6 <i>Differential Scanning Calorimetry</i>	46
2.7 <i>X-ray diffraction analysis</i>	46
2.8 <i>In vitro release studies</i>	47
<b>3. Results and discussion</b>	47
3.1 <i>Synthesis of pH-sensitive GL-grafted microspheres</i>	47
3.2 <i>Characterization of gelatin microspheres</i>	48
3.3 <i>In vitro release studies</i>	52
<b>4. Conclusions</b>	57

## CHAPTER 3

### BIODEGRADABLE GELATIN-BASED NANOSPHERES AS pH-RESPONSIVE DRUG DELIVERY SYSTEMS

<b>1. Introduction</b>	58
<b>2. Experimental Section</b>	60
2.1 <i>Materials</i>	60
2.2 <i>Preparation of gelatin nanoparticles</i>	61
2.3 <i>Shape and surface morphology</i>	61
2.4 <i>Dimensional distribution</i>	61
2.5 <i>Water content of gelatin nanospheres</i>	61
2.6 <i>Enzymatic degradation of gelatin nanoparticles</i>	62
2.7 <i>Drug stability at pH 1.0 and 7.0</i>	63
2.8 <i>Drug loading by soaking procedure</i>	63



2.9 <i>In vitro</i> release studies	65
<b>3. Results and discussion</b>	65
3.1 <i>Synthesis and characterization of gelatin nanospheres</i>	65
3.2 <i>Water uptake experiments</i>	67
3.3 <i>Enzymatic degradation</i>	68
3.4 <i>In vitro</i> release studies	70
<b>4. Conclusions</b>	78

## CHAPTER 4

### TEMPERATURE-SENSITIVE HYDROGELS BY GRAFT POLYMERIZATION OF CHITOSAN AND N- ISOPROPYLACRYLAMIDE FOR DRUG RELEASE

<b>1. Introduction</b>	79
<b>2. Experimental section</b>	81
2.1 <i>Materials</i>	81
2.2 <i>Synthesis of CS-g-NIPAAm hydrogels</i>	82
2.3 <i>Characterization of thermo-responsive hydrogels</i>	82
2.4 <i>Drug stability</i>	84
2.5 <i>Drug loading by soaking procedure</i>	84
2.6 <i>In vitro</i> release studies	85
<b>3. Results and discussion</b>	86
3.1 <i>Synthesis of thermo-responsive hydrogel</i>	86
3.2 <i>Characterization of hydrogels</i>	87
3.3 <i>In vitro</i> release studies	92
3.4 <i>Pulsatile drug release experiments</i>	94
<b>4. Conclusions</b>	96

## SECTION II

### BIOPOLYMER-ANTIOXIDANT CONJUGATE

INTRODUCTION	97
--------------	----

#### CHAPTER 5

##### INNOVATIVE ANTIOXIDANT THERMO-RESPONSIVE HYDROGELS BY RADICAL GRAFTING OF CATECHIN ON INULIN CHAIN

<b>1. Introduction</b>	107
<b>2. Experimental section</b>	108
2.1 <i>Materials</i>	108
2.2 <i>Instrumentation</i>	109
2.3 <i>Synthesis of antioxidant thermo-responsive hydrogels</i>	110
2.4 <i>Characterization of antioxidant thermo-responsive hydrogels</i>	111
2.5 <i>Evaluation of the antioxidant activity</i>	112
<b>3. Results and discussion</b>	114
3.1 <i>Synthesis of antioxidant thermo-sensitive network</i>	114
3.2 <i>Characterization of antioxidant thermo-responsive hydrogel</i>	116
3.3 <i>Evaluation of the antioxidant activity</i>	121
<b>4. Conclusions</b>	123

#### CHAPTER 6

##### STARCH-QUERCETIN CONJUGATE BY RADICAL GRAFTING: SYNTHESIS AND BIOLOGICAL CHARACTERIZATION

<b>1. Introduction</b>	124
<b>2. Experimental section</b>	126
2.1 <i>Materials and Instruments</i>	126
2.2 <i>Synthesis of Starch Conjugate</i>	127
2.3 <i>Characterization of Starch Conjugate</i>	128
2.4 <i>Gallic acid loading by the soaking procedure</i>	134

2.5 <i>Stability studies</i>	135
<b>3. Results and discussion</b>	136
3.1 <i>Synthesis and characterization of starch-queracetin conjugate</i>	136
3.2 <i>Characterization of starch-queracetin conjugate</i>	137
3.3 <i>Determination of the antioxidant properties</i>	139
3.4 <i>Drug stabilization</i>	142
3.5 <i>Enzymatic activities</i>	143
<b>4. Conclusions</b>	145

## CHAPTER 7

### BIOLOGICAL ACTIVITY OF A GALLIC ACID-GELATIN CONJUGATE

<b>1. Introduction</b>	146
<b>2. Experimental Section</b>	148
2.1 <i>Materials</i>	148
2.2 <i>Instrumentation</i>	148
2.3 <i>Synthesis of Gel-GA Conjugate</i>	149
2.4 <i>Characterization of Gel-GA Conjugate</i>	149
2.5 <i>Anticancer Activity</i>	152
<b>3. Results and discussion</b>	153
3.1 <i>Synthesis and Antioxidant Function of the Gel-GA Conjugate</i>	153
3.2 <i>Characterization of starch-queracetin conjugate</i>	154
3.3 <i>Anticancer Activity</i>	158
<b>4. Conclusions</b>	161

## SECTION III

### MODIFICATION OF BIOMATERIAL FOR THE CELL MICROENCAPSULATION

INTRODUCTION	162
--------------	-----

#### CHAPTER 8

### DEVELOPMENT OF HYBRID HYDROGEL BASED ON Na-alg-PEG INTENDED FOR BIOMEDICAL AND BIOTECHNOLOGICAL APPLICATIONS

<b>1. Introduction</b>	170
<b>2. Experimental Section</b>	172
2.1 <i>Materials</i>	172
2.2 <i>Synthesis of heterobifunctional PEG</i>	172
2.3 <i>Preparation of hydrogels</i>	175
<b>3. Results and discussion</b>	179
3.1 <i>Synthesis of heterobifunctional PEG</i>	179
3.2 <i>Hydrogel formation</i>	184
<b>4. Conclusions</b>	186

## PREFACE

### SYNTHESIS AND CHARACTERIZATION OF NOVEL BIOPOLYMERS FOR BIOMEDICAL APPLICATIONS

Nowadays, innovations in biomedical field can count on several polymers for the realization of novel functional materials for specific applications in biological, pharmaceutical, cosmetic and nutraceutical sectors. Indeed, polymeric applications are often used with success in different and active areas of biomedical research, such as in:

- *Pharmaceutical field*, in particular, in the development of innovative devices for drug delivery applications, for example :

- hydrogel systems
- drug conjugate
- biodegradable release systems

Especially, one of the most important opportunities in polymer drug delivery applications are the responsive delivery systems, with which it is possible to deliver drugs through implantable devices, for example, to deliver a drug precisely to a targeted site.

- *Surgery*, in a wide range of implantable applications, such as:

- intraocular lenses;
- degradable orthopedic rods;
- cardiac pacing and defibrillation devices;
- catheters;

These materials must demonstrate several favorable prerequisites:

- Mechanical performance (e.g. flexibility);
- Mechanical durability;
- Physical properties (e.g. permeability).

- *Tissue engineering* , as biological substitutes to restore, maintain, or improve bio-function of tissue, and more specifically in :
  - Tissue-engineered vessels
  - Repair cartilages
  - Realization of artificial bone

The materials that can be used as a scaffold in tissue engineering must satisfy several requirements. These include biocompatibility, biodegradation and no toxicity, ability to support cell growth and proliferation, and appropriate mechanical properties, as well as maintaining mechanical strength during most part of the regeneration process.

In all these context, is necessary to avoid any possible toxic reaction of the materials used, such as undesirable by-products of degradation and, moreover, any surgery required to remove the implant system. For these reasons, the main features of these kind of applications should be the biodegradability and biocompatibility, to minimize any host-body reactions, such as inflammatory, antigenic, and immunogenic problems.

Introducing reactive chemical functions, deriving from synthetic polymers, within or along natural polymer backbones is an attractive route to generate functional polymers for medicine, to be of real interest and have a future for effective applications. Specifically, natural biodegradable polymers, (or biopolymers), such as polysaccharides, represent the most characteristic family of these natural polymers, and proteins, that can be used to produce biodegradable materials. These natural polymers are suited for pharmaceutical, cosmetic and nutraceutical products development, as emulsifying agent, adjuvant and adhesive in packaging. The presence of the natural parts guarantees important features grouped under the terms of biocompatibility, biodegradability and bio-functionality, while polymers of synthetic origin are able to improve the physical and mechanical properties or to modify the degradation of these hybrid systems.

## PREFACE

Among several materials used for the achievement of novel biomedical devices, hydrogels are the most interesting systems, for their countless properties, especially as regards the compatibility of these systems with the human body. Polysaccharides cannot form stable hydrogels and an effective method is represented by the interaction with a synthesized polymer gel networks to form natural and synthesized polymer blend hydrogels, which is becoming an interesting subject in the research field as well as of industrial interest. Poly(hydroxyethyl methacrylate), poly(vinyl alcohol) poly(propylene oxide)(PPO), or poly(N-isopropylacrylamide) are the most common synthetic polymers employed for the realization of hydrogels suitable for biomedical applications. For the same purpose, as documented by many studies in literature, among the various natural polymers, such as polysaccharides, the most used are:

- *Alginate*, is known to form hydrogel in the presence of divalent cations, such as calcium ( $\text{Ca}^{2+}$ ), which act as cross-linkers between the functional groups of alginate chains;
- *Chitosan*, for several positive characteristics, such as hydrophilicity, functional amino groups and a net cationic charge, that made chitosan suitable hydrogel for the intelligent delivery of macromolecular compounds, such as , oligonucleotides, proteins, antigens <sup>1</sup>.
- *Dextran*, as macromolecular carriers in which the drug can be incorporated, can be obtained in various ways, based on either chemical<sup>2</sup> (e.g. radical polymerization) or physical crosslinking<sup>3</sup>(e.g. ionic interactions, stereo-complexes).
- *Starch*, due to its no toxicity, biodegradable, cost-effective, and quite stable in the biological environment, is a good candidate for use in drug delivery applications.

---

<sup>1</sup>Bergera, J.; Reista, M.; Mayera, J.M.; Feltb, O.; Gurnyb, R. *Eur. J. Pharm. Biopharm.* **2004**, *57*, 35–52.

<sup>2</sup> Gupta, P.; Vermani, K.; Garg, S.; *Drug. Discov. Today*.**2002**, *7*, 569-579.

<sup>3</sup> Bos, G.W.; Jacobs, J.J.L.; Koten, J.W.; Van Tomme, S.R.; Veldhuis, T.F.J. van Nostrum, C.F.; Den Otter, W.; Hennink, W.E. *Eur. J. Pharm. Sci.* **2004**, *21*, 561-567.

## PREFACE

Furthermore, also proteins are often used, as natural backbones, for formulating a variety of pharmaceutical products. Some of these are:

- *Albumin*, which is the most abundant protein in plasma and has a high affinity for a wide range of materials and compounds such as , fatty acids, amino acids, and many drugs; it acts as a carrier for such materials in the blood stream <sup>4</sup>. In addition, recent recombinant technology development has enabled the production of a large quantity of human albumin without any risk of pathogen contamination, which guarantees the safety for the use of albumin, as a hydrogel constituent, in a drug delivery system<sup>5</sup>.
- *Gelatin*, which, in general, exhibits a poor mechanical property that is too brittle when fully dried or too soft when fully wet and is easily soluble in aqueous media<sup>6</sup>. To mitigate this, cross-linking can be introduced for the realization of hydrogel, in the development of drug devices.

On the basis of all these considerations, the overall goals of my PhD thesis were the development of novel functional materials based on biopolymers, such as polysaccharides and proteins, with the possible applications in biomedical fields. In particular, the research project has been focused in three main topics:

- I. The first section describes the synthesis and characterization of novel stimuli-responsive hydrogels, with the pH or temperature sensibility, as potential drug delivery systems.

In particular, much attention has been paid to the realization of different types of gelatin-based hydrogels, as possible pH-sensitive drug delivery devices, suitable for the oral administration of drugs.

Moreover, a potential drug carrier based on a polysaccharide , the chitosan, with the temperature sensibility, thus able to modulate the

---

<sup>4</sup> Tada, D.; Tanabe, T.; Tachibana, A.; Yamauchi, K. *Mater. Sci. Eng. C*. **2007**, *27*, 895.

<sup>5</sup> Tada, D.; Tanabe, T.; Tachibana, A.; Yamauchi, K. *J. Biosci. Bioeng.* **2005**, *100*, 551.

<sup>6</sup> Rattanaruengsrikul, V.; Pimpha, N.; Supaphol, P. *Macromol. Biosci.* **2009**, *10*, 1004-15.



## PREFACE

release of drugs in relation to temperature changes, was synthesized and characterized.

- II. The second section report on the realization of biopolymer-antioxidant conjugate as a potential ingredient for pharmaceutical, cosmetic and nutraceutical formulations.

The possibility to promote the conjugation between biopolymer and antioxidant molecules is of high interest to biomedical fields, because the resulting system have the properties of the starting biopolymer (e.g. no-toxicity, biocompatibility and biodegradability) and the activity of their conjugated molecules (e.g. higher stability and slower degradation rate).

- III. The third section developed during the work done during my research period in the Laboratory for Regenerative Medicine and Pharmacobiology, EPFL University (École Polytechnique Fédérale de Lausanne) , is focused on the realization of a novel heterobifunctional PEG system, as potential candidate for biomaterial modification, and in particular for the cell microencapsulation. The choice of a suitable material preserving the viability and functionality of enclosed cells becomes fundamental if a therapeutic aim is intended.

## SECTION I

### STIMULI RESPONSIVE HYDROGELS AS DRUG DELIVERY DEVICES

#### 1.1 Hydrogel as attractive materials for biomedical applications

Hydrogels are the first biomaterials designed for use in the human body<sup>7</sup> and among several synthetic materials used for the realization of biomedical devices, hydrogels are the most interesting systems for their countless properties, that make them very similar with the human tissues. The high water content and the consequent biocompatibility, the interior network for the incorporation of therapeutics, a large surface area for multivalent bio-conjugation, are only some of the interesting features of these materials. Hydrogels may be chemically stable or they may degrade and eventually disintegrate and dissolve, known as physical gels<sup>8</sup>. Hydrogels are called ‘reversible’, or ‘physical’ gels when the networks are held together by molecular entanglements, and/ or secondary forces including ionic, H-bonding or hydrophobic forces<sup>9</sup>. Polymers can interact by charge interaction or by forming hydrogen bonds between them acting as a physical crosslink between the polymers. Charge interaction can occur between a polymer and a small molecule or between two oppositely charged polymers<sup>10</sup>.

---

<sup>7</sup> Kopecek, J.; Yang, *J. Polym. Int.* **2007**, *56*, 1078–98.

<sup>8</sup> Hoffman, A.S. *Adv. Drug Deliver. Rev.* **2002**, *54*, 3-12.

<sup>9</sup> Campoccia, D.; Doherty, P.; Radice, M.; Brun, P.; Abatangelo, G.; Williams, D.F.; *Biomater.* **1998**, *19*, 2101-2127.

<sup>10</sup> Hoare, T.R.; Kohane, D.S.; *Polym.* **2008**, *49*, 1993-2007.

From a physical point of view, the association of polymer–polymer, polymer–drug, or polymer–bioactive components can be established by means of: electrostatic interactions, hydrogen bonding, donor–acceptor, van der Waals forces, or even metal–ion coordination. There are clear examples of supramolecular systems in the living tissues constituted by this mechanism and even it is the basis for metabolic functions, cell growth and proliferation, or the pharmacological action of a great number of drugs<sup>11</sup>. Instead, are called ‘permanent’ or ‘chemical gels when they are covalently-crosslinked networks. Covalent interactions are much stronger than non-covalent, providing excellent mechanical stability. The chemical approach gives excellent opportunities for the design and development of bioactive polymer systems and polymer drugs, with a lot of possibilities for the modulation and control of the targeting of these very interesting bioactive systems<sup>12</sup>. Copolymerization<sup>13</sup>, suspension polymerization<sup>14</sup>, chemical reaction of complementary groups<sup>15</sup>, and crosslinking using enzymes<sup>16</sup> are some of common examples of approaches for the realization of chemical hydrogels. The realization of functional hydrogels, which respond in a programmed way to a change in temperature, pH, electric, or magnetic fields or some other external stimuli, is widely investigate in several biomedical fields, for the several promising potential application, such as in drug delivery systems<sup>17</sup>, tissue engineering<sup>18</sup>, artificial organs<sup>19</sup>, (micro-) actuator and sensor materials<sup>20</sup>, affinity separations and immunoassays<sup>21</sup>, bio-adhesion

---

<sup>11</sup> Ottenbrite, R.M.; Park, K.; Okano, T. *Biom. Appl. Hydrog. Handbook*, 1st Edition., **2010**.

<sup>12</sup> Stojanović, S.; Nikolić, L.; Nikolić, V.; Petrović, S.; Stanković, M.; Mladenović-Ranisavljević, I. *Phys. Chem. Techn.* **2011**, *9*, 37 – 56.

<sup>13</sup> Wang, Zh.; Hou, X.; Mao, Zh.; Ye, R.; Mo, Y.; Finlow, D.E. *Iran. Polym. J.* **2008**, *17*, 791-798.

<sup>14</sup> Zhang, Y.; Zhu, W.; Ding, J.; *J Biomed Mater Res Part A*, **2005**, *75*, 342-349.

<sup>15</sup> Oh, E.J.; Kang, S.W.; Kim, B.S.; Jiang, G.; Cho, I.H.; Hahn, S.K. *J. Biomed. Mater. Res. Part A*, **2008**, *86*, 685-693.

<sup>16</sup> Garcia, Y.; Collighan, R.; Griffin, M.; Pandit, A. *J. Mater. Sci. Mater. Med.* **2007**, *18*, 1991-2001.

<sup>17</sup> Bhattarai, N.; Gunn, J.; Zhang, M. *Adv. Drug. Deli. Rev.*, **2010**, *62*, 83–99.

<sup>18</sup> Sun, L.; Huang, W. M. *Mater. Design.*, **2010**, *31*, 2684–2689.

<sup>19</sup> Robbins, G. P.; Jimbo, M.; Swift, J.; Therien, M. J.; Hammer, D. A.; Dmochowski, I. J. *J. Am. Chem. Soc.*, **2009**, *131*, 3872–3874.

<sup>20</sup> Caldorera-Moore, M.; Peppas, N. A. *Adv. Drug. Deliv. Rev.*, **2009**, *61*, 1391–1401.

mediators, and many more. These particular hydrogel systems are sometimes called smart polymers, sometimes stimuli-responsive polymers or, also, intelligent polymers. Modifications in shape, solubility and surface features, formation of an intricate molecular assembly or a sol-to-gel transition are just some of the direct consequences of the responses of these stimuli, behavioral changes which are possible to exploit in the development of drug delivery by stimuli-responsive gels, intelligent drug delivery with auto-feedback mechanism that release the drug when it is needed.

### **1.2 Stimuli-responsive hydrogel as Drug Delivery Systems**

Stimuli-sensitive hydrogels are ideal candidates for the realization of self-regulated drug delivery systems. Hydrogels represent a material of choice for drug delivery applications due to their hydrophilicity which enhances the in vivo circulation time of the delivery device by avoiding the host immune response. Hydrogels can control drug release by changing the gel structure in response to environmental stimuli. External or internal stimuli, such as pH, temperature, electric, magnetic, mechanical, solvent/ions can drive these kinds of changes. Through the action of different stimuli-generating devices, that are generated externally controlled systems, which ultimately results in pulsed drug delivery. In the internally regulated systems, or self-regulated devices, a feedback mechanism, that is produced within the body, to control the structural changes in the polymer network and to promote the desired drug release, controls the rate of release, and unlike the externally controlled release systems, doesn't require the use of external intervention. The human body is characterized by several physiological variations that particularly concern the pH and temperature. For this reason, hydrogels responsive to temperature and pH have been the most widely studied systems since these two factors have a physiological significance. The gastro-intestinal tract, vagina, blood are some of the body districts in which

---

<sup>21</sup> Lin, Chien-Chi.; Boyer, P. D.; Aimetti, A. A.; Anseth, K. S. *J. Controlled Rel.*, **2010**, *142*, 384–391.

the variation of the pH is quite pronounced and in which the applications of the systems sensible to the variation of the pH then becomes interesting.

On the other side, hydrogels that are responsive to temperature are another important class of stimuli-sensitive hydrogel widely used in biomedical field. Temperature may act as both an external and internal stimulus. Physiologically, thermal stimuli devices are very important, for example, to counteract an increase in temperature during fever, because there is an elevation of body temperature due to the presence of pyrogens or also in the case of an inflammation. In the next session will be analyzed in detail the main aspects of each type of hydrogels with the pH- and temperature-sensitivity, and the description, in the first four Chapters (*Chapter 1-4*), focusing the attention on the synthesis, characterization and potential application of the stimuli responsive hydrogels designed.

### **1.3 pH-responsive hydrogels: general properties and applications**

Solubility, volume and chain conformation of the pH-responsive polymers can be manipulated by several factors, primarily by changes in pH, but also in co-solvent and electrolytes. In particular, the properties of the polymer (charge, concentration and pKa of the ionizable group, degree of ionization, cross-link degree and hydrophilicity or hydrophobicity) and the properties of the swelling medium (pH and ionic strength), are the main parameters that influence the degree of swelling of ionic polymers.

All the pH-sensitive polymers contain pendant acidic (e.g. carboxylic and sulfonic acids) or basic (e.g. ammonium salts) groups that either accept or release protons in response to changes in environmental pH<sup>22</sup>.

- *pH-sensitive polymers with acidic functional groups*

Poly(acrylic acid) and poly(sulfonic acid) are the major polyanions employed in drug delivery. In particular, in neutral and alkaline fluids, the electrostatic

---

<sup>22</sup>Qiu, Y.; Park, K. *Adv. Drug. Deli. Rev.* **2001**, *53*, 321-339.

repulsion of the pendant acidic groups of these kinds of polymers, influence the physical properties of the polymer.

As regards the applicability of these systems, for example, the poly(acrylic acid) polymers are often used for the realization of the oral drug delivery where they retain their therapeutic cargo in the acidic environment of the stomach but release the encapsulated drug in the alkaline environment of the small intestine due to ionization of the carboxylic acid groups and swelling of the polymer matrix (Figure 1).

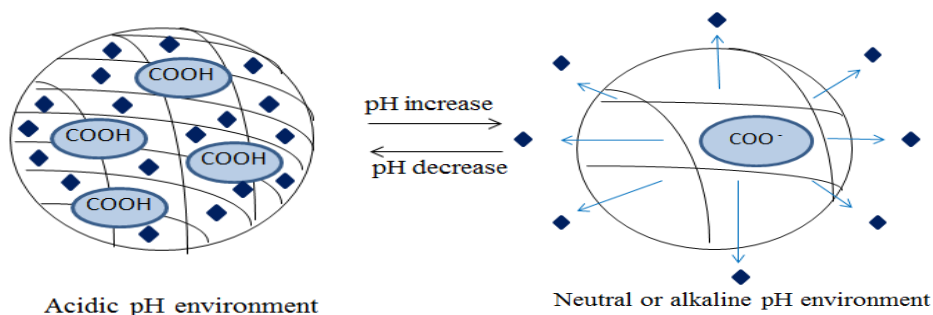


**Figure1.** Schematic drawing of a drug-loaded particle using poly(acrylic acid) polymers

- *pH-sensitive polymers with basic functional groups*

Polymers with amine groups become ionized at low pH values. At basic pH, such as around 8 or for higher values of pH, these systems show a variation in their conformations.

Drug-loaded systems obtained using these types of pH-sensitive polymers, in a neutral or alkaline environment are characterized by unionized amine groups with the consequent entrapment of the loaded drug. Instead, at acidic pH, these polymers become protonated and the electrostatic repulsion between the positive charged groups cause the swelling of the polymeric networks and consequently the release of the loaded drug molecules into the surrounding medium (Figure 2).

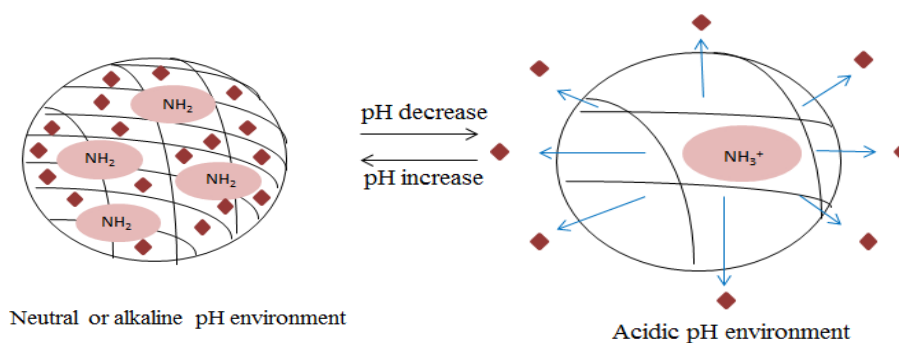


**Figure 2.** Schematic drawing of a drug-loaded particle using poly (vinyl amine) polymers

#### 1.4 Biopolymer-based pH-sensitive hydrogels

One of the limitations linked to the use of synthetic pH-sensitive polymers is their non-biodegradability. To overcome this problem, a considerable interest has been focused on the development of biodegradable, pH-sensitive hydrogels based on polypeptides, proteins and polysaccharides. Natural polysaccharides and their derivatives represent a group of polymers widely used in the pharmaceutical and biomedical fields, such as for the controlled release of drugs. Polysaccharides (e.g. chitosan, alginate, guar gum, pectin, ecc..) present several advantages over the synthetic polymers, because they are nontoxic, less expensive, biodegradable, and freely available, compared to their synthetic counterparts. These polysaccharides offer desired chemical and biological advantages; several saccharide residues provide assorted functionalities for chemical modification and crosslinking to produce biocompatible polysaccharide hydrogels. For all these reason, several research studies in literature focus the attention on the realization of novel biomedical applications based on natural polymer, using polysaccharides backbones. *Atif et al*<sup>23</sup>, for example, developed a pH-sensitive enteric coating of aspirin with biocompatible polymer, to improve the biocompatibility of this device. Indeed, this pH-

<sup>23</sup> Atif, I.; Tariq, Y.; Ijaz, B.; Muhammad, R. *J.Appl. Polym. Sci.* **2012**, *124*, 4184–4192.

sensitive hydrogel was realized from chitosan and poly(vinyl alcohol) and crosslinked with tetraethoxysilane. The resulting system, which has proven a good pH-sensitivity at neutral environment, may be considered a suitable for drug delivery applications. *Kulkarni et al.*<sup>24</sup> fabricated different pH-sensitive polysaccharide-based hydrogel bead systems for controlled drug delivery. They prepared ketoprofen-loaded polyacrylamide-g-alginate beads by ionotropic gelation/covalent cross-linking. The copolymer exhibited considerable pH-sensitive behavior and a predominant drug release at neutral pH (pH 7.2). Moreover, systems based on proteins including gelatin, collagen, casein, albumin and whey protein have been studied for delivering drugs, nutrients, bioactive peptides and probiotic organisms<sup>25</sup>. Proteins represent good raw materials since they have the advantages of synthetic polymers together with the advantages of absorbability and low toxicity of the degradation products<sup>26</sup>.

#### 1.4.1 Gelatin-based pH-responsive hydrogel

One of the natural polymers, extensively studied for the realization of stimuli-responsive bioconjugated hydrogel, useful for biomedical applications, is certainly the gelatin<sup>27</sup>. Gelatin has been widely used in pharmaceutical and medical fields as ingredients in drug formulations, carriers for the delivery of drugs or other therapeutic substances.

Gelatin has a number of advantages as a biomaterial. Indeed, is a natural macromolecule, its natural source is from animals. It is obtained mainly by acidic or alkaline, but also thermal or enzymatic degradation of the collagen. However, gelatin, in general, exhibits a poor mechanical property that is too brittle when fully dried or too soft when fully wet and is easily soluble in

---

<sup>24</sup> Kulkarni, R.V.; Sa, B. *J. Biomater. Sci., Polymer Edn.*, **2009**, *20*, 235-251.

<sup>25</sup> Elzoghby, A.O; Abo El-Fotoh,W.S.; Elgindy, N .A. *J. Control. Release*,**2011**, *153*, 206–216.

<sup>26</sup> Sahin,S.; Selek,H.; Ponchel, G.; Ercan,M.T.; Sargon,M.A.; Hincal, A.; Kas, H.S. *J. Control. Release* ,**2002**,*82*, 345–358.

<sup>27</sup>Raafat, A.I. *J Appl Polym Sci*.**2010**, *118*, 2642-2649.



aqueous media. To mitigate this drawbacks, cross-linking can be introduced<sup>28</sup>. Due to its intrinsic protein structure, characterized by a high number of different functional groups, several modifications can be performed for the realization of novel biomedical applications, by coupling, for examples, of cross-linkers agents. Indeed, different chemical cross-linking methods have been described for gelatin in order to improve its mechanical behavior in physiological conditions, as well as control its rate of biodegradability<sup>29</sup>. In this first part of PhD thesis, the gelatin was selected as natural polymer for the realization of different pH-sensitive hydrogels, in which the natural portions of the natural protein employed, improve the biocompatibility and biodegradability of the synthesized materials. The covalent conjugation of a biodegradable macromolecule, as the gelatin backbone, to a radical monomer represents a versatile strategy to produce intelligent biodegradable hydrogels, suitable for pharmaceutical and biomedical applications.

These pH-sensitive devices were realized employing different synthetic approaches based on the radical polymerization processes. One of this approach, involves the chemical modification of the bio-macromolecules to introduce functionality able to undergo radical polymerization reactions.

It also, biopolymers, without any functional changes in their basic structure, can take part in graft radical polymerization reactions through the involvement of the heteroatoms of the substrates. The following paragraphs briefly describe these two different synthetic approaches.

---

<sup>28</sup> Konishi, M.; Tabata, Y.; Kariya, M.; Hosseinkhani, H.; Suzuki, A.; Fukuhara, K.; Mandai, M.; Takakura, K.; Fujii, S. *J. Controlled Release*, **2005**, *103*, 7.

<sup>29</sup> Tabata, Y.; Nagano, A.; Ikada, Y. *Tissue. Eng.* **1999**, *5*, 127-38.

## 1.5 Synthesis of pH-responsive hydrogels

### 1.5.1 Radical polymerization of biomacromolecules derivatives

Several natural polymers were functionalized with various methacrylates, yielding methacrylated derivative of biopolymers. These biomacromonomers were polymerized to prepare biodegradable hydrogels and micro-/nano-gels for several applications.

The aim of the functionalization of biopolymer is mainly the introduction of useful functional groups, susceptible to radical polymerization, into the polymeric backbone, to realize new systems with innovative features.

As documented in literature, different gelatin derivatives were realized with the aim to obtain novel tissue engineering scaffolds and drug delivery carriers. For example, *Barbetta et al.*<sup>30</sup> have exploited the reaction between primary amines groups of the gelatin with an excess of methacrylic anhydride to realize gelatin methacrylate as a biomacromonomer for the realization of scaffolds for tissue engineering applications.

*Koepff et al.*<sup>31</sup> reported, instead, the derivatization of enzymatic gelatin hydrolisate with glycidylmethacrylate that reacts with both amino and acidic groups and leads to polymerizable gelatin.

In my research project I have turned the attention on the realization of an useful biomacromonomer, through the functionalization of the hydrolyzed gelatin backbone with the methacrylic anhydride, with the aim to obtain a system, with the pH-sensibility, for the realization of a potential drug delivery device for the oral administration.

This work will be described in the *Chapter 1*.

---

<sup>30</sup> Barbetta, A.; Dentini, M.; Zannoni, E.M.; De Stefano, M.E. *Langmuir*, **2005**, *21*, 12333-12341.

<sup>31</sup> Koepff, P.; Braumer, K.; Babel, W. U.S. Pat. Appl. US, **1998**.

### 1.5.2 Biomacromolecules by grafting reaction

Among the prime techniques for polymer modifications, the grafting reaction is one of the most significant. Graft copolymers are branched macromolecules in which the branches are of a different type from the backbone.

They have a variety of potential applications resulting from the wide range of properties available when different polymer chains are connected to form hybrid branched macromolecules<sup>32</sup>.

There are different techniques of graft co-polymerization of different monomers on polymeric backbones. These techniques include chemical, radiation, photochemical, plasma-induced techniques and enzymatic grafting. In the chemical process, for example, the role of initiator is very important as it determines the path of the grafting process. Graft copolymerization reaction introduces side chains and makes various molecular designs possible, thus affording novel types of tailored hybrid materials composed of natural and synthetic polymers.

In the chemical process, free radicals are produced from the initiators and transferred to the substrate to react with monomer to form the graft copolymers<sup>33</sup>.

The free radical polymerization reaction, have several positive features, such as:

- the applicability to the polymerization of a wide range of monomers such as (meth)acrylates, (meth)acrylamides, styrene, butadiene, vinyl acetate and the water-soluble monomers such as acrylic acid, hydroxyl acrylates and N-vinyl pyrrolidone<sup>34</sup>;
- the endurance to a several type of functional groups (e.g. OH, COOH, NR<sub>2</sub>, ecc...);
- the tolerance to different reaction condition (bulk, emulsion, mini-emulsion, solution, suspension).

---

<sup>32</sup>Bhattacharya, A.; Rawlins, J.W.; Ray, P. *Polym. Graft. Crosslink.*, **2009**, 122.

<sup>33</sup> Bhattacharya, A.; Misra, B.N.; *Prog. Polym. Sci.*, **2004**, 29, 767–814.

<sup>34</sup> Roy, D.; Semsarilar, M.; Guthrie, J.T.; Perrier, S. *Chem. Soc. Rev.*, **2009**, 38, 2046-2064.

*Chapter 2* and *Chapter 3*, report on the preparation of novel drug carriers based on gelatin, exploiting the simple and versatile grafting reaction of gelatin, employing sodium methacrylate and N,N'-ethylenebisacrylamide as pH-sensitive monomer and cross-linker agent, respectively.. These hydrogels were obtained by reverse-phase suspension polymerization and their potential applications in drug delivery field demonstrated.

In particular, in the *Chapter 3* I describe a new synthetic approach based on a reverse-phase suspension polymerization employing a natural organic solvent, as dispersed phase.

## **1.6 Thermo-responsive hydrogels**

Temperature-sensitive hydrogels are, together with the pH-sensitive hydrogels, the most studied class of environmentally sensitive polymer systems, applied in drug delivery research. Several polymers show a temperature-responsive phase transition behavior. Hydrophobic groups, such as methyl, ethyl and propyl groups characterized the temperature-sensitive polymer structure.

There are two important types of temperature sensitive hydrogels and in particular:

- Negatively thermo-responsive hydrogels, characterized by a lower critical solution temperature (LCST) below which the hydrogel is in its hydrophilic, swollen state. A common negative thermo sensitive hydrogel with the LCST equal to 32°C is poly(N-isopropyl acrylamide) (PNIPAAm);
- Positively thermo-responsive hydrogels, characterized by a upper critical solution temperature (UCST) behavior. Above the UCST, the hydrogel is in a swollen state and, upon cooling, the hydrogel shrinks

and deswells. Poly(acrylic acid) and polyacrylamide (PAAm) perform as positively thermosensitive hydrogels<sup>35</sup>.

Several bioresponsive hydrogels have been developed for drug delivery based on poly(*N*-isopropylacrylamide) (PNIPAAm) because it exhibits a volume phase transition at a lower critical solution temperature (LCST) in water around 32 °C, which is close to body temperature (Figure 4).

Several researchers have focused the attention on the association between biopolymers with NIPAAm in order to overcome the problem of absent biodegradability and the inability to sustained drug release under physiological condition, of PNIPAAm polymer.

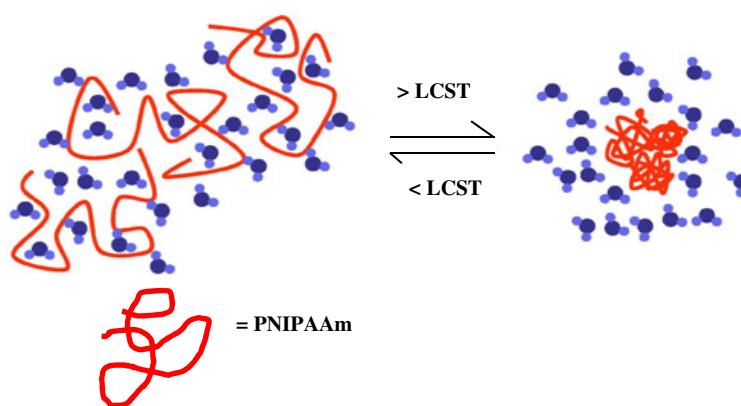


**Figure4.** Schematic drawing of behavior of PNIPAAm hydrogel

### 1.6.1 Chitosan-based thermo-responsive hydrogel

Several thermo-responsive PNIPAAm hydrogels have problems in nonbiodegradability under physiological conditions. Several studies, in literature, have shown that the combination of PNIPAAm with polymer of natural origin, such as polysaccharides and proteins, leads to the formation of biological intelligent hydrogels. In particular, one of the natural polymer, widely investigated for the realization of thermo-responsive bioconjugated

<sup>35</sup>Qifang, W.; Sanming, L.; Zhongyan, W.; Hongzhuo, L.; Chaojie, L. *J. Appl. Polym. Sci.*, **2009**, *3*, 1417-1425.

hydrogel, is the chitosan. Chitosan is a polyelectrolyte with reactive functional groups, gel-forming capability, high adsorption capacity and biodegradability. In addition, it is innately biocompatible and non-toxic to living tissues as well as having antibacterial, antifungal and antitumor activity<sup>36</sup>. These features highlight the suitability and extensive applications that chitosan has in medicine.

Chitosan gels are a promising biocompatible and biodegradable vehicle for treatment of local inflammation<sup>37</sup>.

An important way to obtain the chemical modification of chitosan, with the aim to improve its performance, and enlarging its potential applications<sup>38</sup>, is represented by radical grafting polymerization.

This technique may be considered as an approach to achieve novel biopolymer based materials with improved properties including all the expected usefulness of these biomaterials<sup>39</sup>. This method of reaction is considered one of the most versatile and attractive approaches for the realization of novel types of hybrid materials composed of natural biopolymers and synthetic polymers. Chitosan, in particular, has two types of reactive groups that can be grafted. First, the free amine groups on deacetylated units and secondly, the hydroxyl groups on the C<sub>3</sub> and C<sub>6</sub> carbons on acetylated or deacetylated units (Figure 5).

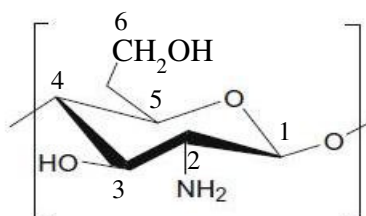


Figure 5. Chitosan structure

<sup>36</sup> Dash, M.; Chiellini, F.; Ottenbrite, R.M.; Chiellini, E. *Prog. Polym. Sci.*, **2011**, *36*, 981-1014.

<sup>37</sup> Prabakaran, M.; Mano, J.F.; *Macromol Biosci.*, **2006**, *6*, 991-1008.

<sup>38</sup> Zhang, H.; Zhong, H.; Zhang, L.; Chen, S.; Zhao, Y.; Zhu, Y. *Carbohydr Polym.*, **2009**, *77*, 785-790.

<sup>39</sup> Maiti, S.; Ranjit, S.; Sa, B. *Int. J. Pharm. Tech. Res.*, **2010**, *2*, 1350-1358.

### 1.6.2 Synthesis of Thermo-Responsive Hydrogels

Several NIPAAm hydrogel systems have been realized and analyzed by different approaches. For example, the simplest material can be obtained by the polymerization of NIPAAm in the presence of a multifunctional vinyl monomer (for instance N,N'-methylenebisacrylamide). More versatile gels have been obtained by copolymerization with other vinyl monomers<sup>40</sup> or by the formation of interpenetrated polymer networks (IPN)<sup>41</sup> or semi-IPN<sup>42</sup>.

Clinical applications of NIPAAm-based thermosensitive hydrogels have limitations since they are not biodegradable but have been evaluated as drug release carriers consisting in semi- or full-IPN of PNIPAAm and different polysaccharides, such as chitosan, alginate, cellulose and dextran, to form biological intelligent hydrogels.

*Kim and Healy*<sup>43</sup>, for example, have synthesized poly(*N*-isopropylacrylamide-co-acrylic acid) hydrogels with degradable peptide cross-linkers.

PNIPAAm/chitosan semi-interpenetrating polymer network hydrogel particles were realized by *Xiaochun et al.*<sup>44</sup>, employing inverse suspension polymerization method. The prepared particles were sensitive to both temperature and pH, and they had good reversibility in solution at different temperatures and pH values.

The aim of the work which will be described in the *Chapter 4*, was the realization of a thermo-responsive hydrogel, based on chitosan, exploiting the covalent conjugation of the biodegradable macromolecule, to thermo-sensitive monomer, combining the features of biocompatibility and biodegradability of chitosan with thermoresponsivity of NIPAAm. This device was realized by adopting a free radical-induced grafting procedure, with the aim to promote the binding of NIPAAm to amino group of chitosan, in presence of a radical initiator.

<sup>40</sup> Yıldız, B.; Isık, B.; Kıs, M.; *Polymer*, **2001**,42, 2521.

<sup>41</sup> Zhang, J.; Peppas, N.A. *Macromolecules*, **2000**,33, 102.

<sup>42</sup> Ju, H.K.; Kim, S.Y.; Lee, Y.M. *Polymer*, **2001**,42,6851.

<sup>43</sup> Kim, S.; Healy, K.E.; *Biomacromol.*, **2003**,4, 1214.

<sup>44</sup> Xiaochun, C.; He, S.; Ting, F.; Jianxin, B.; Jian, X.; Hanjie, Y. *J. Appl. Polym. Sci.*, **2010**, 116, 1342-1347.

Moreover, was verified the ability of this thermo-sensitive system to act as drug delivery carriers, in order to confirm its possible pharmaceutical application.



## *Chapter 1*

### **pH-SENSITIVE DRUG DELIVERY SYSTEMS BY RADICAL POLYMERIZATION OF GELATIN DERIVATIVES**

#### **1. Introduction**

There is a growing attention regarding the development of new materials such as hydrophilic polymers, and especially their cross-linked forms, because this important class of biomaterials, known as hydrogels, have demonstrated great potential application in biological and medical sectors<sup>45</sup>. For the realization of useful biomedical applications, is possible, in particular, take advantages from the numerous properties of an interesting class of hydrogel system, that are capable to modified their gel structures in response to different environmental stimuli (pH, temperature, ecc..) . In particular, hydrogel with pH-sensibility have a potential application in the human body, e.g. as drug carriers, because are capable to control the drug release in relation to the variation of the pH that occur in a specific area of the body.

pH-responsive polymeric systems provide the possibility of fabricating tailorable “smart” functional materials; hence they have found many potential commercial applications, such as in controlled drug delivery, personal care, industrial coatings, biological and membrane science.

This type of stimuli responsive hydrogel are even more interesting when they do not cause toxic reactions or harmful to the human body.

One way to try to increase the compatibility with the human body of these stimuli responsive hydrogels, is represent by the use of natural polymers appropriately cross-linked with the monomer that impart the desired stimulus.

---

<sup>45</sup> Peppas, N.A.; Bures, P.; Leobandung, W.; Ichikawa, H. *Eur. J.Pharm. Biopharm.*, **2000**, *50*, 27-46.

Introduction of functional groups, deriving from synthetic polymeric structure, to a natural polymeric backbone, provide an efficient way to tailor the properties of the resultant polymers, such as hydrophilicity, biodegradability and bioactivity<sup>46</sup>.

Hydrogels from natural proteins such as gelatin, have received particular attention due to the biocompatibility and biodegradability, which are the main attractive features of this natural polymer. A diverse range of applications have been studied for gelatin carrier-mediated pharmaceutical drug delivery and, in particular, gelatin microspheres, have been widely investigated for drug controlled release. Microgels are crosslinked hydrogel particles that are confined to smaller dimensions. Microgels/nanogels have high water content and adjustable chemical and mechanical properties. In addition, they have tunable size from submicrons to tens of nanometers, a large surface area for multivalent bioconjugation, and an interior network for the incorporation of therapeutics. These unique properties offer great potential for the utilization of microgels/hydrogels in applications for medical implants, bionanotechnology, and drug delivery<sup>47</sup>.

In this work, modifying the basic structure of the native gelatin and obtaining an interesting gelatin derivative, hydrolyzed methacrylate gelatin (HGL-MA) which act as pro-hydrophilic monomer/crosslinker, were obtained pH-sensitive microspheres, in presence of methacrylic sodium salt (NaMA), that was selected as pH-sensitive monomer and N,N'-methylenebisacrylamide (MEBA), acting as additionally crosslinking agent. The aim of this approach of radical polymerization reaction it was to obtain protein moieties bearing polymerizable functionalities (HGL-MA) in order to promote directly the copolymerization with a stimuli-responsive monomer (NaMA), thus producing a network in which the polypeptide chains are linked by hydrocarbon bridge and randomly interrupted by growing chains of the functional monomer.

---

<sup>46</sup> Chiu,H.C.; Hsiue,G.H.; Lee, Y.P.; Huang,L.W., *J. Biomater. Sci. Poly. Ed.*,**1999**,*10*, 591–608.

<sup>47</sup> Oh, J.K.; Drumright, R.; Siegwart, D.J.; Matyjaszewski, K. *Prog. Polym. Sci.*, **2008**, *33*,448–77.

Besides, the applicability of these pH-microspheres ,for the oral administration, was verified by loading, in the synthesized hydrogels, an anti-inflammatory drug, Diclofenac sodium salt (DC), in order to mimic the release of drug in an environment simulating the gastro-intestinal tract, thus realizing the release profiles at pH 1.0 and 7.0.

The microspheres were obtained by reverse-phase suspension polymerization, using ammonium persulfate/ N,N,N',N'-tetramethylethylenediamine (TMEDA) as initiator system, and characterized by scanning electronic microscopy, Fourier transform infrared (FT-IR) spectrophotometry, particle size distribution, and swelling analyses. Finally, to estimate the diffusional contribute on the delivery of the drug semi-empirical equations were employed.

## 2. Experimental Section

### 2.1 Materials

Gelatin (Ph Eur, Bloom 160) (GL), methacrylic anhydride (MA), potassium hydroxide, sodium methacrylate (NaMA), hydrochloride acid, N,N'-methylenebisacrylamide (MBA), sorbitan trioleate (Span 85), polyoxyethylene sorbitan trioleate (Tween 85), TMEDA, ammonium persulfate, sodium hydrogen phosphate, disodium hydrogen phosphate, ammonium acetate, and diclofenac sodium salt were provided from Sigma–Aldrich (Sigma Chemical Co, St. Louis, MO).

Acetonitrile, methanol, and water were from Carlo Erba Reagents (Milan, Italy) and all of high-pressure liquid chromatography (HPLC) grade. 2-propanol, ethanol, acetone, n-hexane, chloroform, glacial acetic acid, and diethyl ether were from Carlo Erba Reagents and all of analytical grade (Milan, Italy); *n*-hexane and chloroform were purified by standard procedures<sup>48</sup>.

---

<sup>48</sup> Vogel, A. I.; Tatchell, A. R.; Furnis, B. S.; Hannaford, A. J.; Smith, P. W. G. *Practical Organic Chemistry*, 5th ed.; Longmans: London, **1989**.

## 2.2 Functionalization of gelatin: synthesis of methacrylated gelatin hydrolyzate (HGL-MA)

Derivatization of hydrolyzed gelatin with MA was realized according to the literature with some modifications<sup>49</sup>. In particular, the gelatin, suitably dissolved in water, was undergoes to the basic hydrolysis, in presence of sodium hydroxide, and the resultant solution was heated to 130°C. Then, after cooling to room temperature, a suitable amount of MA was added to the reaction mixture. After a reaction time of 5 h, the mixture was adjusted with dilute hydrochloride acid to a pH value of 7.0. The hydrolyzate was precipitated by adding the polymeric solutions to an excess volume of acetone under agitation at room temperature. The suspensions were filtered by sintered glass filter funnel (Pyrex, Ø30 mm; porosity 3) and washed with diethyl ether, and the recovered HGL-MA was dried in a vacuum oven at 40 °C.

## 2.3. Microspheres preparation (standard procedure)

Microspheres based on HGL-MA, NaMA, and MBA were produced by reverse-phase suspension polymerization<sup>50</sup>. Briefly, a mixture of *n*-hexane and chloroform was placed in a round-bottomed cylindrical glass reaction vessel fitted with an anchor-type stirrer and thermostated at 30°C, then treated, after 30 min of N<sub>2</sub> bubbling, with an aqueous solution of HGL-MA, the comonomer (NaMA), the crosslinker (MBA), and ammonium persulfate as radical initiator. The density of the organic phase was adjusted by the addition of chloroform or *n*-hexane, so that the aqueous phase sank slowly when stirring stopped. Under stirring at 1000 rpm, the mixture was treated with Span 85 and Tween 85, then after 10 min, with TMEDA and stirring was continued for another 60 min. The Table I reports on the experimental conditions of each polymerization reactions. The microspheres were filtered, washed with 50 mL portions of 2-propanol, ethanol, acetone and diethyl ether, and dried overnight under vacuum at 40°.

<sup>49</sup> Iemma, F.; Spizzirri U. G.; Puoci, F.; Cirillo, G.; Curcio, M.; Parisi, O. I.; Picci, N. *Colloid. Polym. Sci.* **2009**, 287, 779-787.

<sup>50</sup> Iemma, F.; Spizzirri, U. G.; Puoci, F.; Muzzalupo, R.; Trombino, S.; Cassano, R.; Leta, S.; Picci, N. *Int J Pharm.*, **2006**, 312, 151-157.

**Table I.** Experimental conditions of copolymerization of HGL-MA with NaMA.

Aqueous dispersed phase			Organic continuous phase	Hydrogel	
HGL-MA Mg	NaMA mg/mmol	MBA mg/mmol	CHCl <sub>3</sub> / <i>n</i> -hexane ml/ml	mg conv %	Code
100	300/2.77	100/0.59	22/22	440 (88%)	<b>HG-1</b>
200	300/2.77	100/0.59	23/23	350 (59%)	<b>HG-2</b>
300	300/2.77	100/0.59	23/23	470 (67%)	<b>HG-3</b>

For all polymerizations, the amount of aqueous phase is 2.5 ml; initiator system is (NH<sub>4</sub>)<sub>2</sub>S<sub>2</sub>O<sub>8</sub>/TMEDA (200 mg/150 μl); surfactants are Span 85/Tween 85 (240 μl/50 μl)

## 2.4 Characterization of pH-responsive microspheres

### 2.4.1 FT-IR Spectroscopy

FT-IR spectra of HGel-MA, NaMA, MBA, HG-1, HG-2, and HG-3 were measured as pellets in KBr with a FT-IR spectrophotometer (model Jasco FT-IR 4200) in the wavelength range of 4000–400 cm<sup>-1</sup>. Signal averages were obtained for 100 scans at a resolution of 1 cm<sup>-1</sup>.

### 2.4.2 Shape and Surface Morphology

The shape and surface morphology of the microspheres were studied using scanning electron microscopy (SEM). The sample was prepared by lightly sprinkling the microspheres powder on a double adhesive tape, which was stuck on aluminium stub. The stubs were then coated with gold to thickness of about 300 Å, using a sputter coater then viewed under scanning electron microscopy (Leo stereoscan 420) and shown in photomicrographs.

### 2.4.3 Dimensional Distribution

The particle size distribution was carried out using an image processing and analysis system, (Stereomicroscope Motic BA 300 Pol). This image processor calculates the particle area and converts it to an equivalent circle diameter.

### 2.4.4 Water Content of Microspheres

The swelling characteristics were determined in order to check hydrophilic affinity of microspheres. Typically, aliquots (40–50 mg) of the microspheres dried to constant weight were placed in a tared 5-mL sintered glass filter ( $\varnothing$ 10 mm; porosity, G3), weighted, and left to swell by immersing the filter plus support in a beaker containing the swelling media (PBS solution  $10^{-3}$  M, pH 7.0, and HCl 0.1N at 37°C). After 24 h, the excess water was removed by percolation at atmospheric pressure. Then, the filter was placed in a properly sized centrifuge test tube by fixing it with the help of a bored silicone stopper, and then centrifuged at 3500 rpm for 15 min and weighted. The filter tare was determined after centrifugation with only water. The weights recorded at the different times were averaged and used to give the water content percent (WR%) by equation (1):

$$WR(\%) = \frac{W_s - W_d}{W_s} \times 100 \quad (1)$$

Where  $W_s$  and  $W_d$  are weights of swollen and dried microspheres respectively. The WR (%) for all prepared materials are reported in Table II.

**Table II.** Swelling behaviors, dimensional parameters and drug loading parameters of hydrophilic pH-responsive microspheres.

Hydrogel	Water Content			Drug loading parameters		
	pH 1.0	pH 7.0	S <sub>r</sub>	Average diameter (μm)	LE (%)	DL (%)
<b>HG-1</b>	62±4	841±2	13.6	87±4	96.3±0.3	9.8±0.2
<b>HG-2</b>	63±2	779±4	12.4	48±3	92.1±0.2	9.6±0.1
<b>HG-3</b>	67±4	646±3	9.6	21±2	88.2±0.4	9.5±0.1

### 2.5 Incorporation of Drug into Preformed Microspheres

Incorporation of Diclofenac sodium salt into the microspheres was performed as follow: 200 mg of preformed empty microspheres were wetted with 2.0 mL in a concentrated drug solution (10 mg/mL). After 3 days, under slow stirring at 37 °C, the microspheres were filtered and dried at reduced pressure in presence of P<sub>2</sub>O<sub>5</sub> to constant weight. The loading efficiency percent (LE%) of all samples are determined by HPLC analysis of filtered solvent according to equation (2):

$$LE (\%) = \frac{C_i - C_0}{C_i} \times 100 \quad (2)$$

Here,  $C_i$  is the concentration of drug in solution before the loading study,  $C_0$  the concentration of drug in solution after the loading study. The values of calculated LE percent and the drug loaded percent (DL%) in each matrix are listed in Table II, according to equation (3):

$$DL(\%) = \frac{\text{Amount of drug in the beads}}{\text{Amount of beads}} \times 100 \quad (3)$$

### 2.6 Differential Scanning Calorimetry analyses

The calorimetric analyses of DC, empty microspheres and DC-loaded microspheres were performed using a Netzsch DSC200 PC. The analyses were performed on the dry samples from 70 to 290°C under an inert atmosphere with a flow rate of 25 mL/min and a heating rate of 10°C/min.

### 2.7 Drug stability

Drug stability was studied at 37°C and at different pH (1.0 and 7.0). Aliquots of drug (10 mg) were incubated at 37°C in HCl 0.1M (pH 1.0) and phosphate buffer solution (PBS)  $10^{-3}$  M (pH 7.0). At scheduled time intervals, corresponding to the condition of the drug release experiments, the samples were withdrawn and assayed by HPLC, in order to determine the drug concentration. The HPLC conditions were a mixture of aqueous solution of ammonium acetate, methanol, and acetonitrile (40/ 30/30, v/v/v). The pH of the aqueous mobile phase portion of ammonium acetate buffer was adjusted with glacial acetic acid. The mobile phase was filtered, degassed, and pumped isocratically at a flow rate of 0.6 mL/min; UV detection at 284 nm<sup>51</sup>. The HPLC analyses were carried out using a Jasco PU- 2080 liquid chromatography equipped with a Rheodyne 7725i injector (fitted with a 20-IL loop), a Jasco UV-2075 HPLC detector, and Jasco-Borwin integrator. A reversed-phase C18 column ( $\mu$ Bondapak, 10  $\mu$ M of 150 x 4.6 mm internal diameter obtained from Waters, Milford, MA) was used. Retention time 4.2 min; limit of detection 0.7  $\mu$ M limit of quantification 14  $\mu$ M.

---

<sup>51</sup> Malliou, E. T.; Markopoulou, C. K.; Koundourellis, J. E. *J. Liq. Chrom. Relat. Tech.*, **2004**, 27, 1565.



### 2.8 *In vitro* release studies

*In vitro* drug release profiles were obtained by HPLC analyses. Aliquots (10 mg) of drug-loaded microspheres were dispersed in flasks containing 10.0 mL of PBS solutions (pH 7.0,  $10^{-3}$ M), at  $37.0^{\circ}\text{C} \pm 0.1^{\circ}\text{C}$ , and sink conditions were maintained throughout the experiments. The samples, at suitable time intervals, were filtered and the solutions were analyzed by HPLC. Additionally, *in vitro* studies were performed by initial dispersion of aliquots (10 mg) of drug-loaded microparticles in flasks containing HCl 0.1M (pH 1.0, simulating gastric fluid) and maintained at  $37^{\circ}\text{C} \pm 0.1^{\circ}\text{C}$  in a water bath for 2 h with magnetic stirring. After this time, a solution of 0.2M tribasic sodium phosphate was added to raise the pH to 7.0 (simulating intestinal fluid), according to the method reported in USP XXII (drug release test, method A, for enteric-coated particles), and the drug solution concentration was determined at suitable times until 24 h<sup>52</sup>. Sink conditions were maintained throughout the experiment. Then at suitable time intervals, samples were filtered and the solutions were analyzed by HPLC. All the experiments were done in triplicate and the results were in agreement within 6 5% standard error.

## 3. Results and Discussion

### 3.1 *Synthesis of microspheres based on hydrolyzed gelatin*

Chemical groups susceptible to radical polymerization were introduced onto hydrolyzed gelatin by acylation with methacrylic anhydride to synthesized polymerizable polypeptide species.

The hydrolyzates gelatin, compared to the native protein, are characterized by several important features, e.g, by enhanced water solubility and by a greater number of nucleophilic groups disposable for the reaction with the acylating agent.

---

<sup>52</sup> U.S. Pharmacopeial Convention. United States Pharmacopeia XXII/National Formulary XVII, Suppl 4; USP: Rockville, MD, 1991, 2510.

In addition to the thiolic groups of cysteine, hydroxyl groups of serine and tyrosine, and with the amino groups in the side chain of lysine residues, the terminal amino groups, derived from the alkaline hydrolysis of the peptide bonds, represent, indeed, reactive sites toward the derivatization with MA. The goal of this study was the realization of protein moieties bearing polymerizable functionalities to be directly copolymerized with a stimuli- responsive monomer, producing a network in which the polypeptide chains are linked by hydrocarbon bridge and randomly interrupted by growing chains of the functional monomer. To synthesize useful spherical polymeric materials, showing pH-responsive behavior, biocompatibility characteristics and hydrophilic properties, the HGL-MA was copolymerized with NaMA and MBA, acting as pH-sensitive and crosslinking agent, respectively, as reported in Figure 1.1.

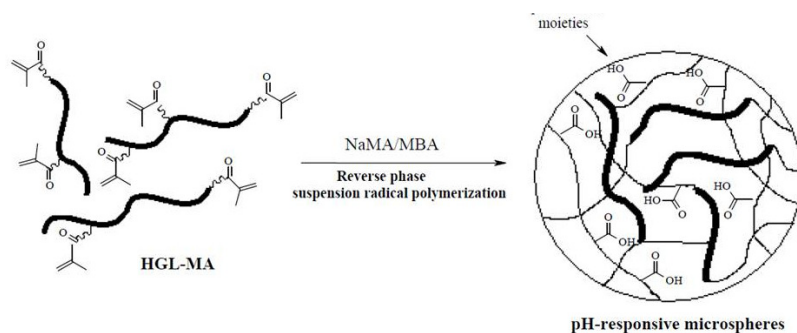


**Figure 1.1.** Copolymerization of HGel-MA monomers with NaMA and MBA

Besides, the choice to obtain hydrogels characterized by spherical shape was dictated by the fact that this kind of materials are ideal vehicles for many controlled delivery applications, due to their ability to encapsulate a variety of drugs, biocompatibility, high bioavailability, and sustained drug release characteristics<sup>53</sup>. The microspheres were synthesized by free-radical suspension polymerization, in which TMEDA and ammonium persulfate was used as initiator system. The optimization of the polymerization method was performed, and it was observed that hydrophilic/lipophilic balance (HLB) of surfactants

<sup>53</sup> Cirillo, G.; Iemma, F.; Puoci, F.; Parisi, O. I.; Curcio, M.; Spizzirri, U. G.; Picci, N., *J. Drug Target*.,**2009**, *17*, 72-77.

represents an important parameter to produce a water-in-oil emulsion consisting of water drops uniformly dispersed in the organic phase ( $\text{CHCl}_3/n$ -hexane) when stirring was stopped. Varying the HGL-MA/NaMA/MBA molar ratio in the polymerization feed, three different hydrogels were prepared, as reported in Table I. In particular, NaMA/ MBA molar ratio was 4.7, while the amount of hydrophilic crosslinker (HGL-MA) was 20.0% (w/w) for HG-1 and was increased to 33.3 and 42.8% for HG-2 and HG-3, respectively. In the proposed polymerization protocol, we found that the change of both the crosslinking degree and the hydrophilic/hydrophobic balance of the polymeric networks seem to greatly influence the water affinity of the microspheres. The increased amount of pH-sensitive monomer in the hydrogel reduces the crosslinking degree of the network enhancing water-polymer affinity.

### **3.2 Characterization of gelatin microspheres**

The materials were characterized by FT-IR spectrophotometry, morphological analyses, particle size distribution, and swelling behavior.

#### *3.2.1 FT-IR Spectroscopy*

The FT-IR spectra of native and hydrolyzed methacrylate gelatin, reported in Figure 1.2(A), showed the appearance of the typical band of carbon–carbon double bond confirming the functionalization reaction.

In addition, the FT-IR spectra of all samples [Figure 1.2(B)] showed the disappearance of band at  $917\text{cm}^{-1}$  ascribable to carbon–carbon double bond of methacrylic functionalities of acidic monomer and HGL-MA, the appearance of the typical absorption bands of the reactive species involved in the polymerization process.

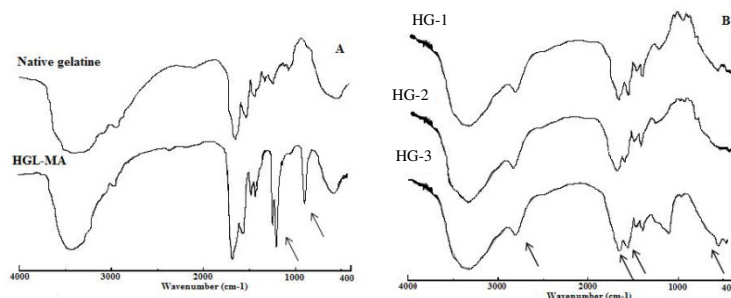


**Figure 1.2.** FT-IR spectra of native gelatin and HGL-MA (A) and of pH-responsive hydrogels HG-1, HG-2, and HG-3 (B)

In particular, the broad band at 3550–3350  $\text{cm}^{-1}$  due to N-H stretching of the secondary amide and hydroxyl group of protein and monomer, carbonyl groups stretching at 1655  $\text{cm}^{-1}$ , N-H bending between 1570 and 1510  $\text{cm}^{-1}$ , N-H out of plane wagging at 675  $\text{cm}^{-1}$  and C-H stretching at 2925 and 2860  $\text{cm}^{-1}$  are visible in the spectra of the hydrogels.

### 3.2.2 Shape and Surface Morphology

Using scanning electron microscopy, informations about the shape and the surface properties of the microparticles were obtained. In Figure 1.3(A) the spherical shape of sample HG-2 was evident, while Figure 1.3(B) shows outside surface of HG-1, characterized by a rough surface. Similar results were obtained for all of the spherically synthesized samples. The shape and the morphology of the microparticles suggest their potential use as drug delivery systems.

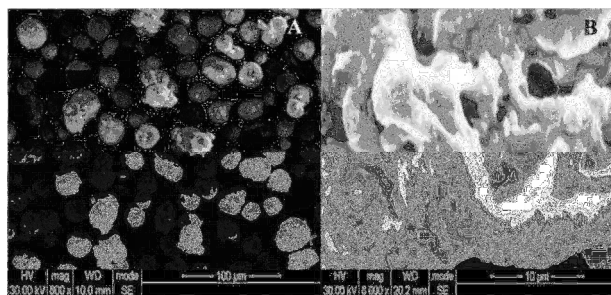


**Figure 1.3.** SEM micrographs of HG-2 (A) and HG-1 outside surface (B)

### 3.2.3 Dimensional Distribution

The dimensional distribution of the spherical microparticles was determined by using an optical stereomicroscope equipped with an image processor that calculates the particle area and converts it to an equivalent circle diameter. In this experiment, the particle diameter was in the dimensional range 60– 80  $\mu\text{m}$  for HG-1, 40–60  $\mu\text{m}$  for HG-2, and 20–40  $\mu\text{m}$  for HG-3 and for each sample a distributional profile was recorded (Figure 1.4). A broad particle size distribution was recorded for HG-3, while the dimensional profile distributions of HG-1 and HG-2 were much narrower than HG-3.

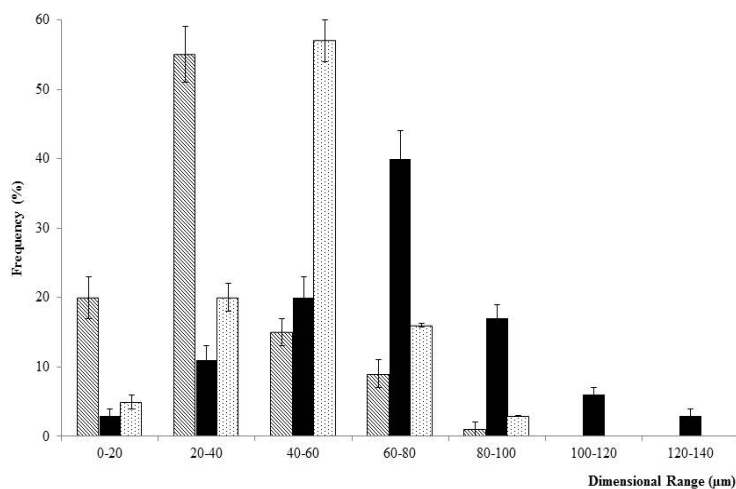


**Figure 1.4.** Size distribution profiles for HG-1 (grey bars), HG-2 (white bars) and HG-3 (black bars)

The particle mean diameter of the hydrogels was 87  $\mu\text{m}$  for HG-1, 48  $\mu\text{m}$  for HG-2, and 21  $\mu\text{m}$  for HG-3. The microparticle diameters were strictly depending on the amount of crosslinkers (HGL-MA and MBA) and the ratio of the reactive species in the polymerization feed; the values of mean particle diameter, in general, decrease as HGL-MA amount increases in the polymerization mixture composition.

### 3.2.4 *Water Content of Microspheres*

Investigation of the applicability of these hydrogels in controlled release was done by studying their swelling behavior. The values of contained water percentage were determined in aqueous media that simulates biological fluids, such as gastric (pH 1.0) and intestinal (pH 7.0) at 37°C. The data reported in Table II illustrate the water uptake, in grams per grams of dry copolymer, for each composition and pH studied. The prepared materials show different water affinity at pH 7.0 and acid pH due to pendant acidic groups in the polymeric chains. In particular, at pH 1.0 there is a considerable lowering of the water affinity due to acidic groups unionized at this pH value. When the pH is 7.0, the water content is greater than that found at pH 1.0 for all copolymers. It is possible to explain this behavior as a consequence of electrostatic repulsions between polymeric chains due to the increase of dissociated groups at pH 7.0. The hydrophilic/hydrophobic balance of the polymeric networks and the amount of the pH-sensitive monomer [ranging from 60% (w/w) for HG-1 to 42% for HG-3] justified the values recorded in the water uptake experiments. In particular, the hydrogel HG-1 showed highest water affinity at neutral pH as consequence of the both increased acidic moieties in the polymeric backbone and lower crosslinking degree, while the Sr value increased as a function of the number of pH-sensitive monomeric units in the hydrogel ranging from 13.6 for HG-1 to 9.6 for HG-3.

### 3.3 *In vitro* release studies

The stimuli-responsive microgels were tested as site specific delivery devices for DC, a well-known no-steroidal anti-inflammatory drug (NSAID), selected for its pharmacokinetics properties and safety concerns. The microgels were loaded by soaking procedure and the loading efficiency (LE%) and the DL% of all samples were determined by HPLC analysis (Table II). DC was loaded on the beads with a LE% > 88% for all copolymers. In our experiments, drug-loaded copolymers with DL% ranging from 9.5 to 9.8 were produced.

Considering the DSC analyses of drug, drug-loaded and unloaded microparticles (Figure 1.5), the nature of the drug inside the polymer matrix can be assessed. This one may emerge in solid solution, metastable molecular dispersion or crystallization and may display relevant properties during *in vitro* release.<sup>28</sup> The onset melting peak of DC was observed at 288°C. However, no characteristic peak of DC was observed in the DSC curves of the drug-loaded microparticles, suggesting that the drug is molecularly dispersed in the polymer matrix.<sup>29</sup>

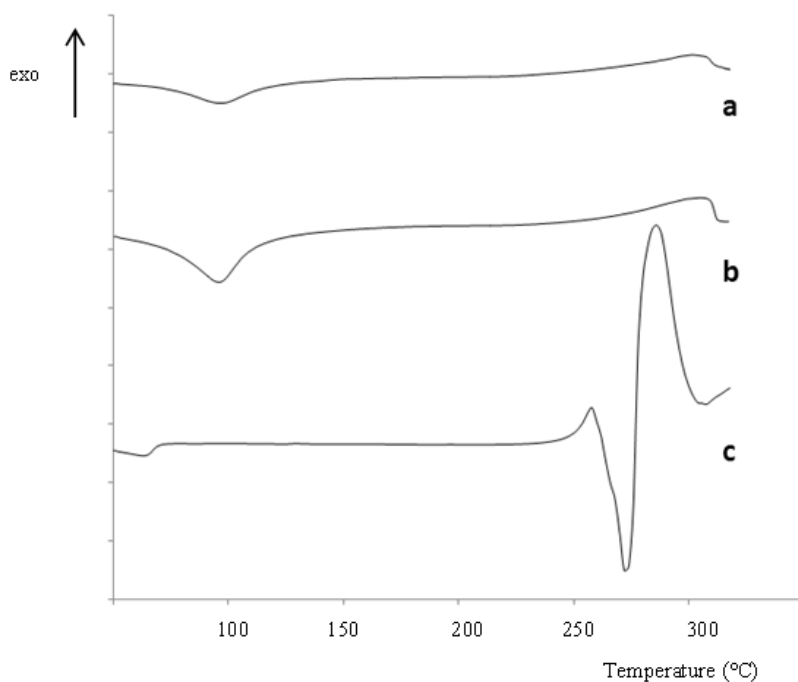


**Figure 1.5.** Differential scanning calorimetric thermograms of DC-unloaded HG-1 microspheres (a) and DC-loaded HG-1 microspheres (b) and pure DC (c). Analogous results have been found for all materials

Drug release profiles were determined by HPLC analyses and the amount of drug released was expressed as percent of drug delivered ( $M_t$ ) related to the effectively entrapped total dose ( $M_0$ ), as a function of time at 37°C in PBS solution (pH 7.0, 1mM) for all microgels (Figure 1.6).

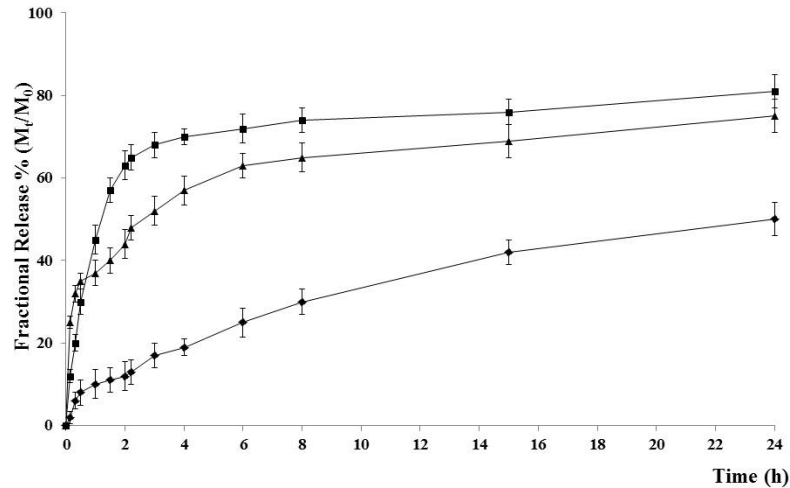


**Figure 1.6.** Drug release expressed as percent of DC delivered ( $M_t$ ) related to the effectively entrapped total dose ( $M_0$ ), as a function of time for microspheres HG-1 (■), HG-2 (▲) and HG-3 (◆) at 37°C and pH 7.0 (1 mM, PBS solution)

In addition, in order to simulate gastrointestinal tract, in vitro release studies at 37°C and at pH 1.0 for 2 h, and then at pH 7.0 for 22 h using the pH change method, were performed. Because of the presence of strong ionizable groups in the polymeric network, pH of the swelling medium induces a change in the degree of ionization of the polyelectrolyte and therefore in the swelling capacity of the microgel. The experimental data showed an increase of DC release for all samples at pH 7.0 due to the repulsion of negative charges of carboxyl groups in the polymeric backbone. The acidic groups are undissociated after 2 h at pH 1.0 and low amounts of drug ( $M_t/M_0$  percent < 10.0) are released. When the pH is 7.0, the swelling of the network increases and the drug molecules easily diffuse through the polymeric structure (Figure 1.7).



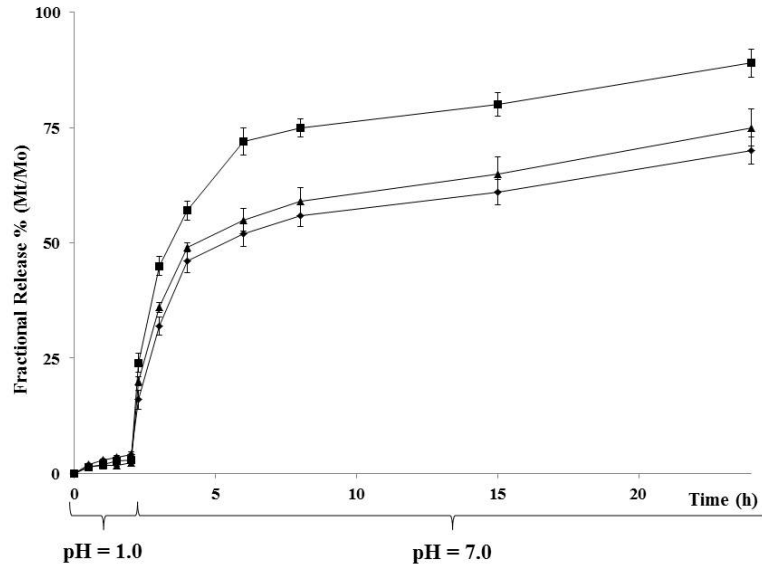


**Figure 1.7.** Drug release expressed as the percent of DC delivered ( $M_t$ ) related to the effectively entrapped total dose ( $M_0$ ), as a function of time using the pH change method for microspheres HG-1 (■), HG-2 (▲) and HG-3 (◆) at 37°C

Since the microparticles have a well-defined geometry and a narrow dimensional distribution, the mechanism of drug release (Fickian or non-Fickian) was determined. In particular, the kinetics of DC release at 37°C and pH 7.0 were analyzed by the semi-empirical equation (4) for  $M_t/M_0 \leq 0.6$ .<sup>12</sup>

$$\frac{M_t}{M_0} = Kt^n \quad (4)$$

where  $M_t/M_0$  is the drug fraction released at time  $t$ ,  $K$  and  $n$  are a constant and the kinetic exponent of drug release, respectively. Although the use of this equation requires detailed statistical analysis, the calculated exponent,  $n$ , gives an indication of the release kinetics. If  $n = 0.43$ , the drug diffuses and releases out of the polymer matrix following a Fickian diffusion, while a Case II transport occur if  $n = 0.85$ . With  $0.43 \leq n \leq 0.85$ , transport lies between Fickian and Case II. With  $n < 0.43$ , pseudo-Fickian diffusion behavior occurs, where sorption curves resemble Fickian curves, but with a slower approach to equilibrium. Finally,  $n > 0.85$  implies that solvent (or drug) transport rate

accelerates as equilibrium is approached (Super-Case II transport). The least-squares estimations of the fractional release data along with the estimated correlation coefficient values,  $r$ , are presented in Table III. As the results shown, the exponents  $n$  in the release experiments at 37°C and pH 7.0 for the HG-1 and HG-2 were 0.32 and 0.31, respectively, which were meant the polymers at this temperature and pH mainly followed a pseudo-Fickian diffusion way. For the hydrogel HG-3 the  $n$  value was 0.47 which meant that the transport lies between Fickian and Case II with a more pronounced Fickian behavior. A more informative analysis can be obtained by fitting the data with the model proposed by Peppas and Sahlin.<sup>13</sup> The equation for this model is:

$$\frac{M_t}{M_0} = K_1 \cdot t^{1/2} + K_2 \cdot t \quad (5)$$

with  $M_t/M_0 \leq 0.95$ . In this equation, the first term is the Fickian contribution and the second term is the Case II relaxational contribution. Table III reports  $K_1$  and  $K_2$  values according to equation (5).

**Table III.** Release kinetics parameters of different formulations

Sample	$\frac{M_t}{M_0} = K t^n$ (4)			$\frac{M_t}{M_0} = K_1 \cdot t^{1/2} + K_2 \cdot t$ (5)		
	$K 10^3$ (min <sup>-n</sup> )	$n$	$r$	$K_1 10^3$ (min <sup>-1/2</sup> )	$K_2 10^3$ (min <sup>-1</sup> )	$r$
<b>HG-1</b>	45.24±1.65	0.32±0.04	0.97	48.77±1.16	-4.90±0.13	0.94
<b>HG-2</b>	39.96±0.98	0.31±0.02	0.97	39.45±1.14	-5.17±0.11	0.96
<b>HG-3</b>	9.29±0.05	0.47±0.03	0.98	8.05±0.70	0.51±0.09	0.98

For all samples the term  $K_1t^{1/2}$  is greater than the term  $K_2t$ , indicating that the predominant release mechanism of DC is the Fickian diffusion through the swollen microparticles. Thus, the drug release was determined by two factors: the swelling rate of polymer and the diffusivity of the drug through the network. Because, at the same temperature, there are no marked differences of the diffusivity of drug in each polymer, the swelling rate of the polymer was the dominating factor. When the dried gels are placed in the release media, water molecules begin to diffuse into the gel network and the matrix swelled. At the same time, drug molecules start to diffuse through the gel layer and to the medium.

#### 4. Conclusions

In this work, pH-responsive microspheres (HG-1, HG-2 and HG-3) based on methacrylated gelatin hydrolyzed, were prepared and tested as site-specific delivery devices of diclofenac sodium salt. Reverse-phase suspension polymerization was chosen as synthetic methodology to obtain microparticles with spherical shape, porous surface and narrow size distribution. The copolymerization of all components was verified by FT-IR spectra, while water uptake experiments at pH 1 and 7 confirmed the pH-responsivity of all hydrogels; in particular, it was observed that, increasing the amount of pH-sensitive monomer in the polymeric feed, and thus reducing the crosslinking degree, the water affinity enhances, raising the highest value for HG-1 matrix. After drug loading, DSC analyses were performed to demonstrate the homogeneous distribution of DC in the polymer matrices and release experiments at neutral pH and in gastro-intestinal simulating fluid were performed. Finally, in order to estimate the diffusional contribute on the drug delivery, semi-empirical equations were employed showing, for each sample, the predominant role of the diffusional component in the release mechanism.

## *Chapter 2*

### **GRAFTED GELATIN MICROSPHERES AS POTENTIAL**

#### **pH-RESPONSIVE DEVICES**

##### **1. Introduction**

The area of stimuli-responsive polymer, which include mostly the pH- and temperature-responsive systems, represent an interesting sector in the field of medicine. In particular, pH-sensitive hydrogels are frequently used to realize controlled release formulations, so as to ensure a targeted release in a particular area of the body.

pH-sensitive polymer are usually obtained by adding pendant acidic or basic functional groups to the polymeric structure; these either accept or release protons in response to appropriate pH and ionic strength changes in aqueous media <sup>54</sup>. The bioconjugation between biopolymer, such as proteins, and ionic polymers, such as poly(acrylic acid), poly(methacrylic acid), allows to obtain different biomaterials with pH-sensibility that find their large use in controlled-release applications.

This is an interesting strategy for designing novel hydrogel drug delivery systems, combining the positive aspects of bioresponsive activity, deriving from the use of pH-responsive monomer, and the biodegradable features, deriving from the biopolymer employed.

The aim of this work it was the synthesis of pH-sensitive microspheres, for oral drug administration, by graft polymerization of gelatin with methacrylic acid sodium salt (NaMA), as pH-sensitive monomer, and N,N'-ethylenebisacrylamide (EBA), acting as crosslinking agent.

---

<sup>54</sup> Langer R, Peppas NA.. *AICHE J*, **2003**; 49, 2990–3006.

Graft copolymerization is a simple and versatile mechanism of reaction and for this reason is of great interest in the scientific community because it is a convenient method to add new properties to a natural polymer with minimum loss of the initial properties of the substrate, as previously reported.

The radical insertion of native gelatin, without any modification in the basic protein backbone, in a cross-linked structure, exploiting the simple and versatile grafting reaction, allows obtain biomacromolecules-based materials with interesting applications in biomedical and pharmaceutical fields.

In this study, the grafted gelatin microspheres were obtained by reverse phase suspension polymerization and characterized by scanning electronic microscopy (SEM), Fourier Transform IR spectrophotometry, particle size distribution and swelling analyses. In order to verify the suitability of these materials as pH-responsive devices for drug delivery, a commonly used anti-inflammatory drug, Diclofenac sodium salt, was loaded on the polymeric structures and the release profiles at pH 1.0 and 7.0 were evaluated. *In vitro* release studies in simulated gastrointestinal fluids have showed the influence of the environmental pH and the chemical nature of entrapped drug on release profiles and hydrogels crosslinking degree. Finally, to estimate the diffusional contribute on the delivery of the drug semi-empirical equations were employed<sup>55,56</sup>.

## 2. Experimental Section

### 2.1 Materials

Gelatin (GL) (Ph Eur, Bloom 160), sodium methacrylate (NaMA), *N,N'*-ethylenebisacrylamide (EBA), sorbitan trioleate (Span 85), polyoxyethylene sorbitan trioleate (Tween 85), *N,N,N',N'*-tetramethylethylenediamine (TMEDA), ammonium persulfate (APS), sodium hydrogen phosphate, disodium hydrogen phosphate, ammonium acetate and DC were provided from Sigma-Aldrich (Sigma Chemical Co, St. Louis, MO). Acetonitrile, methanol and water were

<sup>55</sup> Ritger P.L.; Peppas, N.A. *J. Contr. Rel.*, **1987**; 5, 23-36.

<sup>56</sup> Peppas, N.A.; Sahlin, J.J. *Int. J. Pharm.*, **1989**; 57, 169-72.

from Carlo Erba Reagents (Milan, Italy) and all of HPLC grade. 2-Propanol, ethanol, acetone, glacial acetic acid and diethyl ether were from Carlo Erba Reagents (Milan, Italy) and all of analytical grade. *n*-hexane and chloroform, purchased from Carlo Erba Reagents, were purified by standard procedures.

### *2.2. Microspheres preparation (standard procedure)*

Microspheres based on GL, NaMA and EBA were produced by radical copolymerization technique. In brief, a mixture of *n*-hexane and chloroform was placed in a round-bottomed cylindrical glass reaction vessel fitted with an anchor-type stirrer and thermostated at 30 °C, then treated, after 30 min of N<sub>2</sub> bubbling, with an aqueous solution of GL, NaMA, EBA and APS as radical initiator. The density of the organic phase was adjusted by the addition of chloroform or *n*-hexane so that the aqueous phase sank slowly when stirring stopped. Under stirring at

1,000 rpm, the mixture was treated with Span 85 and Tween 85, then after 10 min with TMEDA, and stirring was continued for another 60 min. The Table I reports on the experimental conditions of each polymerization reaction. The microparticles were filtered by a sintered glass filter (Ø10 mm ; porosity, G3), serially washed with portion (3 x 50 mL) of acetone and ethanol to remove unreacted species and reaction solvent and dried overnight under vacuum at 40°C.

**Table I.** Experimental conditions of copolymerization of GL with NaMA.

Aqueous dispersed phase			Organic continuous phase	Hydrogel	
GL mg	NaMA mg/m mol	EBA mg/m mol	CHCl <sub>3</sub> /n-hexane ml/ml	mg conv %	Code
300	150/1.39	100/0.59	22/22	450 82%	<b>H-1</b>
200	250/2.31	100/0.59	22/23	427 78%	<b>H-2</b>
150	300/2.77	100/0.59	23/22	411 75%	<b>H-3</b>

For all polymerizations, the amount of aqueous phase is 2.5 ml; initiator system is (NH<sub>4</sub>)<sub>2</sub>S<sub>2</sub>O<sub>8</sub>/TMEDA (200 mg/150  $\mu$ l); surfactants are Span 85/Tween 85 (250  $\mu$ l/60  $\mu$ l).

## 2.3 Characterization of pH-responsive microspheres

### 2.3.1 FT-IR Spectroscopy

Fourier-Transmission IR (FT-IR) spectra of starting monomers and hydrogels were measured as pellets in KBr with a FT-IR spectrophotometer (model Jasco FT-IR 4200) in the wavelength range of 4000–400 cm<sup>-1</sup>. Signal averages were obtained for 100 scans at a resolution of 1 cm<sup>-1</sup>.

### 2.3.2 Shape and Surface Morphology

The shape and surface morphology of the microspheres were studied using scanning electron microscopy. The samples were prepared by lightly sprinkling the microspheres powder on a double adhesive tape, which was stuck on aluminium stub. The stubs were then coated with gold to thickness of about 300 Å using a sputter coater then viewed under scanning electron microscopy (Leo stereoscan 420) and shown in photomicrographs.

### 2.3.3 Dimensional Distribution

The particle size distribution was carried out using an image processing and analysis system, (Stereomicroscope Motic BA 300 Pol). This image processor calculates the particle area and converts it to an equivalent circle diameter.

### 2.3.4 Water Content of Microspheres

The hydrophilic properties of grafted microspheres were determined as follows. Aliquots (40–50 mg) of the microparticles dried to constant weight were placed in a tared 5-ml sintered glass filter ( $\varnothing$ 10 mm; porosity, G3), weighted, and left to swell by immersing the filter plus support in a beaker containing the swelling media (PBS solution, pH = 7.0 and HCl 0.1 N, pH 1.0). After 24 h the excess of water was removed by percolation at atmospheric pressure. Then, the filter was placed in a properly sized centrifuge test tube by fixing it with the help of a bored silicone stopper, then centrifuged at 3500 rpm for 15 min and weighted. The filter tare was determined after centrifugation with only water. The weights recorded at the different times were averaged and used to give the water content percent, WR (%), by the following equation (1):

$$WR(\%) = \frac{W_s - W_d}{W_s} \times 100 \quad (1)$$

Where  $W_s$  and  $W_d$  are weights of swollen and dried microparticles, respectively.

The WR (%) for all prepared materials are reported on Table II.

Aqueous dynamic was determined by observing, through an optical stereomicroscope equipped with an image processor (Motic BA 300 Pol), the variation of the microparticle diameter in PBS solution (pH = 7.0,  $10^{-3}$  M) at room temperature until the microparticles achieved the full swollen equilibrium with a diameter  $d_\infty$ . The values of the normalized diameter,  $d_t/d_0$ , were determined,  $d_t$  being the diameter of the swollen microparticles at time  $t$  and  $d_0$  the diameter of the dry microparticles. The experiment carried out by analysing 20 microparticles of each sample.



**Table II.** Swelling behaviors, dimensional parameters and drug loading parameters of hydrophilic pH-responsive microspheres

Hydrogel	Water Content			Dimensional analysis		Drug loading parameters	
	pH 1.0	pH 7.0	S <sub>r</sub>	Average diameter (μm)	Equilibrium normalized diameter d <sub>e</sub> /d <sub>0</sub>	LE (%)	DL (%)
H-1	195±4	717±2	3.7	105±1	1.82±0.03	98.3±0.3	9.8±0.2
H-2	210±2	1010±4	4.8	129±2	2.16±0.05	99.5±0.2	9.9±0.1
H-3	212±4	1073±3	5.1	170±3	2.65±0.06	96.2±0.4	9.7±0.1

#### 2.4 Drug stability

The DC stability was studied at pH 1.0 and pH 7.0 at 37°C. Aliquots of drug (10 mg) were incubated in phosphate buffer solution 10<sup>-3</sup> M at pH 7.0. At scheduled time intervals, corresponding to the condition of the drug release experiments, the samples were withdrawn and assayed by High-Pressure Liquid Chromatography (HPLC), in order to determine the drug concentration. The HPLC conditions were a mixture of aqueous solution of ammonium acetate, methanol and acetonitrile (40/30/30, v/v/v). The pH of the aqueous mobile phase portion of ammonium acetate buffer (pH 7.0, 10<sup>-3</sup> M) was adjusted with glacial acetic acid. The mobile phase was filtered, degassed, and pumped. The HPLC analyses were carried out using a Jasco PU-2080 liquid chromatography equipped with a Rheodyne 7725i injector (fitted with a 20 μl loop), a Jasco UV-2075 HPLC detector and Jasco-Borwin integrator. A reversed-phase C18 column (μBondapak, 10 μm of 150×4.6 mm internal diameter obtained from Waters) was used. Retention time 4.2 min; Limit of Detection (LOD) 0.7 μM; Limit of Quantification (LOQ) 14 μM.

### 2.5. Drug loading by soaking procedure

Incorporation of DC into microspheres was performed as follows: 200 mg of preformed empty microspheres were wetted with 2.0 ml in a concentrated aqueous solution of drug (10 mg/ml). After 3 days, under slow stirring at 25°C, the microspheres were filtered and dried at reduced pressure in presence of P<sub>2</sub>O<sub>5</sub> to constant weight. The loading efficiency percent, LE (%), of all samples was determined by HPLC analysis of filtered solvent according to equation (2):

$$LE(\%) = \frac{C_i - C_0}{C_i} \times 100 \quad (2)$$

Here  $C_i$  was the concentration of drug in solution before the loading study,  $C_0$  the concentration of drug in solution after the loading study. The calculated LE (%) values of different copolymers are listed on Table 2. In addition, the drug loaded percent, DL(%), in each matrix was calculated and the values were listed on Table 2, according to equation 3:

$$DL(\%) = \frac{\text{Amount of drug in the beads}}{\text{Amount of beads}} \times 100 \quad (3)$$

### 2.6 Differential Scanning Calorimetry

The calorimetric analyses of DC, empty microspheres and DC-loaded microspheres were performed using a Netzsch DSC200 PC. The analyses were performed on the dry samples from 70 to 290°C under an inert atmosphere with a flow rate of 25 ml/min and a heating rate of 10°C/min.

### 2.7 X-ray diffraction analysis

X-ray diffraction analysis was performed using a diffractometer Philips PW 1729 X-ray generator. The experimental parameters were: Cu K $\alpha$  radiation, tube setting 40 kV, 20 mA; angular speed 2° (2 $\theta$ /min); range recorded 10–40° (2 $\theta$ /min); time constant 1 s, chart speed 2 cm/min.

## 2.8. *In vitro* release studies

### 2.8.1 *In vitro* release studies at pH 7.0

Release studies were carried out using the dissolution method described in the USP XXIV (Apparatus 1-basket stirring element). Aliquots (10 mg) of drug-loaded microparticles were dispersed in flasks containing PBS solution (pH 7.0) and maintained at  $37.0\pm 0.1^{\circ}\text{C}$  in a water bath. At suitable time intervals, an aliquot of the release medium was withdrawn, filtered (Iso-Disc<sup>TM</sup> Filters PTFE 25-4 25mm x 0.45  $\mu\text{m}$ , Supelco) and the solutions were analysed by HPLC.

### 2.8.2 *In vitro* drug release at pH 1.0 and 7.0

Aliquots (10 mg) of drug-loaded microparticles were dispersed in flasks containing HCl 0.1 M (pH 1.0, simulating gastric fluid) and maintained at  $37\pm 0.1^{\circ}\text{C}$  in a water bath for 2 h with magnetic stirring. After this time, a solution of 0.2 M tribasic sodium phosphate was added to raise the pH to 7.0 (simulating intestinal fluid), according to the method reported in USP XXII (drug release test, method A, for enteric-coated particles). Sink condition were maintained throughout the experiment. Then at suitable time intervals, samples were filtered and the solutions were analysed by HPLC.

## 3. Results and Discussion

### 3.1 Synthesis of pH-sensitive GL-grafted microspheres

Graft copolymerization is an effective method to impart the features of the grafting molecule to a macromolecular structure. The residues in the side chains of gelatin, because of their susceptibility to undergo oxidative modifications, represent suitable target groups to prepare composite materials showing both protein and grafting molecule characteristics. In this study the radical polymerization between the GL and specific functional monomers was proposed to prepare gelatin-based stimuli responsive hydrogels. In particular, we report on the synthesis of pH-sensitive hydrogels by grafting reaction on native GL of

NaMA and EBA, as functional monomer and co-crosslinker respectively, using APS/TEMED as chemical initiator system. The free-radical suspension polymerization technique was employed to obtain the covalent insertion of all the reactive species in a three-dimensional polymeric network.

In the graft reaction the anionic radicals, produced by thermal dissociation of APS, attack the H-atoms in hydroxyl, thiolic or amino groups in the side chain of gelatin, forming macroradicals with several active sites which, in presence of acrylic monomers, propagate as regular radical polymerization. Varying the amount of gelatin in the polymerization feed, three different hydrogels were prepared (Table I) and the optimization of the polymerization method required several attempts to produce devices showing a spherical shape. It was observed that hydrophilic/lipophilic balance (HLB) of surfactants is important. Many tests were carried out to determine the correct ratio of Span 85 (HLB = 1.8) and Tween 85 (HLB = 11). Finally, a system with a total HLB = 3.6 was able to stabilize the aqueous dispersed phase.

### 3.2 Characterization of gelatin microspheres

The materials were characterized by FT-IR spectrophotometry, morphological analyses, particle size distribution, and swelling behavior.

#### 3.2.1 FT-IR Spectroscopy

The FT-IR spectra of all samples showed the disappearance of band at  $917\text{ cm}^{-1}$  ascribable to carbon-carbon double bond of NaMA and the appearance of the typical absorption bands of the commercial gelatin. In particular, the broad band at  $3500\text{-}3350\text{ cm}^{-1}$  due to N-H stretching of the secondary amide and hydroxyl group of protein and monomer, carbonyl groups stretching at  $1650\text{ cm}^{-1}$ , N-H bending between  $1550$  and  $1500\text{ cm}^{-1}$ , N-H out of plane wagging at  $670\text{ cm}^{-1}$  and C-H stretching at  $2922$  and  $2850\text{ cm}^{-1}$  are visible in the spectra of the hydrogels.

### 3.2.2 Shape and Surface Morphology

Using scanning electron microscopy information about the shape and the surface properties of the microparticles were obtained. In Figure 2.1a the spherical shapes of sample H-2 are evident, while Figure 2.2b shows outside surface of H-1, characterized by a high degree of porosity. Similar results were obtained for all of the spherical synthesized samples. The shape and the morphology of the prepared microparticles suggest their potential use as drug delivery systems<sup>57</sup>.

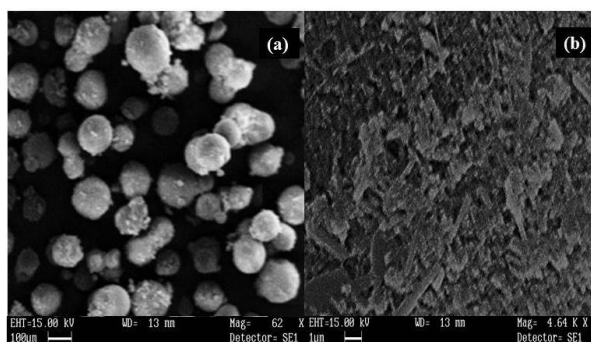


**Figure 2.1.** Morfological analyses (a) SEM micrographs of H-2, (b) outside surface of H-1

### 3.2.3 Dimensional Distribution

The dimensional distribution of the spherical microparticles was determined by using an optical stereomicroscope equipped with an image processor that calculates the particle area and converts it to an equivalent circle diameter. In our experiments, the particle diameter was in the dimensional range 80–120  $\mu\text{m}$  for H-1, 120–160  $\mu\text{m}$  for H-2, and 160–200  $\mu\text{m}$  for H-3 and for each sample a narrow distributional profile was recorded (Figure 2.2). The particle mean diameter of the hydrogels was 170  $\mu\text{m}$  for H-3, 129  $\mu\text{m}$  for H-2 and 105  $\mu\text{m}$  for H-1. The microparticle diameters were strictly depending on the crosslinker amount and hydrophilic/hydrophobic balance of the polymerization feed; the

<sup>57</sup> Iemma, F.; Spizzirri, U.G.; Puoci, F.; Muzzalupo, R.; Trombino, S.; Picci, N. *Drug Deliv.*, **2005**, *12*, 179.

values of mean particle diameter, in general, decrease as the cross-link density increases.

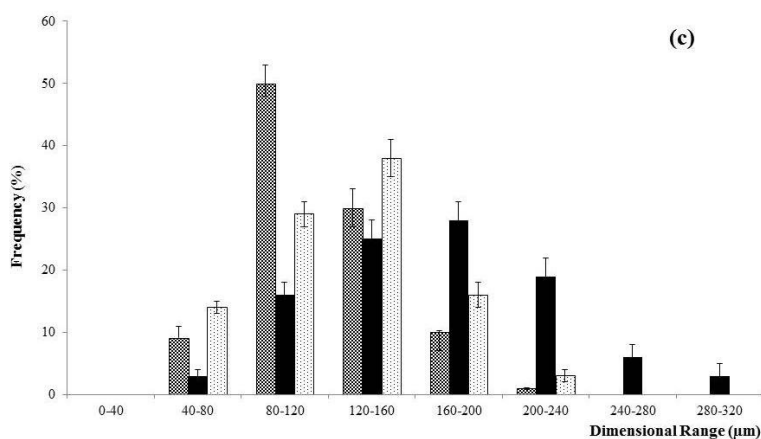


**Figure 2.2.** Size distribution profiles for H-1 (grey bars), H-2 (white bars) and H-3 (black bars)

### 3.2.4 Water Content of Microspheres

Investigation of the applicability of these hydrogels in controlled release was done by studying their swelling behaviour. The value of contained water percentage was determined in aqueous media which simulates some biological fluids, such as gastric (pH 1.0) and intestinal (pH 7.0) at 37°C. The data reported in Table II illustrate the water uptake, in grams per grams of dry copolymer, for each composition and pH studied. We reported also the ratio between the swelling at pH 7.0 and pH 1.0 ( $S_r$ ) for all samples. The microspheres show different water affinity at pH 7.0 and acid pH due to pendant acidic groups in the polymeric chains. In particular, at pH 1.0 there is a considerable lowering of the water affinity due to acidic groups unionized at this pH value. When the pH is 7.0, the water content is greater than that found at pH 1.0 for all copolymers. It is possible to explain this behaviour as a consequence of electrostatic repulsions between polymeric chains due to the increase of dissociated groups at pH 7.0. The hydrophilic/hydrophobic balance and the pH-sensitive monomer amount of the polymeric networks justified the values recorded in the water uptake experiments. In particular, the hydrogel H-3 showed highest water affinity both

acidic and neutral pH as consequence of the increased NaMA amount in the polymerization feed while the  $S_r$  value increased as a function of the number of pH-sensitive monomeric units in the hydrogel ranging from 3.7 for H-1 to 5.1 for H-3.

In addition the Figure 2.3 shows, as an example, the photomicrography of an isolated H-2 microparticle before (a) and after (b) the swelling experiment. As can be observed, after the water penetration, the microparticle maintains its spherical shape but appears translucent and has a greater dimension (analogous results were obtained for samples H-1 and H-3). Therefore, considering that the swelling process is reflected in the change of sample dimension as a function of time, a dynamic swelling study was performed, evaluating through an optical stereomicroscope equipped with an image processor the variation of the microparticle diameter as a function of time when sample are immersed in distilled water. The results of the dynamic swelling measurements are reported in Figure 2.3c as normalized diameter values ( $d_t/d_0$ ) as a function of time for all the samples investigated. As can be observed, the diameter of the microparticles increases monotonically towards the equilibrium swollen value ( $d_\infty$ ) according to the different degree of cross-linking and hydrophilic/hydrophobic balance of the microparticles investigated. In particular, the values of the equilibrium normalized diameter ( $d_\infty/d_0$ ) reported on Table II decrease following the same trend of water regain as the values previously discussed. In addition, the samples investigated swell with a different rate, in particular H-1 microparticles to reach the greatest  $d_\infty$  value swell for a longer time (up to about 10 min), whereas for H-2 and H-3 microparticles an instantaneous swelling in the aqueous medium was observed.

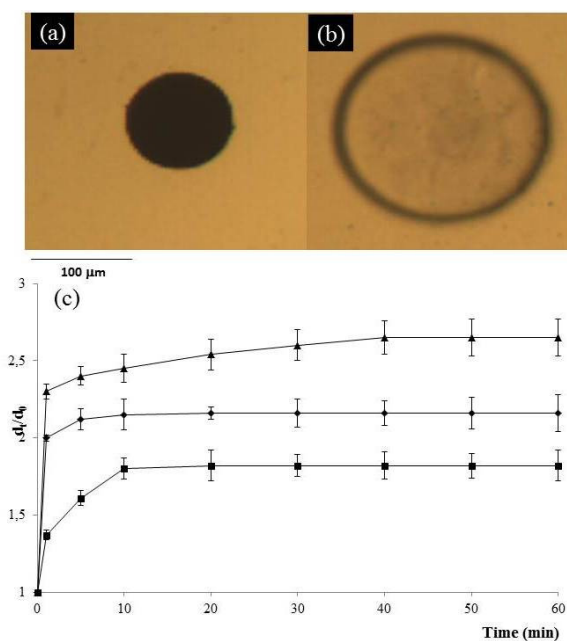


**Figure 2.3.** Photomicrographs of isolated dried H-2 microparticle (a) and isolated swollen H-2 microparticle (b); normalized diameter values ( $d_t/d_0$ ) versus time for H-1 ( $\blacksquare$ ), H-2 ( $\blacklozenge$ ) and H-3 ( $\blacktriangle$ ) microparticles in PBS solution (pH = 7.0,  $10^{-3}$  M) (c)

### 3.3 *In vitro* release studies

To test the microspheres as drug delivery devices these were loaded with DC, by soaking procedure and the loading efficiency (LE%) and the drug loading percent (DL%) of all samples were determined by HPLC analysis (Table II).

Considering the DSC analysis of drug, drug-loaded and unloaded microparticles (Figure 2.4a), the nature of the drug inside the polymer matrix can be assessed. This one may emerge in solid solution, metastable molecular dispersion or crystallization and may display relevant properties during *in vitro* release<sup>58</sup>. The onset melting peak of DC was observed at 288°C. However, no characteristic peak of DC was observed in the DSC curves of the drug-loaded microparticles, suggesting that the drug is molecularly dispersed in the polymer matrix<sup>59</sup>. Information about the drug dispersion state in the microgels were also obtained

<sup>58</sup> Abdel-Tawab, M.; Zettl, H.; Schubert-Zsilavecz, M. *Curr Med Chem.*, **2009**, *16*, 2042.

<sup>59</sup> Stubbe, B.G.; Hennink, W.E.; De Smedt, S.C.; Demeester, J. *Macromolecules*, **2004**, *37*, 8739-8744.



by X-ray analysis. Figure 2.4b shows the X-ray diffraction patterns of pure drugs (curves I), unloaded (curves II) and drug-loaded H-1 microgels (curves III). The characteristic peaks of DC were not found in the loaded microparticles, confirming that no crystalline drug was detected, in accordance with DSC results. Analogous results have been obtained for all the microgels.

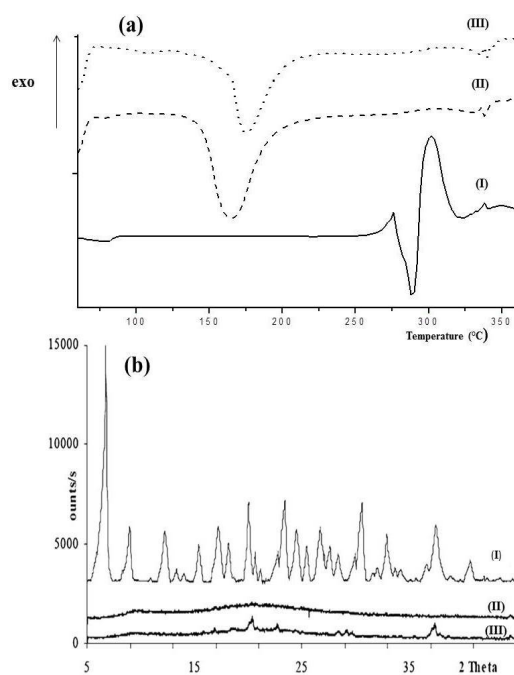


**Figure 2.4.** (a) Differential scanning calorimetric thermograms of pure DC (I), DC-unloaded H-1 microspheres (II) and DC-loaded H-1 microspheres (III); (b) X-ray diffraction patterns of pure DC (I), DC-unloaded H-1 microspheres (II) and DC-loaded H-1 microspheres (III)

Drug release profiles were determined by HPLC analysis and the amount of drug released was expressed as percent of drug delivered ( $M_t$ ) related to the effectively entrapped total dose ( $M_0$ ), as a function of time at 37°C in PBS solution (pH 7.0,  $1.0 \cdot 10^{-3}$  M) for all microgels (Figure 2.5a).

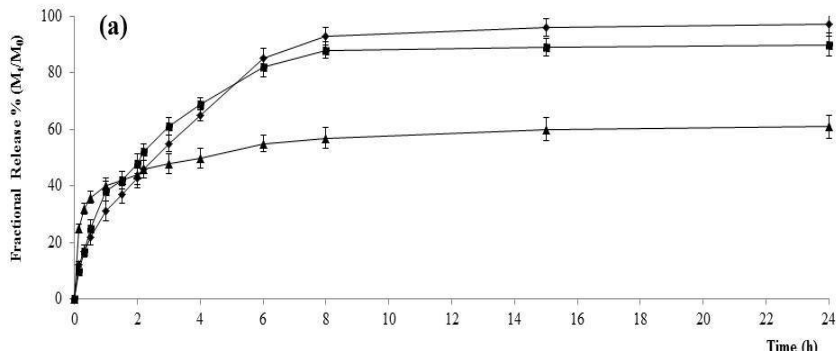


**Figure 2.5 (a)** Drug release expressed as percent of DC delivered ( $M_t$ ) related to the effectively entrapped total dose ( $M_0$ ), as a function of time at 37°C and pH 7.0 (1 mM, PBS solution)

*In vitro* release studies were carried out at 37°C and at pH 1.0 for 2 h, and then at pH 7.0 using the pH change method. Due to the presence of strong ionizable groups in the polymeric network, pH of the swelling medium induces a change in the degree of ionization of the polyelectrolyte and therefore in the swelling capacity of the microgel. The experimental data showed an increase of DC release for all samples at pH 7.0 due to the repulsion of negative charges of carboxyl groups in the polymeric backbone. The acidic groups are undissociated after 2 h at pH 1.0 and low amounts of drug ( $M_t/M_0$  percent < 20.0) are released. When the pH is 7.0, the swelling of the network increases and the drug molecules easily diffuse through the polymeric structure (Figure 2.5b).

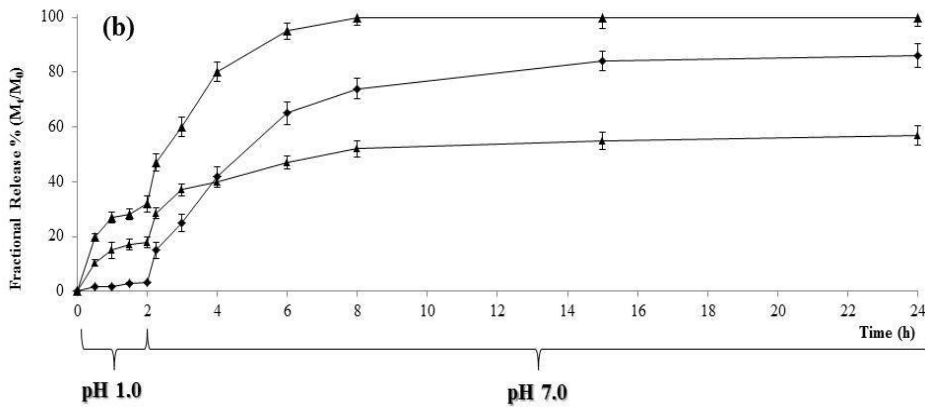


**Figure 2.5 (b)** Drug release expressed as percent of DC delivered ( $M_t$ ) related to the effectively entrapped total dose ( $M_0$ ), using the pH change method at 37°C (b) for microspheres H-1 (■), H-2 (◆) and H-3 (▲)

Since the microparticles have a well-defined geometry and a narrow dimensional distribution, the mechanism of drug release (Fickian or non-Fickian) was determined. In particular, the kinetics of DC release at 37°C and pH 7.0 were analyzed by the semi-empirical equation (4) for  $M_t/M_0 \leq 0.6$ :<sup>12</sup>

$$\frac{M_t}{M_0} = Kt^n \quad (4)$$

where  $M_t/M_0$  is the drug fraction released at time  $t$ ,  $K$  and  $n$  are a constant and the kinetic exponent of drug release, respectively. Although the use of this equation requires detailed statistical analysis, the calculated exponent,  $n$ , gives an indication of the release kinetics. If  $n = 0.43$ , the drug diffuses and releases out of the polymer matrix following a Fickian diffusion, while a Case II transport occur if  $n = 0.85$ . With  $0.43 \leq n \leq 0.85$ , transport lies between Fickian and Case II. With  $n < 0.43$ , pseudo-Fickian diffusion behavior occurs, where sorption curves resemble Fickian curves, but with a slower approach to equilibrium. Finally,  $n > 0.85$  implies that solvent (or drug) transport rate accelerates as equilibrium is approached (Super-Case II transport). The least-squares estimations of the fractional release data along with the estimated correlation coefficient values,  $r$ , are presented in Table III. As the results shown, the exponents  $n$  in the release experiments at 37°C and pH 7.0 for the H-1 and H-2 were 0.32 and 0.31, respectively, which were meant the polymers at this temperature and pH mainly followed a pseudo-Fickian diffusion way. For the hydrogel H-3 the  $n$  value was 0.47 which meant that the transport lies between Fickian and Case II with a more pronounced Fickian behavior. A more informative analysis can be obtained by fitting the data with the model proposed by Peppas and Sahlin.<sup>13</sup> The equation for this model is:

$$\frac{M_t}{M_0} = K_1 \cdot t^{1/2} + K_2 \cdot t \quad (5)$$

with  $M_t/M_0 \leq 0.95$ . In this equation, the first term is the Fickian contribution and the second term is the Case II relaxational contribution. Table III reports  $K_1$  and  $K_2$  values according to equation (5). For all samples the term  $K_1 t^{1/2}$  is greater than the term  $K_2 t$ , indicating that the predominant release mechanism of DC is the Fickian diffusion through the swollen microparticles. Thus, the drug release was determined by two factors: the swelling rate of polymer and the diffusivity of the drug through the network. Because, at the same temperature, there are no marked differences of the diffusivity of drug in each polymer, the swelling rate of the polymer was the dominating factor.

**Table III.** Release kinetics parameters of different formulations

Sample	$\frac{M_t}{M_0} = K t^n$ (4)			$\frac{M_t}{M_0} = K_1 \cdot t^{1/2} + K_2 \cdot t$ (5)		
	$K \cdot 10^3$ (min <sup>-n</sup> )	n	r	$K_1 \cdot 10^3$ (min <sup>-1/2</sup> )	$K_2 \cdot 10^3$ (min <sup>-1</sup> )	r
<b>H-1</b>	30.75±0.39	0.52±0.01	0.99	39.87±0.83	-3.89±0.44	0.99
<b>H-2</b>	34.29±0.87	0.52±0.03	0.98	43.58±1.30	-5.08±0.36	0.98
<b>H-3</b>	39.27±0.53	0.17±0.08	0.98	59.60±3.79	-18.30±2.73	0.94

When the dried gels are placed in the release media, water molecules begin to diffuse into the gel network and the matrix swelled. At the same time, drug molecules start to diffuse through the gel layer and to the medium.

#### 4. Conclusions

In this work, a novel class of pH-responsive microgels were designed and synthesized by reverse phase suspension radical polymerization of native gelatin with a hydrophilic pH-sensitive monomer (NaMA). The possibility of inserting commercial gelatin in a crosslinked structure bearing pH-sensitive moieties, by radical process, represents an interesting innovation that significantly improves the device performance, opening new applications in the pharmaceutical fields as gastrointestinal carrier.

The grafting mechanism allows the insertion of commercial gelatin in a crosslinked structure without any other derivatization reaction, obtaining materials characterized by improved mechanical properties, pH-responsive swelling mechanism, a spherical shape, the most suitable geometry for a drug delivery device. The degree of swelling of the hydrogels depends on the concentration of cross linking agent as well as on the pH of the environment. Materials with different compositions were tested as drug carriers for DC release, which was found to be greatly influenced by the hydrogels crosslinking degree and the drug-polymer interactions. Depending on the pH of the surrounding environment, the DC release takes place by volume changes of the hydrogels and by diffusion of the therapeutic through the polymeric network. In order to estimate the diffusional contribute on the drug delivery, semi-empirical equations were employed, showing the enhanced role of the diffusional component in the release mechanism at acidic pH values. Experimental release data suggest that the synthesized microparticles could be ideal candidates for the release in the intestinal tract of nonsteroidal antiinflammatory drugs thus reducing ulcerogenic effects on the gastric mucosa.

## Chapter 3

### BIODEGRADABLE GELATIN-BASED NANOSPHERES AS pH-RESPONSIVE DRUG DELIVERY SYSTEMS

#### 1. Introduction

Nanoparticles used as drug delivery vehicles are generally < 100 nm in at least one dimension, and consist of different biodegradable materials such as natural or synthetic polymers<sup>60</sup>.

Nanoparticles can be used in targeted drug delivery at the site of disease to improve the uptake of poorly soluble drugs<sup>61</sup>, the targeting of drugs to a specific site, and drug bioavailability.

Among the several types of nanomaterials that have been developed as drug carriers, nanogels or nano-hydrogels are extremely promising. Nanogels are hydrophilic networks constructed starting from both synthetic and natural materials, characterized by high specific surface area and biocompatibility. Many biopolymers, such as polysaccharides and proteins, used as base-materials for the synthesis of hydrogels and nanogels, possess a large amount of functional groups which can be utilized for further bioconjugation, allowing to adapt the hydrogel performances to the desired application.

To obtain efficient drug delivery devices it is important to understand the interactions of nanomaterials with the biological environment and their compatibility therein.

Controlled drug release and subsequent biodegradation are important for developing successful devices.

---

<sup>60</sup> Suri, S.; Fenniri, H.; Singh, B., *J. Occup. Medic. Tox.*, **2007**, 2:16.

<sup>61</sup> Ould-Ouali, L.; Noppe, M.; Langlois, X.; Willems, B.; Te Riele, P.; Timmerman, P.; Brewster, M.E.; Arien, A.; Preat, V., *J. Control. Release*, **2005**, 102, 657-668.

Biodegradability features is an important requirement for the realization of medical devices, to avoid, for example, a second operation to remove them, or to gradually release a drug. Indeed, in the field of controlled drug delivery, biodegradable polymers offer tremendous potential either as a drug delivery system alone or in conjunction to functioning as a medical device<sup>62</sup>. Biodegradable polymers should be:

- non-toxic;
- capable of maintaining good mechanical integrity until degraded;
- capable of controlled rates of degradation.

Different mechanisms can promote the degradation of biodegradable polymers, such as chemical and enzyme-catalyzed degradation of the polymer chains into biologically acceptable, and progressively smaller, compounds<sup>63</sup>. It is very important that the degradation products do not result toxic.

This work proposes a new emulsion polymerization method employing sunflower seed oil and L- $\alpha$ -phosphatidilcoline, or lecithin as biocompatible organic phase and emulsifier, respectively, to obtain gelatin-based particles with spherical shape and nanometric size range.

For the synthesis of nanospheres, radical graft polymerization of gelatin with methacrylic acid sodium salt (NaMA) and N,N' ethylenebisacrylamide (EBA), acting as crosslinking agent, was employed. Scanning Electron Micrograph, particle size distribution, swelling experiments and biodegradation studies were performed in order to characterize the nanospheres. Moreover, drug release experiments in different media were performed using Diclofenac sodium salt as model drug.

In this work the attention has been focused also on the characterization of biodegradability properties of the obtained pH-sensitive hydrogels in order to test the stability of the synthesized hydrogel after their interaction with the environment of the gastro-intestinal tract. For this reason, enzymatic

---

<sup>62</sup> Middleton, J.C.; Tipton, A.J. *Med. Plast. Biomat. Magazine*, **1998**.

<sup>63</sup> Asifm, M.; Arayne, S.; Sultana, N.; Hussain, F. *Pak. J. Pharm. Sci.*, **2006**, *19*, 73-84.

degradation tests were performed in pepsin and pancreatin solution, in order to test the stability of the synthesized nanoparticles towards the enzymes of gastrointestinal tract.

## 2. Experimental Section

### 2.1 Materials

Gelatin (Ph Eur, Bloom 160) (GL), sunflower seed oil from *Helianthus annuus*, sodium methacrylate (NaMA), *N,N'*-ethylenebis(acrylamide) (EBA), *N,N,N',N'*-tetramethylethylenediamine (TMEDA), ammonium persulfate (APS), sodium dihydrogen phosphate, disodium hydrogen phosphate, diclofenac sodium salt, pancreatin from porcine pancreas, and pepsin from porcine gastric mucosa were purchased from Sigma–Aldrich (Sigma Chemical Co, St. Louis, MO). L- $\alpha$ -phosphatidilcoline was purchased in a local market. Ethanol, acetone, diethyl ether, hydrochloric acid (37 % w/w), all of analytical grade, were provided by Carlo Erba reagents (Milano, Italia). Acetonitrile, water and acetic acid, all of high-performance liquid chromatography (HPLC) grade, were supplied from Carlo Erba Reagents (Milan, Italy).

**Table I.** Experimental conditions for biodegradable pH-responsive nanospheres synthesis

Aqueous dispersed phase			Natural Surfactant Lecithin (mg)	Hydrogel	
GL mg	NaMA mg/mmol	EBA mg/mmol		mg/conv %	Code
200	250/2.31	100/0.59	80	436/79.0	GL-1
200	250/2.31	100/0.59	100	450/81.8	GL-2
200	250/2.31	100/0.59	120	471/85.6	GL-3

For all polymerizations, the amount of aqueous phase is 2.5 ml; initiator system is  $(\text{NH}_4)_2\text{S}_2\text{O}_8$ /TMEDA (200 mg/150  $\mu\text{l}$ ); the organic continuous phase is Sunflower seed oil (40 mL)



## 2.2 *Preparation of gelatin nanoparticles*

Gelatin nanoparticles were prepared by a solvent-free emulsion polymerization method. Briefly, 2.5 ml of an aqueous solution of GL, NaMA, EBA and APS (the dispersed phase) was added drop to drop, under continuous stirring at 1200 rpm, to 40 ml of the continuous phase constituted by sunflower seed oil containing different amount of lecithin. After stabilization of the emulsion under continuous stirring, TEMED (100  $\mu$ l) was added and stirring was continued for 60 min. In Table I the experimental conditions of each polymerization reaction was reported. The obtained nanoparticles were exhaustively washed in n-hexane, acetone and ethanol and dried overnight under vacuum at 40°C.

## 2.3 *Shape and surface morphology*

Scanning electron microscopy was employed to study the shape and surface morphology of the nanoparticles. The samples were prepared by lightly sprinkling the microspheres powder on a double adhesive tape, which was stuck on aluminium stub. The stubs were then coated with gold to thickness of about 300 Å using a sputter coater then viewed under scanning electron microscopy (Leo stereoscan 420) and shown in photomicrographs.

## 2.4 *Dimensional distribution*

The particle size distribution was carried out using an image processing and analysis system, (Stereomicroscope Motic BA 300 Pol). This image processor calculates the particle area and converts it to an equivalent circle diameter.

## 2.5 *Water content of gelatin nanospheres*

The swelling characteristics of gelatin nanospheres were determined in order to check hydrophilic affinity of microparticles. Typically, aliquots (40-50 mg) of the nanoparticles, dried to constant weight, were placed in a tared 5-ml sintered glass filter ( $\varnothing$ 10 mm; porosity, G4), weighted, and left to swell by immersing the filter plus support in a beaker containing the swelling media (HCl 0.1N and

PBS solution, pH = 7.0, at  $37 \pm 0.1^\circ\text{C}$ ). At a predetermined time, the excess water was removed by percolation at atmospheric pressure. Then, the filter was placed in a properly sized centrifuge test tube by fixing it with the help of a bored silicone stopper, then centrifuged at 3,500 rpm for 15 min and weighted. This operation was repeated at different times (1, 4, and 24 h). The filter tare was determined after centrifugation with only water. The weights recorded at the different times were averaged and used to give the water content percent (WR %) by the following equation. 1:

$$WR (\%) = \frac{W_s - W_d}{W_s} \times 100 \quad (1)$$

$W_s$  and  $W_d$  are the weights of swollen and dried nanoparticles, respectively. The WR (%) for all prepared materials are reported on Table II.

**Table II.** Swelling behaviors, dimensional parameters and drug loading parameters of hydrophilic pH-responsive nanospheres

Hydrogel	Water Content		Dimensional analysis	
	WR-1.0	WR-7.0	$S_r$	Diameter range (nm)
GL-1	54 $\pm$ 2	960 $\pm$ 4	17.8	450-500
GL-2	86 $\pm$ 3	860 $\pm$ 3	10.0	300-350
GL-3	102 $\pm$ 2	800 $\pm$ 2	7.8	100-150

WR-1.0 and WR-7.0 = water content percent at pH 1.0 and 7.0,  
 $S_r$  = swelling ration WR-7.0/ WR-1.0

### 2.6 Enzymatic degradation of gelatin nanoparticles

A weighted amount of each sample (50 mg) was incubated with: a) 10 mL of HCl solution (0.1 N) containing pepsin (final concentration 0.8 mg/ml) for 72h and b) 10 ml of phosphate buffer solution at pH 7.4 containing pancreatin (final concentration 1.0 mg/ml). Samples were kept in a water bath at  $37^\circ\text{C} \pm 0.1^\circ\text{C}$

under continuous stirring (100 r.p.m.). After the incubation time, the samples were removed and washed with distilled water to remove traces of soluble degradation products, enzymes or other impurities, frozen and dried with “freezing-drying apparatus”. The degree of degradation was calculated by weight loss (WL) following the equation 2:

$$WL (\%) = \frac{W_0 - W_t}{W_t} \times 100 \quad (2)$$

where  $W_0$  is the dry weight before degradation and  $W_t$  is the dry weight at time  $t$ .

### 2.7 Drug stability at pH 1.0 and 7.0

The DC stability was studied at pH 1.0 and pH 7.0 at 37°C. Aliquots of drug (10 mg) were incubated in phosphate buffer solution  $10^{-3}$  M at pH 7.0. At scheduled time intervals, corresponding to the condition of the drug release experiments, the samples were withdrawn and assayed by High-Pressure Liquid Chromatography (HPLC), in order to determine the drug concentration. The HPLC conditions were a mixture of aqueous solution of ammonium acetate, methanol and acetonitrile (40/30/30, v/v/v). The pH of the aqueous mobile phase portion of ammonium acetate buffer (pH 7.0,  $10^{-3}$  M) was adjusted with glacial acetic acid. The mobile phase was filtered, degassed, and pumped isocratically at a flow rate of  $0.6 \text{ ml min}^{-1}$ ; UV detection at 284 nm. The HPLC analyses were carried out using a Jasco PU-2080 liquid chromatography equipped with a Rheodyne 7725i injector (fitted with a 20  $\mu\text{l}$  loop), a Jasco UV-2075 HPLC detector and Jasco-Borwin integrator. A reversed-phase  $C_{18}$  column ( $\mu\text{Bondapak}$ , 10  $\mu\text{m}$  of  $150 \times 4.6$  mm internal diameter obtained from Waters) was used. Retention time 4.2 min; Limit of Detection (LOD) 0.7  $\mu\text{M}$ ; limit of Quantification (LOQ) 14  $\mu\text{M}$ .

### 2.8 Drug loading by soaking procedure

Diclofenac sodium salt was chosen as model drug for release studies. To promote the incorporation of DC, 200 mg of preformed empty nanoparticles

were wetted with 3.0 ml in a concentrated aqueous solution of drug (6.6 mg/ml). After 3 days, under slow stirring at 25°C, the nanoparticles were filtered and dried at reduced pressure in presence of P<sub>2</sub>O<sub>5</sub> to constant weight. The loading efficiency percent (LE %) of all samples was determined by HPLC analysis of filtered solvent according to equation (3):

$$LE (\%) = \frac{C_i - C_0}{C_i} \times 100 \quad 3$$

Here C<sub>i</sub> was the concentration of drug in solution before the loading study, C<sub>0</sub> the concentration of drug in solution after the loading study. The calculated LE (%) values of different copolymers are listed on Table 2. In addition, the drug-loaded percent (DL%) in each matrix was calculated, and the values were listed on Table III, according to equation (4):

$$DL (\%) = \frac{\text{Amount of drug in the nanospheres}}{\text{Amount of nanospheres}} \times 100 \quad (4)$$

**Table III.** LE = loading efficiency, DL = drug loading

Hydrogel	Drug loading parameters	
	LE (%)	DL (%)
GL-1	95±2	9.5±0.1
GL-2	93±2	9.3±0.1
GL-3	97±1	9.7±0.1

Calorimetric analyses of DC, empty nanoparticles and DC-loaded nanoparticles were performed using a Netzsch DSC200 PC. The analyses were performed on the dry samples from 70 to 290 °C under an inert atmosphere with a flow rate of 25 ml/min and a heating rate of 10 °C/min.

### 2.9 *In vitro* release studies

Drug release experiments were performed at 37°C in the following release media: pH 1.0 for 2 h, and then at pH 7.0; PBS solution (1.0 mM, pH 7.4); pancreatin solution (1.0 mg/ml in PBS 10<sup>-3</sup> M, pH 7.4). Using the pH change method, to simulate gastrointestinal drug release, aliquots (10 mg) of drug-loaded nanoparticles were dispersed in flasks containing HCl 0.1M aqueous solution, which is almost similar to the stomach medium, and maintained 37±0.1°C in a water bath for 2 h with magnetic stirring. After this time, a solution of 0.2 M tribasic sodium phosphate was added to raise the pH to 7.4, simulating intestinal environment. At different time intervals, each sample solution were withdrawn, filtered (Iso-Disc™ Filters PTFE 25-4 25mm x 0.45 µm, Supelco), and then the solutions were analyzed by HPLC. Moreover, aliquots (10 mg) of drug-loaded microparticles were dispersed in flasks containing PBS solution (pH 7.4) and maintained at 37.0±0.1°C in a water bath. At suitable time intervals, an aliquot of the release medium was withdrawn, filtered (Iso-Disc™ Filters PTFE 25-4 25mm x 0.45 µm, Supelco) and the solutions were analysed by HPLC. The same procedure was carried out in pancreatin solution (1.0 mg/ml in PBS 10<sup>-3</sup> M, pH 7.4).

## 3. Results and discussion

### 3.1 *Synthesis and characterization of gelatin nanospheres*

In this work, a new solvent-free emulsion polymerization method to obtain biocompatible and biodegradable pH-sensitive nanospheres was proposed. Sunflower seed oil and lecithin were employed as continuous phase and surfactant, respectively, in order to completely overcome any problems of toxicity related to the uses of potentially harmful organic solvents in the polymerization process.

For the synthesis of hydrogels, a free radical grafting procedure, involving the covalent insertion of a pH-sensitive monomer, NaMA, and a crosslinking agent,

MBA, was exploited, and, in order to determine the influence of the surfactant on the hydrogels performances, three different polymeric materials (GL-1, GL-2 and GL-3) were prepared varying the amount of lecithin in the organic phase from 0.2% w/w of GL-1 to 0.3% w/w of GL-3 (Table I). The obtained materials were characterized by scanning electron micrograph, dimensional analysis and water uptake experiments.

In Figure 3.1, SEM of hydrogels were reported. As it is possible to observe, all the synthesized materials showed a nanosized dimension and spherical shape, confirming the suitability of the proposed polymerization procedure to obtain materials as drug delivery devices.

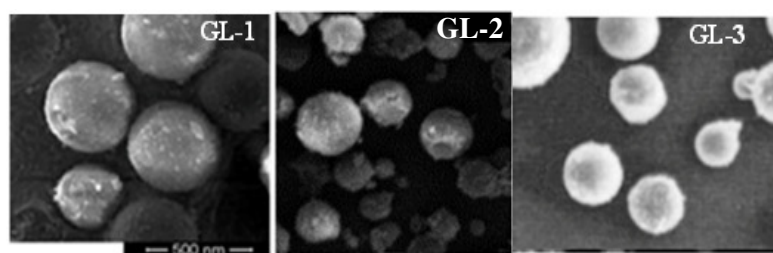


**Figure 3.1.** SEM micrographs of biodegradable pH-sensitive nanogels

Dimensional analyses were also performed in order to evaluate the influence of lecithin concentration on the particle size. It was found that the particle diameter decreases as the amount of surfactant enhances (Table II). In particular, the dimensional parameter decrease ranging from 450-500 nm for GL-1 to 100-150 nm for GL-3, according to the increasing amount of lecithin in the polymerization feed (Figure 3.2).

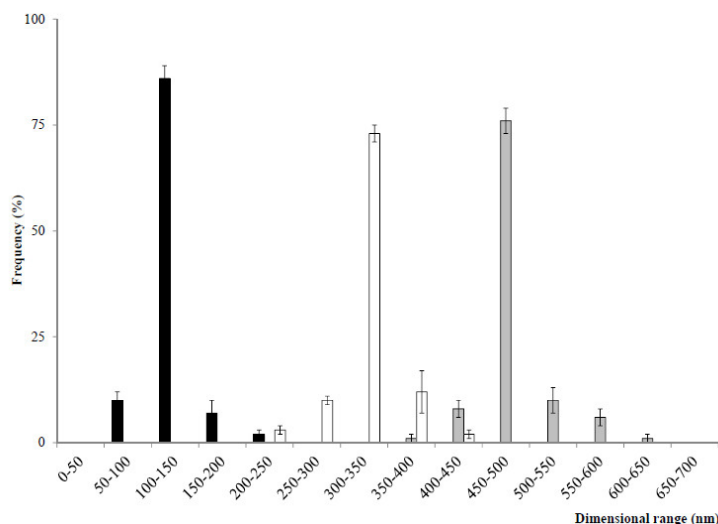


**Figure 3.2.** Size distribution profiles for GL-1 (grey bars), GL-2 (white bars) and GL-3 (black bars)

As reported in literature<sup>64</sup>, these results can be explained considering the role of surfactant in a conventional emulsion polymerization process. The surfactant stabilizes the droplets of the emulsion, forming a thin layer on their surface and preventing coalescence phenomenon. A lecithin amount of 0.3% w/w is sufficient to completely cover the droplets of the emulsion and allows to obtain the particles with the lowest dimensions; concentrations between 0.2 and 0.3 %w/w are adequate to obtain particles with spherical shape but not sufficient to cover the droplets, which thus aggregate forming larger particles with a lower surface area and higher dimensions. Finally, a surfactant amount lower than 0.2% w/w is not sufficient to stabilize the emulsion, and particles with irregular shape were obtained (data not shown).

### 3.2 Water uptake experiments

Swelling experiments were performed in order to test the applicability of the synthesized materials as drug delivery devices. The water affinity was tested at

<sup>64</sup> El-Mahdy, M.; Ibrahim, E.S.; Safwat, S.; el-Sayed, A.; Ohshima, H.; Makino, K.; Muramatsu, N.; Kondo, T. *J. Microencap.*, **1998**, 15, 661-673.

37°C in aqueous media simulating gastric (pH 1.0) and intestinal (pH 7.0) fluids. In Table II the values of water uptake, expressed in grams per gram of dry copolymer, are reported. Because of the presence of pendant acidic groups, each sample showed pH-responsive properties: the higher water affinity at pH 7.0, compared to pH 1.0, is ascribable to the electrostatic repulsions of dissociated carboxylic pendant groups in the hydrogels. At acidic pH, however, the networks are in a collapsed state because of undissociated acidic groups, and water uptake values are considerably lower. Depending of lecithin amount in the emulsion system, a slight difference in the water affinity values were recorded. The nanogel GL-1 showed the higher Sr (17.8), reflecting the higher water uptake at pH 7.0 (960 %) and the lower at pH 1.0 (52 %). Increasing the lecithin amount the Sr decrease for GL-2 and GL-3 which showed values of 10.0 and 7.8, respectively. This behavior could be ascribable to the different amount and distribution of the pH-sensitive monomer in the dispersed phase.

### 3.3 Enzymatic degradation

Biodegradability is a desirable characteristic for a drug delivery device<sup>65</sup>. Biodegradation can occur as a result of different mechanisms, such as chemical and enzyme-catalyzed degradation of the polymer chains into biologically acceptable, and progressively smaller, compounds<sup>66</sup>. In this work, enzymatic biodegradability studies was performed in pepsin and pancreatin solution, in order to test the stability of the synthesized nanoparticles towards the enzymes of gastrointestinal tract. During degradation, the mass of the material may undergo changes, and these changes can be monitored by comparing the mass before and after the degradation period, thus by calculating the percentages of weight loss. After degradation, the sample were washed thoroughly with distilled water to remove traces of soluble degradation products, enzymes, salts, or other impurities and dried under vacuum conditions until constant weight.

<sup>65</sup> Park, J.H.; Ye, M.; Park, K. *Molec.*, **2005**, *10*, 146-161.

<sup>66</sup> Asif, M.; Arayne, M.S.; Sultana, N.; Hussain, F. *Pakist. J. Pharm. Sci.*, **2006**, *19*, 73-84.



Generally, the degradation rate is affected both by polymers intrinsic properties (chemical structure, molecular weight, water content) and by formulation properties, such as particle size<sup>67</sup>.

When incubated in pepsin solution, after 72 h, no significant weight loss was observed for GL-1, GL-2 and GL-3, while, when placed in pancreatin solution, an increasing of the polymer degradation rate as the particle size decreases was verified. The nanoparticles synthesized with the highest amount of emulsifier agent (GL-3), and characterized by the smallest diameter values, indeed, are characterized by a higher weight loss (58%) compared to GL-1 and GL-2 (20 and 37 %, respectively) (Table IV).

**Table IV.** Enzymatic degradation weight loss (%)

Hydrogel	Enzymatic degradation	
	Weight loss (%)	
	Pepsin 1.0 mg/ml	Pancreatin 1.0 mg/ml
GL-1	none	20±1
GL-2	none	37±2
GL-3	none	58±2

As reported in literature<sup>68</sup>, the influence of particle size on the degradation can be ascribable to the fact that, in smaller particles, the products of degradation forming during the degradation process can diffuse easily to the surface, while in the larger particles degradation products have a longer path to the surface of the particle. The first degradation event after contact with water molecules is the hydrolytic scission of the polymer chains leading to a decrease in the molecular weight. At this initial stage, the first degradation products are not small enough to become soluble, and no significant change in the material weight is detected. With increasing time, the molecular weight of degradation products is reduced

<sup>67</sup> Göpferich, A. *Biomat.*, **1996**, *17*, 103-114.

<sup>68</sup> Dunne, M.; Corrigan, O.I.; Ramtoola, Z. *Biomat.*, **2000**, *21*, 1659-1668.

by further hydrolysis, which allows them to diffuse from the material to the surface and then to the solution, causing significant weight loss. In addition, the erosion phenomena was more evident in the hydrogel with the lower dimensional range, due to the higher specific surface for the enzymatic action. The obtained results suggest that it is possible to design an oral drug delivery system that can be degraded by the digestive enzymes and release the entrapped drug at or before specific region of the GI tract.

### 3.4 *In Vitro* Release Studies

The potential use of the nanoparticles as drug delivery device was tested by loading experiments with a model drug, the antiinflammatory Diclofenac sodium salt (DC), by soaking procedure. The loading efficiency of all samples (LE %) was determined by HPLC analysis as reported in the experimental part (Table III). The uniform dispersion of the drug inside the polymeric network is an important requirement for a drug delivery system, in order to avoid that it could affect drug release experiments<sup>69</sup> emerging in solid solution, metastable molecular dispersion or crystallization. Differential Scanning Calorimetric thermograms (DSC) on DC, DC-loaded and unloaded nanoparticles confirmed the effective incorporation of drug inside the polymeric networks (Figure 3.3): the onset melting peak of DC was observed at 288°C. However, no characteristic peak of DC was observed in the DSC curves of the drug-loaded nanoparticles, suggesting that the drug is molecularly dispersed in the polymer matrix.

---

<sup>69</sup>Sairam, M.; Babu, V.R.; Naidu, B.V.K.; Aminabhavi, T. M. *Intern. J. Pharma.*, **2006**, 320, 131-136.

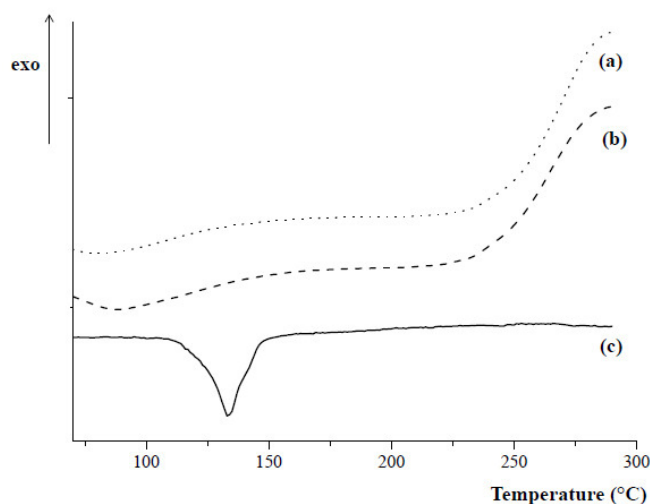


**Figure 3.3.** Differential scanning calorimetric thermograms of pure DC (a), DC-unloaded GL-1 nanospheres (b) and DC-loaded GL-1 nanospheres (c). Analogous results have been found for all materials

Then, drug release experiments were performed at 37°C using the pH change method (at pH 1.0 for 2 h, and then at pH 7.0). Due to the presence of ionizable carboxylic pendant groups, for each sample the swelling capacity and the drug release percentages, are strongly affected by the pH variations of the medium. At pH 1.0 the acidic groups are undissociated and low amounts of drug ( $M_t/M_0$  percent < 15.0) are released. After 2h, when pH jumps to 7.0, the hydrogels swell because of the repulsion of negative charges of carboxyl groups and the drug molecules easily diffuse through the polymeric structure (Figure 3.4). Moreover, figure 4 shows that, at the same experimental time, the release percentages are greater as the particle diameter increases; this behavior can be explained considering the higher swelling capacity of GL-1 sample compared to GL-2 and GL-3.

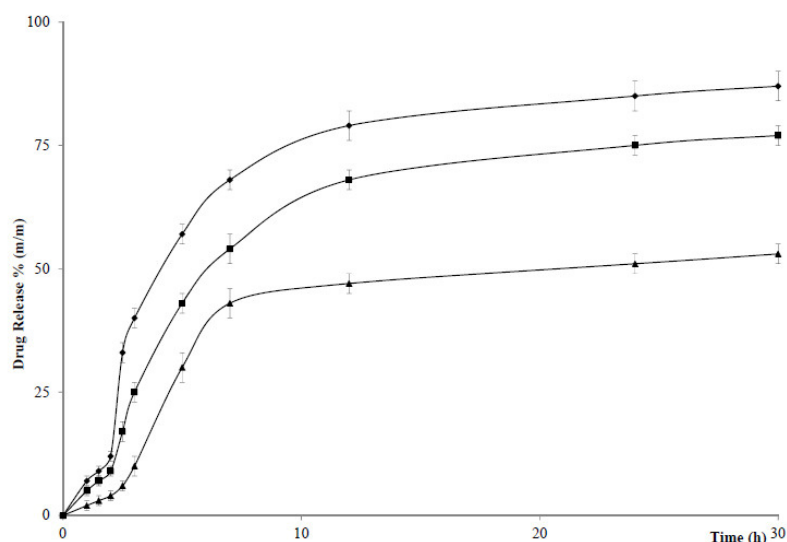


**Figure 3.4.** Drug release expressed as the percent of DC delivered ( $M_t$ ) related to the effectively entrapped total dose ( $M_0$ ), as a function of time using the pH change method for nanospheres GL-1 (♦), GL-2 (■) and GL-3 (▲) at 37°C.

In addition, to evaluate the potential application of the synthesized materials as parenteral drug vehicles, DC release profiles were studied in PBS solution (1.0 mM, pH 7.4). The amount of released drug was expressed as percent of DC delivered ( $M_t$ ) related to the effectively entrapped total dose ( $M_0$ ), as a function of time (Figure 3.5). In these conditions, a correlation between drug release percentages and particle diameters was verified. At each experimental time, indeed, GL-1 nanogels showed a DC release percentage higher than that recorded for GL-2 and GL-3. Moreover, it can be also observed that, even after 30 h, the release is not yet complete ( $M_t/M_0$  percent after 30 h equal to 66.0, 57.0 and 55.0 for GL-1, GL-2 and GL-3, respectively). In addition, the same release experiments were performed in pancreatin solution (1.0 mg/ml in PBS  $10^{-3}$  M, pH 7.4). Similarly to what observed in PBS experiments, at each experimental time, the drug release percentages are higher for the materials with higher particle diameter. However, in this experimental condition, due to the enzymatic degradation of the polymeric network that accelerates drug release, a  $M_t/M_0$  percent > 95.0 for all the synthesized nanospheres was recorded (Figure

3.5). Because of the surface enzyme action a considerable increase of drug release was recorded in the first hours of the experiments for all formulations.

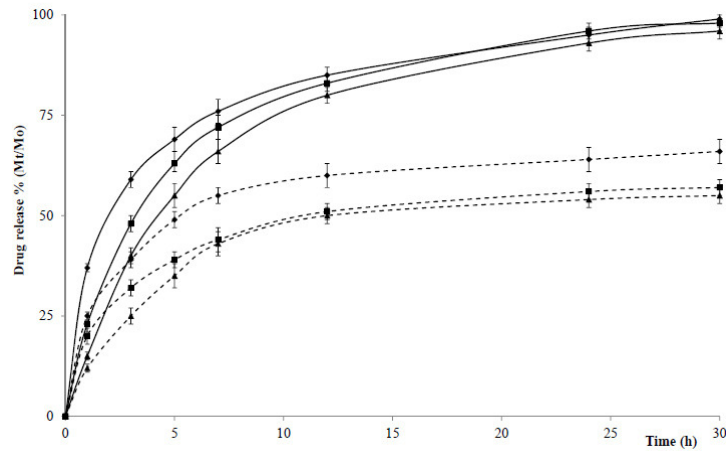


**Figure 3.5.** Drug release expressed as percent of DC delivered ( $M_t$ ) related to the effectively entrapped total dose ( $M_0$ ), as a function of time for microspheres GL-1 (◆), GL-2 (■) and GL-3 (▲) at 37°C, pH 7.4 (1 mM, PBS solution) (—) and 37°C, 1.0 mg/ml pancreatin solution (PBS  $10^{-3}$  M, pH = 7.4) (- - - -)

The drug transport inside pharmaceutical systems and its release sometimes involves multiple steps provoked by different physical or chemical phenomena, making it difficult, or even impossible, to get a mathematical model describing it in the correct way. These models better describe the drug release from pharmaceutical systems when it results from a simple phenomenon or when that phenomenon, by the fact of being the rate-limiting step, conditions all the other processes. The release models with major appliance and best describing drug release phenomena are, in general, the Higuchi model, zero order model, Weibull model and Ritger–Peppas model. The Higuchi and zero order models represent two limit cases in the transport and drug release phenomena, and the Ritger–Peppas model can be a decision parameter between these two models. Since the nanoparticles have a well-defined geometry and a narrow dimensional distribution, the mechanism of drug release (Fickian or non-Fickian) was

determined. In particular, the kinetics of DC release at 37°C and pH 7.4 were analyzed by the semi-empirical equation (5) for  $M_t/M_0 \leq 0.6$ <sup>70</sup>:

$$\frac{M_t}{M_0} = Kt^n \quad (5)$$

where  $M_t/M_0$  is the drug fraction released at time  $t$ ,  $K$  and  $n$  are a constant and the kinetic exponent of drug release, respectively. Although the use of this equation requires detailed statistical analysis, the calculated exponent,  $n$ , gives an indication of the release kinetics. If  $n = 0.43$ , the drug diffuses and releases out of the polymer matrix following a Fickian diffusion, while a Case II transport occur if  $n = 0.85$ . With  $0.43 \leq n \leq 0.85$ , transport lies between Fickian and Case II. With  $n < 0.43$ , pseudo-Fickian diffusion behavior occurs, where sorption curves resemble Fickian curves, but with a slower approach to equilibrium. Finally,  $n > 0.85$  implies that solvent (or drug) transport rate accelerates as equilibrium is approached (Super-Case II transport). The least-squares estimations of the fractional release data along with the estimated correlation coefficient values,  $r$ , are presented in Table V. As the results shown, the exponents  $n$  was 0.34 for GL-1, 0.27 for GL-2 and 0.24 for GL-3 in the experiments at 37°C and pH 7.4 which were meant the polymers at this temperature mainly followed a pseudo-Fickian diffusion release.

A more informative analysis can be obtained by fitting the data with the model proposed by Peppas and Sahlin<sup>71</sup>. The equation (6) for this model is:

$$\frac{M_t}{M_0} = K_1 \times t^{1/2} + K_2 \times t \quad (6)$$

with  $M_t/M_0 \leq 0.95$ . In this equation, the first term is the Fickian contribution and the second term is the Case II relaxational contribution. Table V (a) reports  $K_1$  and  $K_2$  values according to equation (5). For all samples the term  $K_1 t^{1/2}$  is much

<sup>70</sup> Ritger, P.L.; Peppas, N.A. *J. Control. Rel.*, **1987**, *5*, 37-42.

<sup>71</sup> Peppas, N.A.; Sahlin, J.J. *Intern. J. Pharma.* **1989**, *57*, 169-72.

greater than the term  $K_2t$ , indicating that the predominant release mechanism of DC is the Fickian diffusion through the swollen nanoparticles. Thus, the drug release was determined by two factors: the swelling rate of polymer and the diffusivity of the drug through the network. Because, at the same temperature, there are no marked differences of the diffusivity of drug in each polymer, the swelling rate of the polymer was the dominating factor. When the dried gels are placed in the release media, water molecules begin to diffuse into the gel network and the matrix swelled. At the same time, drug molecules start to diffuse through the gel layer and to the medium. In addition, the mechanism of drug release was studied at 37°C and in 1.0 mg/ml of pancreatin solution (PBS  $10^{-3}$  M, pH = 7.4). In erodible drug delivery systems also known as degradable or absorbable release systems, drug release is mediated by the rate of surface erosion. In matrix devices, the drug is dispersed within the three-dimensional structure of the hydrogel. Drug release is controlled by drug diffusion through the gel or erosion of the polymer. In true erosion controlled devices, the rate of drug diffusion will be significantly slower than the rate of polymer erosion and the drug is released as the polymer erodes.

**Table V(a).** Release kinetics parameters of different formulations (equation5)

Sample	$\frac{M_t}{M_0} = Kt^n$ (5)		
	K 10 <sup>3</sup> (min <sup>-n</sup> )	n	R <sup>2</sup>
GL-1	27.2±2.1	0.34±0.04	0.96
GL-2	24.5±2.0	0.27±0.03	0.94
GL-3	19.4±3.2	0.24±0.06	0.97
GL-1*	44.5±2.8	0.25±0.02	0.95
GL-2*	34.7±2.1	0.32±0.04	0.94
GL-3*	27.8±2.2	0.38±0.05	0.93

One of the earliest mathematical models, where the release mechanism only depends on matrix erosion rates, was developed by Hopfenberg<sup>72</sup>. A binomial equation, in which the contribution of the relaxation or erosion mechanism and of the diffusive mechanism can be quantified<sup>73</sup>, was adapted to pharmaceutical problems by Peppas and Sahlin (Equation 6) (Table V b) and the kinetic parameters are reported in the table 3. For all samples the term  $K_1t^{1/2}$  is much greater than the term  $K_2t$ , indicating that the predominant release mechanism of DC is the Fickian diffusion through the swollen nanoparticles as confirmed by

<sup>72</sup>Hopfenberg, H.B.; Hsu, K.C. *Polym. Engin. & Sci.*, **1978**, 18, 1186–1191.

<sup>73</sup>Colombo, P.; Bettini, R.; Santi, P.; Peppas, N.A. *Pharma.Sci. Techn. Tod*, **2000**, 3, 198-204.



the n values calculated fitting the experimental data with the Ritger-Peppas equation.

**Table V(b).** Release kinetics parameters of different formulations (equation 6)

Sample	$\frac{M_t}{M_0} = K_1 \cdot t^{1/2} + K_2 \cdot t \quad (6)$		
	$K_1 10^3$ ( $\text{min}^{-1/2}$ )	$K_2 10^3$ ( $\text{min}^{-1}$ )	$R^2$
<b>GL-1</b>	28.1±0.6	-3.0±0.1	0.99
<b>GL-2</b>	22.3±0.1	-2.2±0.1	0.99
<b>GL-3</b>	19.3±1.3	-1.7±0.3	0.97
<b>GL-1*</b>	39.3±1.0	-4.0±0.2	0.99
<b>GL-2*</b>	33.5±0.8	-2.8±0.3	0.99
<b>GL-3*</b>	28.3±1.1	-1.9±0.2	0.97

#### 4. Conclusions

In this work, bioerodible pH-responsive nanospheres based on commercial gelatin sodium methacrylate and N,N'-ethylenebisacrylamide were prepared and tested as site-specific delivery devices of diclofenac sodium salt. The polymeric devices, synthesized by an eco-friendly emulsion polymerization (W/O) using sunflower seed oil containing different amount of lecithin as continuous phase, were characterized by morphological analysis, particle size distribution, determination of swelling properties and enzymatic biodegradability studies in pepsin and pancreatin solutions. Depending on the pH of the surrounding environment, the DC release takes place by volume changes of the hydrogels and by diffusion of the therapeutic through the polymeric network and the release percentages recorded after 30 hours were lower than 70% for all nanopolymers. In order to estimate the diffusional contribute on the drug delivery, semi-empirical equations were employed, showing the enhanced role of the diffusional component in the release mechanism. Carrying out the release experiment in the presence of pancreatin a complete delivery of DC was observed in 24 h with an increased release of the drug in the first time of the experiment due to the enzymatic surface erosion. The analysis of the kinetic parameters also in this case suggested a predominant diffusional contribute to the release. Experimental release data suggest that the synthesized nanospheres could be ideal candidates for the release in the intestinal tract of nonsteroidal antiinflammatory drugs thus reducing ulcerogenic effects on the gastric mucosa.

## *Chapter 4*

### **TEMPERATURE-SENSITIVE HYDROGELS BY GRAFT POLYMERIZATION OF CHITOSAN AND N- ISOPROPYLACRYLAMIDE FOR DRUG RELEASE**

#### **1. Introduction**

Hydrogels that are responsive to temperature are an interesting class of stimuli-sensitive hydrogel widely used in biomedical field.

Exploiting the ability of this “intelligent gel” to undergoing a volume phase transition under the change of temperature, several research studies have focused the attention on the development of these materials in a variety of applications, e.g. controlled drug delivery <sup>74</sup>, immobilization of enzymes <sup>75</sup> and cell separation processes <sup>76</sup>.

From a physiological point of view, thermo-responsive hydrogel acquire considerable importance, e.g. during a fever there is an increase of body temperature due to the presence of pyrogens. Changes in temperature that can trigger drug delivery can be either due to increased body temperature in a disease state or due to modulated external temperature (for example in the form of heat-triggered sub-dermal implants, etc). PNIPAAm is the most employed synthetic temperature-responsive polymer in the field of drug delivery. PNIPAAm remains in a soluble state in aqueous solution below its lower critical solution temperature (LCST), but forms a hydrogel above this temperature.

The main reason for its frequent use is because its phase transition occurs at approximately body temperature.

---

<sup>74</sup> Wu, M.H.; Bao, B.R.; Chen, J.; Xy, Y.J.; Zao, S.R.; Ma, Z.J.. *Radiat. Phys. Chem.*, **1999**, 56,341.

<sup>75</sup> Park, T.G.; Hoffmann, A.S.. *J. Biomed. Res.*, **1990**,24,21.

<sup>76</sup> Freitas, R.F.S.; Cussler, E.L.. *Sep. Sci. Technol.*, **1987**; 22, 911.

It, indeed, exhibits phase transition at 32 °C in water, and for the purposes of drug targeting, its phase-transition temperature can easily be adjusted to an appropriate temperature (around 40°C) by the introduction of a hydrophilic comonomer, such as *N,N*-dimethylacrylamide<sup>77</sup>.

A prominent application of thermo-responsive hydrogels is represented by the “on-off drug delivery systems” in response to a stepwise temperature change<sup>78</sup>. An example of this application is the release of antipyretics only when the body temperature rises.

Medical applications of NIPAAm-based thermo-responsive hydrogels present restrictions in terms of applicability since they are not biodegradable. To improve this limitation are evaluated thermo-sensitive devices consisting in semi- or full- IPN of NIPAAm with natural polymer, such as dextran<sup>79</sup>, chitosan<sup>80</sup> and xanthan<sup>81</sup>.

The aim of this bioconjugation is the realization of hydrogels which present, at the same time, properties of biocompatibility, biodegradability and thermosensitivity.

Among the polysaccharides which have been largely used to form thermo-responsive hydrogels, in presence of specific thermo-responsive monomers, the chitosan is one of the most studied<sup>82</sup>.

In literature, different methods to obtain chitosan-based, temperature-sensitive hydrogels are reported. *Lee et al.* synthesized NIPAAm-grafted chitosan hydrogels by the direct grafting method using the NIPAAm monomer and ceric ammonium nitrate (CAN) as a radical initiator. The NIPAAm chains of the present study were grafted by forming the amide linkage with chitosan after the

---

<sup>77</sup> Gan, L. H.; Roshan, D. G.; Loh, X. J.; Gan, Y. Y. *Polymer*, **2001**, *42*, 65-9.

<sup>78</sup> Bae, Y. H.; Okano, T.; Kim, S. W. *Pharm. Res.*, **1991**, *8*, 624-628.

<sup>79</sup> Huan, X.; Nayak, B.R.; Lowe, T.L. *J. Pol. Sci. Part A. Pol. Chem.*, **2004**, *42*, 5054-5066.

<sup>80</sup> Yueqin, Y.; Xianzhi, C.; Hansheng, N.; Shusheng, Z. *Cent. Eur. J. Chem.*, **2008**, *6*, 107-113.

<sup>81</sup> Hamcerencu, M.; Desbrieres, J.; Khoukh, A.; Popa, M.; Riess, G., *Pol. Inter.*, **2011**, *60*, 1527-1534.

<sup>82</sup> Bhattarai, N.; Gunn, J.; Zhang, M. *Adv. Drug Del. Rev.*, **2010**, *62*, 83-99.

NIPAAm monomers were polymerized with carboxylic group in the chain end to graft efficiently and control the grafted regions and chain length of NIPAAm<sup>83</sup>.

In the present work, a thermoresponsive material based on chitosan, as possible drug delivery device, was realized exploiting the covalent conjugation of the biodegradable macromolecule, to a thermo-responsive monomer, by free radical-induced grafting procedure, using ammonium persulfate (APS) as initiator system.

The ability of the different systems to act as a controlled release vehicle for drug was evaluated and the diclofenac sodium salt (DS), an anti-inflammatory drug, was chosen as model drug. The obtained materials were characterized by FT-IR spectrophotometry, calorimetric analyses, swelling behavior at different temperatures in the range 15–45°C. Finally, to verify the suitability of these hydrogels as thermo-responsive devices, the drug release profiles were studied performing *in vitro* experiments around the swelling-shrinking transition temperatures of the hydrogels.

## 2 Experimental Section

### 2.1 Materials

Chitosan (CS) (degree of deacetylation 72%), *N*-isopropylacrylamide (NIPAAm), ammonium persulfate (APS), sodium dihydrogen phosphate (NaH<sub>2</sub>PO<sub>4</sub>), disodium hydrogen orthophosphate (Na<sub>2</sub>HPO<sub>4</sub>), diclofenac sodium salt (DC), were purchased from Sigma-Aldrich (Sigma Chemical Co., St Louis, MO, USA). Acetonitrile, methanol and water were of HPLC grade and were obtained from Carlo Erba reagents (Milano, Italia). Acetone, diethyl ether, glacial acetic acid provided by Carlo Erba reagents (Milano, Italia) and all reagents used were of analytical grade.

---

<sup>83</sup> Lee, S.B.; Ha, D.I.; Cho, S.K.; Kim, S.J.; Lee, Y.M. *J. Appl. Polym. Sci.*, **2004**; 92, 2612–2620.

## 2.2. Synthesis of CS-g-NIPAAm hydrogels

Thermo-responsive hydrogels based on CS and NIPAAm (CS-g-NIPAAm) were prepared by bulk radical polymerization. Briefly, CS was dissolved in 12 mL of acetic acid solution (1.0 M) and NIPAAm, was added, as reported on Table I. The mixture was treated for 30 minutes with N<sub>2</sub> bubbling and then APS was added to initiate the copolymerization reaction at 40°C, in a thermostatic bath, for 24 h. The resultant bulk rigid polymer was crushed, grounded into powder and sieved through a 63 nm stainless steel sieve. The sieved materials were collected and the very fine powders were washed with distilled water (3 x 100 mL) to remove unreacted species and reaction solvent, frozen and dried with “freezing-drying apparatus” to afford vaporous solids. Freeze drier Micro Modulyo, Edwards was employed.

**Table I.** Composition and thermal properties of the thermo-responsive hydrogels

Chitosan (g)	NIPAAm (g/mmol)	Code	LCST (°C)
0.240	0.560/4.9	P1	34.8±0.2
0.240	1.130/9.9	P2	32.1±0.2
0.240	1.700/14.9	P3	31.4±0.2

Acetic acid (1M, 12 ml); Initiator: Ammonium persulphate (200 mg)

## 2.3 Characterization of thermo-responsive hydrogels

### 2.3.1 FT-IR Spectroscopy

Fourier-Transmission IR (FT-IR) spectra of starting monomers and hydrogels were measured as pellets in KBr with a FT-IR spectrophotometer (model Jasco FT-IR 4200) in the wavelength range of 4000–400 cm<sup>-1</sup>. Signal averages were obtained for 100 scans at a resolution of 1 cm<sup>-1</sup>.

### 2.3.2 Surface Morphology

The surface morphology of the hydrogels were investigated using scanning electron microscopy. The samples were prepared by lightly sprinkling the microspheres powder on a double adhesive tape, which was stuck on aluminium stub. The stubs were then coated with gold to thickness of about 300 Å using a sputter coater then viewed under scanning electron microscopy (Leo stereoscan 420) and shown in photomicrographs.

### 2.3.3 Differential Scanning Calorimetry analyses

The calorimetric analyses were performed using a Netzsch DSC200 PC in order to determinate the Lower Critical Solution Temperature (LCST) of the hydrogels. Hydrogels were immersed in distilled water at room temperature for 24h to reach the equilibrium state. Then, about 20 mg of the swollen sample were placed inside a hermetic aluminum pan and sealed tightly by a hermetic aluminum lid. The thermal analyses were performed in the range of temperature from 25°C to 55°C with a heating rate of 3°C min<sup>-1</sup> on the swollen hydrogel sample under a dry nitrogen atmosphere with a flow rate of 25 mL min<sup>-1</sup>.

### 2.3.4 Swelling behaviour of hydrogels

For the investigation of temperature effects on the equilibrium swelling ratio of hydrogels, the swelling studies were carried out at different temperatures from 15°C to 45°C. Briefly, the dried hydrogels (50 mg) were weighed and placed in a tared 5 mL sintered glass filter (Ø10 mm; porosity, G3) and left to swell by immersing the filter plus support in a beaker containing the swelling media (PBS solution 10<sup>-3</sup> M, pH 7.0). After 24 h, the excess water was removed by percolation at atmospheric pressure. Then, the filter was placed in a properly sized centrifuge test tube by fixing it with the help of a bored silicone stopper, then centrifuged at 3500 rpm for 15 min and weighted. The weight of the wet hydrogel was then measured. The water content percentage (WR%) was determined from the equation (1):

$$WR(\%) = \frac{W_s - W_d}{W_s} \times 100 \quad (1)$$

where  $W_s$  and  $W_d$  are the weights of the equilibrated swollen hydrogels and the dried gels, respectively.

#### 2.4 Drug stability

The DC stability was studied at the release experiment conditions (25 and 40°C, pH 7.0) Aliquots of drug (10 mg) were incubated in phosphate buffer solution  $10^{-3}$  M at pH 7.0. At scheduled time intervals, corresponding to the condition of the drug release experiments, the samples were withdrawn and assayed by High-Pressure Liquid Chromatography (HPLC), in order to determine the drug concentration. The HPLC conditions were a mixture of aqueous solution of ammonium acetate, methanol and acetonitrile (40/30/30, v/v/v). The pH of the aqueous mobile phase portion of ammonium acetate buffer (pH 7.0,  $10^{-3}$  M) was adjusted with glacial acetic acid. The mobile phase was filtered, degassed, and pumped isocratically at a flow rate of  $0.6 \text{ ml min}^{-1}$ ; UV detection at  $284 \text{ nm}^{84}$ . The HPLC analyses were carried out using a Jasco PU-2080 liquid chromatography equipped with a Rheodyne 7725i injector (fitted with a  $20 \mu\text{l}$  loop), a Jasco UV-2075 HPLC detector and Jasco-Borwin integrator. A reversed-phase C18 column ( $\mu\text{Bondapak}$ ,  $10 \mu\text{m}$  of  $150 \times 4.6 \text{ mm}$  internal diameter obtained from Waters) was used. Retention time 4.2 min; Limit of Detection (LOD)  $0.7 \mu\text{M}$ ; Limit of Quantification (LOQ)  $14 \mu\text{M}$ .

#### 2.5 Drug loading by soaking procedure

Incorporation of DC into CS-g-NIPAAm was performed as follows: 200 mg of preformed empty hydrogels were wetted with 2.0 ml in a concentrated aqueous

---

<sup>84</sup> Malliou, E.T.; Markopoulou, C.K.; Koundourellis, J.E. *J Liq Chromatogr Rel Technol.*, **2004**, *27*,1565–1577.



solution of drug (10 mg/ml). After 3 days, under slow stirring at 25°C, the microspheres were filtered and dried at reduced pressure in presence of P<sub>2</sub>O<sub>5</sub> to constant weight. The loading efficiency percent, LE (%), of all samples was determined by HPLC analysis of filtered solvent according to equation (2):

$$LE (\%) = \frac{C_i - C_0}{C_i} \times 100 \quad (2)$$

Here  $C_i$  was the concentration of drug in solution before the loading study,  $C_0$  the concentration of drug in solution after the loading study. The calculated LE (%) values of different copolymers are listed on Table II. In addition, the drug loaded percent, DL(%), in each matrix was calculated and the values were listed on Table II, according to equation 3:

$$DL(\%) = \frac{\text{Amount of drug in the beads}}{\text{Amount of beads}} \times 100 \quad (3)$$

## 2.6 *In vitro* release studies

### 2.6.1 *In vitro* release studies at 25°C and 40°C

Release studies were carried out using the dissolution method described in the USP XXIV (Apparatus 1-basket stirring element). Aliquots (10 mg) of drug-loaded microparticles were dispersed in flasks containing PBS solution (10<sup>-3</sup> M, pH 7.0) and maintained at 25.0±0.1 and 40.0±0.1°C in a water bath. At suitable time intervals, an aliquot of the release medium was withdrawn, filtered (Iso-Disc™ Filters PTFE 25-4 25mm x 0.45 µm, Supelco) and the solutions were analysed by HPLC.

### 2.6.2 *In vitro* pulsatile drug release from 25°C to 40°C

Oscillatory drug release profile of the materials was investigated by immersing the hydrogels in a solution at pH 7.0 (10<sup>-3</sup> M, PBS). The dissolution tube was

alternatively placed in thermostatic water baths at 25 and 40°C, respectively, and, at suitable time intervals, an aliquot of the release medium was withdrawn, filtered (Iso-Disc™ Filters PTFE 25-4 25mm x 0.45 µm, Supelco) and the solutions were analysed by HPLC. The release period was extended over several cycles until no further drug was released (6 hours). Two different experiments were performed: the first starting from 25°C and the second from 40°C. The larger temperature difference was used to help increase the speed of collapse, since DC is a small molecule.

### **3 Results and Discussion**

#### *3.1 Synthesis of thermo-responsive hydrogel*

Graft polymerization between the CS and a specific monomer was proposed to prepare CS-based thermo-responsive hydrogels. The synthesis of the hydrogels by grafting on deacetylated CS of NIPAAm, as functional monomer, using APS as radical initiator system, was reported. Polymer grafting reactions provide the potential for significantly altering the physical and mechanical properties of the starting materials. The reactive C-2 amino groups in chitosan chains were involved in macroradical formation and represent a suitable target groups to prepare composite materials showing both polysaccharides and grafting molecule characteristics. The radical reaction between the formed macromolecular reactive species and the acrylic monomer (NIPAAm) produces a hydrogel characterised by a network where the CS chains are linked by hydrocarbon bridges bearing isopropyl groups able to confer thermo-responsive behaviour to the material (Figure 4.1).

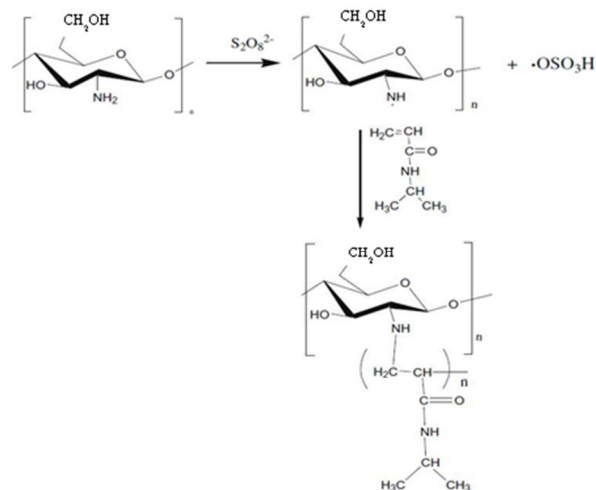


**Figure 4.1.** Schematic representation of thermo responsive CS-g-NIPAAm

Varying the amount of functional monomer in the polymerization feed, three different hydrogels were prepared, labelled P1-3, (Table I).

### 3.2 Characterization of hydrogels

The materials were characterized by FT-IR spectrophotometry, morphological analyses, thermal analyses and swelling behavior.

#### 3.2.1 FT-IR Spectroscopy

The FT-IR spectra of all samples showed the disappearance of bands at 944 and 921  $\text{cm}^{-1}$  ascribable to C-C double bond of NIPAAm. The insertion of the monomer in the polymeric networks was confirmed by the presence of the bands at 3270 (aminic groups), 2974 (hydrocarburic moieties), 1547  $\text{cm}^{-1}$  (amidic groups). Figure 4.2 reports on the FT-IR spectra of chitosan, NIPAAm and P1, respectively. Similar results were recorded for all the hydrogels.

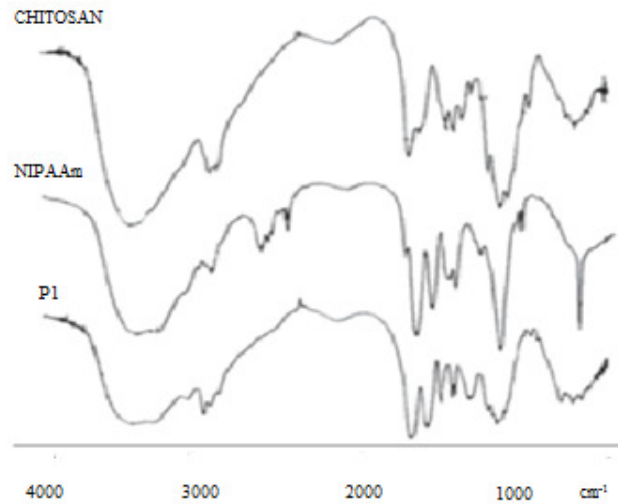


**Figure 4.2.** FT-IR spectra of chitosan, NIPAAm and CS-g-NIPAAm (P1)

### 3.2.2 Surface Morphology

Using scanning electron microscopy information about the surface properties of the hydrogels were obtained. Figure 4.3 showed as the outside surface of the samples was characterized by a high degree of porosity.

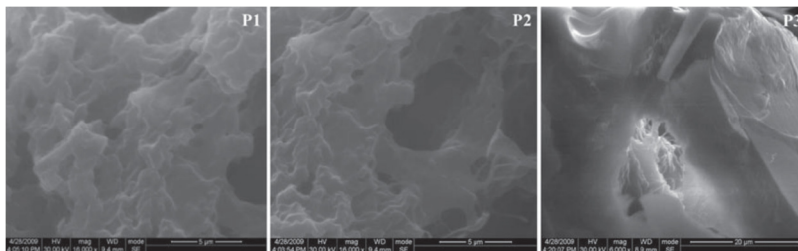


**Figure 4.3.** SEM thermo-responsive hydrogels surface

This feature is important in the design of a drug delivery system because of the presence of pores on the surface of the material determines an high specific surface area able to easily interact with the both drug and solvent molecules.

### 3.2.3 Thermal Analyses

Thermal analyses were performed on the swollen samples from 25 to 55°C and the LCST values were collected on Table I. These values were strictly dependent on the hydrophobic/hydrophilic balance in the polymerization feed and on the chemical and structural properties of hydrophilic monomer/crosslinker. The data indicate that all the copolymers are characterized by a LCST value higher than the pure PNIPAAm hydrogel (30°C)<sup>85</sup>. The increase of the LCST values of the crosslinked copolymers can be attributed to the increased hydrophilic/hydrophobic balance in the polymeric structure. Thermo-responsive behaviour of PNIPAAm hydrogel is strongly influenced by polymer-water affinity; at temperature below its LCST, the hydrophilic groups (amide groups) in the side chains of the PNIPAAm hydrogel interact with the water molecules by hydrogen bonds. However, as the external temperature increases, the copolymer-water hydrogen bonds are broken and the water molecules, rigidly structured around the polymer chains, gain more freedom degrees and can rapidly diffuse across the bulk phase. As a result, hydrogen bonds between solvent molecules in the continuous phase are formed; while, inside the polymeric network, hydrophobic interactions among the isopropyl groups become dominant. When hydrophilic groups are randomly inserted in the polymeric chains, polymer-water interactions significantly increase and more energy is required to destroy hydrogen bond, allowing solvent diffusion. The increase in the LCST recorded in CS-g-NIPAAm hydrogels can be attributed to the increased hydrophilic content with respect to the hydrophobic moiety, from P3 (w/w ratio CS/NIPAAm equal to 0.14) to P1 (w/w ratio CS/NIPAAm equal to 0.43) (Figure 4.4).

---

<sup>85</sup> Iemma, F.; Spizzirri, U.G.; Puoci, F.; Cirillo, G.; Curcio, M.; Parisi, O.I.; Picci, N. *Colloid. Polym. Sci.*, **2009**, 287,779–787.

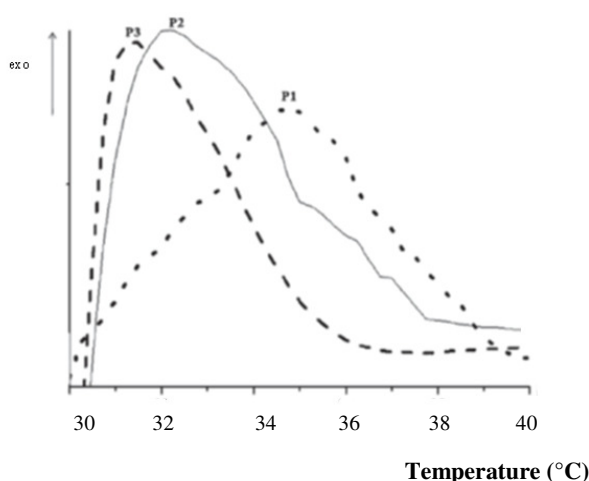


**Figure 4.4** DSC thermograms of the swollen stimuli responsive hydrogels P1 (....), P2 (\_\_\_\_) and P3 (\_\_\_) at a heating rate of 3°C/ min (the temperatures at the maximum points of the exotherms were referred as volume phase transition temperature of the hydrogels)

The insertion in the polymeric network of polysaccharide chains determines, in all the hydrogels, a steep increase in the transition temperature of the macromolecular system, strictly correlated to the CS amount in the polymerization feed. For the graft hydrogels the LCST values were recorded in the 34.8–31.4°C range.

#### 3.2.4 Swelling behaviour of hydrogels

Swelling behaviour of the hydrogels was investigated by determination of the values of contained water percentages in aqueous media (PBS solution pH = 7.0,  $10^{-3}$  M) at different temperatures between 15°C and 45°C (Figure 4.5). The data, reported in Table II, illustrate the water uptake (WR (%)) at 15°C and 45°C, in grams per gram of dry copolymer, for each composition. The thermo-responsive behaviour of the hydrogels was marked by the  $R_s$  parameter, calculated as the ratio between the WR (%) value at 15°C and 45°C. At 45°C, a considerable lowering of the water content was observed, due to the predominance of the

hydrophobic interactions between the pendant hydrophobic groups in the polymeric network.

**Table II.** Swelling and drug loading properties of the hydrogels

Hydrogel	Swelling behaviour		Drug loading parameters		
	WR (%) 15°C	WR (%) 45°C	$R_s$	LE%	DL%
P1	1230±11	392±9	3.1	95.2±0.3	9.7±0.1
P2	1302±10	207±3	6.3	97.8±0.2	9.8±0.1
P3	1756±12	202±3	11.4	98.0±0.3	9.9±0.1

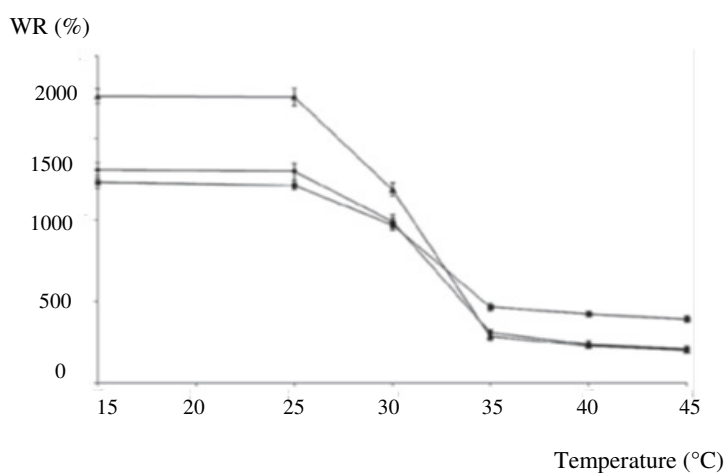


**Figure 4.5.** Swelling behaviour analyses of pH-responsive hydrogels in the 15–45°C temperature range (P1 (◆), P2 (■), P3 (▲))

Water-hydrogel affinity is improved by temperature decreasing to 15°C, and the swelling degree is greater depending on the crosslinking density of the hydrogels, due to the CS content in the polymerization feed. In particular, for the sample P-1, the WR (%) changed from 392% to 1230% ( $R_s = 3.1$ ) when the temperature decreases from 45°C to 15°C. Increasing the amount of monomeric specie in the polymerization bulk, the  $R_s$  values tend to be higher (2.1 and 3.7 times for P-2 and P-3, respectively) as a consequence of increased WR (%) difference between the experimental temperatures. Thus, it can be assumed that

the effect of the hydrogel crosslinking degree is predominant at 15°C, while the increase of the hydrophobic moieties (isopropyl groups), from P1 to P3, produces a more evident collapsed state of the hydrogels.

### 3.3 *In vitro* release studies

In order to estimate the ability of CS-g-NIPAAm hydrogels to act as drug delivery device, the matrices were loaded with diclofenac sodium salt (DC) by soaking procedure and the loading efficiency of all samples (LE %) was determined by HPLC analysis (Table II). The DC, one of non-steroid anti-inflammatory drug, shows therapeutic efficacy by means of pain relief, antifebrile and anti-inflammation and is widely applicable in rheumatic arthritis, osteoarthritis, spastic spondylitis, acute gout, and inflammation or gout of lesion after operation. When DC is orally administered for a long period of time, remarkable side effects were observed. In order to reduce such side effects, studies on the method of formulating DC into a site-specific matrix have actively been in progress. Stimuli responsive hydrogels offer the possibility to act as devices modulating the release of a therapeutic. The DC was loaded on the beads with a LE (%) > 95% for all copolymers in order to have DC-loaded matrix with a DC/carrier ratio (w/w) approximately equal to 0.1 (DL% in the 9.7-9.9% range), as reported on Table II. Considering the DSC analysis of drug, drug-loaded and unloaded hydrogels (Figure 4.6), the nature of the drug inside the polymer matrix can be assessed.

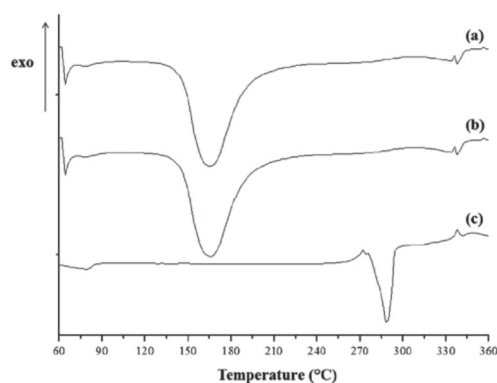


**Figure 4.6.** Differential scanning calorimetric thermograms of DS-unloaded P1 hydrogel (a) and DS-loaded P1 hydrogel (b) and pure DS (c). Analogous results have been found for all materials



This one may emerge in solid solution, metastable molecular dispersion or crystallization and may display relevant properties during *in vitro* release<sup>86</sup>. The onset melting peak of DC was observed at 288°C. However, no characteristic peak of DC was observed in the DSC curves of the drug-loaded hydrogels, suggesting that the drug is molecularly dispersed in the polymer matrix<sup>87</sup>.

Drug release profiles were determined by HPLC analysis and the amount of drug released was expressed as percentage of drug delivered ( $M_t$ ) related to the effectively entrapped total mass ( $M_0$ ), as a function of time at 25°C and 40°C. In figures 7 the release profiles were reported, in PBS solution (pH 7.0,  $10^{-3}$  M), at 25 and 40°C, for all compositions and a different release rate was recorded. The amount of drug molecules that moves from the polymeric beads to the surrounding media was higher at 40°C than 25°C for all microspheres, in each experimental time, and a shape rise at the first 30 minutes was noted at 40°C (burst effect), comparing to a slow increase at 25°C. This jump in the release profile was concerned as a result of rapid collapse of the hydrogel

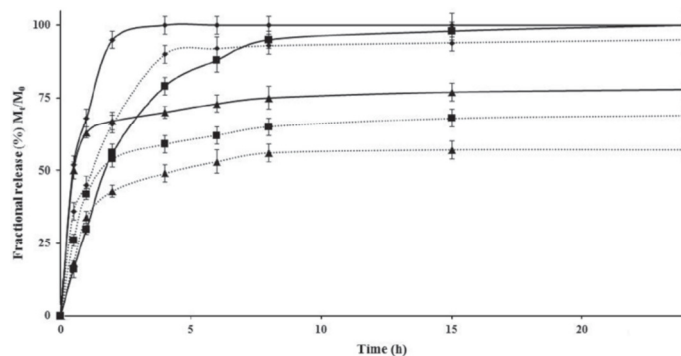


**Figure 4.7.** Drug release expressed as percent of DS delivered ( $M_t$ ) related to the effectively entrapped total dose ( $M_0$ ), as a function of time for microspheres P1 (◆), P2 (■) and P3 (▲) at 25°C (dashed lines) and 40°C (solid lines) and at pH 7.0 (PBS solution  $10^{-3}$  M)

<sup>86</sup> Cirillo, G.; Iemma, F.; Spizzirri, U.G.; Puoci, F.; Curcio, M.; Parisi, O.I. et al. *J Biomater Sci Polym.*, **2011**, 22, 823–844.

<sup>87</sup> Sairam, M.; Babu, V.R.; Vijaya, B.; Naidu, K.; Aminabhavi, T.M. *Int. J. Pharm.*, **2006**, 320, 131–136.

from swelled to shrank state. The drug release was basically determined by two factors, the swelling rate of polymer and the diffusivity of the drug through the network. When the dried gels are placed in the release media, water molecules diffuse into the gel network and the matrix swelled. At the same time, drug molecules diffuse through the gel layer and enter in the medium. When the polymers were at 40°C, above their LCST, the release behaviours were complex and not only diffusional effects of drug through the polymer network has to be considered, but also the squeezing effect of swelled polymer contributed to the apparent release rate. Drug release profiles recorded at different temperatures appear strictly depending on crosslinking degree of the polymeric networks that seems to influence both drug-matrix interaction and the diffusion of the water molecules. In particular, the hydrogel P1, containing the lower CS/NIPAAm w/w ratio (higher crosslinking degree), showed a more marked difference between the release profiles recorded at 25 and 40°C.

#### 3.4 Pulsatile drug release experiments

The reversible volume phase transition of the hydrogels was evaluated cyclically modifying the medium temperature and determining the drug release in each experimental condition. Pulsatile devices may have many applications in areas of medicine where a constant rate of drug release does not match the physiological requirements of the body. To demonstrate reversible on/off-switching of DC release, the microspheres were repeatedly heated above and cooled below their LCST in *in vitro* pulsatile release experiments and the release profiles were reported in Figure 4.8, as a function of the temperature cycling at fixed pH value (PBS solution  $10^{-3}$  M, pH 7.0). In these conditions, the release profiles during 6 hours were found to have good sustaining efficacy and the effect of temperature cycling on drug release may reflect a response rate to various environments. The experiments started placing the samples both in a swelling (25°C) and in a collapsed (40°C) state and recording the amount of DC released, expressed as  $M_t/M_0$  percent, in the surrounding environment after each temperature change. For all samples it can be observed a higher DC amount

released at 40°C versus 25°C. This behaviour is due to the strong hydrophobic interactions between the isopropyl groups of NIPAAm moieties, as the temperature reached the LCST, so that a significant amount of aqueous drug solution was dispelled from the collapsed hydrogels. As a consequence, exposing the DC-loaded samples to a temperature of 40°C, a significant burst effect was observed for all samples, with  $M_t/M_0$  percent values ranged from 25.0 to 45.0 % after 30 minutes. These percentages decrease to values between 5.0 and 15.0 % when the microspheres were initially placed to a temperature of 25°C. These results clearly confirmed that CS-g-NIPAAm hydrogels can be used to effectively modulate the release rate of the DC.

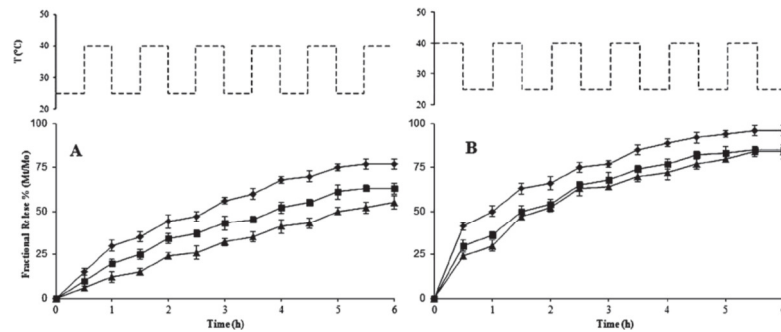


**Figure 4.8.** Temperature dependent stepwise DS release profile expressed as percent of drug delivered ( $M_t$ ) related to the effectively entrapped total dose ( $M_0$ ), as a function of time for microspheres P1 (◆), P2 (■) and P3 (▲) hydrogels first exposed to a temperature of 25°C (A) and 40°C (B), with alternating temperature between 25°C and 40°C at pH 7.0 (PBS solution,  $10^{-3}$  M)

#### 4. Conclusions

Novel thermo-sensitive hydrogels to be used as drug delivery devices were synthesized by free radical grafting reactions in presence of chitosan as biomacromolecules, N-isopropylacrylamide as thermo-responsive monomer and ammonium persulfate as initiator systems. The synthetic strategy was optimized by varying the amount of the thermo-responsive monomer in order to verify the effect of the hydrogel composition on the performance of the macromolecular system. The release experiments, performed at different temperature and the release profile was found to be effected by two factors, the swelling rate of polymer and the diffusivity of the drug through the network. Finally, to demonstrate reversible on/off-switching of DC release, the microspheres were repeatedly heated above and cooled below their LCST in *in vitro* pulsatile release experiments. The obtained results (a higher DC release at 40°C comparing to 25°C) clearly confirmed that the proposed hydrogels can be used to effective modulate the release rate of the DC.

## SECTION II

### BIOPOLYMER-ANTIOXIDANT CONJUGATES FOR BIOMEDICAL APPLICATIONS

#### 2.1. Antioxidant molecules as benefit agents for human health

Our body always reacts with oxygen when our cells produce energy and when we breathe. As a consequence of this activity, highly reactive molecules are produced. These molecules are known as free radicals and they are able to attack important cellular components such as DNA, or the cell membrane, with consequent oxidative damage to proteins, lipids and genes. The oxidative stress is involved in the development of many diseases, such as cancer, Parkinson's and Alzheimer's diseases, diabetes, atherosclerosis, heart failure and many other disorders.

To counter this problem, a valuable aid is represented by agents able to inhibit the oxidation of other molecules: the antioxidants.

Is possible classified the antioxidant molecules in two main groups:

- antioxidant enzymes (e.g. Super Oxide Dismutase (SOD), catalase and glutathione peroxidase);
- non-enzymatic antioxidants (e.g. e vitamin C, vitamin E, beta-carotene, catechin, quercetin, etc.).

An useful way to counteract the effects of free radicals is represent by the addition of antioxidants in the diet or by antioxidant supplements. Indeed, for example fruits and vegetables are good sources of antioxidants and several scientific studies have show that who eats these important sources, have a lower risk of heart disease and some neurological diseases, and also is evident that some types of vegetables and fruits protect against a number of cancers.

Among the antioxidant molecules, polyphenolic compounds (e.g. gallic acid, ellagic acid, etc...) which include also flavonoids (e.g. catechin, quercetin, etc...) are the most used to obtain functional products with high resistance to oxidative stress.

Flavonoids are among the substances most exploited for their antioxidant properties. Good sources of flavonoids include all citrus fruits, berries, tea (especially white and green tea), red wine and dark chocolate.

Several biological effects, such as anti-inflammatory, anti-ischaemic, anti-allergic and antitumoral activities, characterize this group of polyphenolic compounds, that result from their antioxidant properties and free radical scavenging ability. Moreover, flavonoids inhibit the action of several enzymes, including lipoxygenase, cyclooxygenase, monooxygenase, glutathione-S-transferase, phospholipase A2, and protein kinases. The antioxidant activities of flavonoids vary considerably depending upon the different backbone structures and functional groups. The position of hydroxyl groups and other features in the chemical structure of flavonoids are important for their antioxidant and free radical scavenging activities.

In the following works, that will be explored in *Chapter 5, 6 and 7*, major attention was focused on three antioxidants, and specifically on:

- Catechin (Figure 1 a) is the major flavonoid constituent present in green tea leaves. The prevention and treatment of a number of chronic diseases, including cardiovascular diseases and cancers are the most important positive benefits associated with this antioxidant compound although the mechanisms underlying their biological properties are not fully understood<sup>88</sup>.

In addition to antioxidant effects, green tea catechins have effects on several cellular and molecular targets in signal transduction pathways associated with cell death and cell survival. These effects have been

---

<sup>88</sup> Jeong, W-S.; Kong, A-N. T. *Pharmac. Biol.* **2004**, *42*, 84–93.

demonstrated in both neuronal cells and in tumor epithelial/endothelial cells;

- Quercetin, (Figure 1 b) which is one of the most abundant bioflavonoid present in fruit and vegetables, with proven beneficial effect on health<sup>89</sup>. It modulates the activity of several enzyme systems including cyclooxygenase, lipoxygenase, phosphodiesterase and tyrosine kinase. Much in vitro and some preliminary animal and human data indicate quercetin inhibits tumor growth<sup>90</sup>;
- Gallic acid (Figure 1 c) is a natural phenolic antioxidant extractable from several plants, such as green tea<sup>91</sup>. It is largely used in cosmetic, drugs and food to avoid rancidity, induced by lipid peroxidation, and spoilage.

Gallic acid may have a few health benefits especially for those at risk of certain types of cancers and neural disorders.

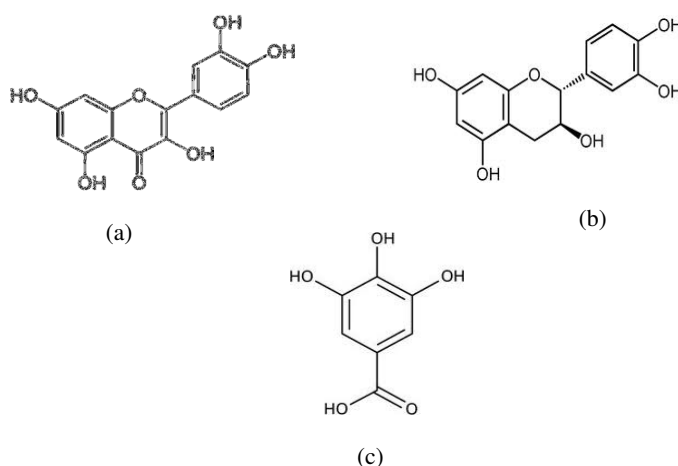


**Figure 1.** Chemical structure of: (a) Quercetin; (b) Catechin; (c) Gallic acid

<sup>89</sup> Kaur, C.; Kapoor, H.C.; *Int. J. Food Sci. Technol.*, **2001**, *36*, 703-725.

<sup>90</sup> Lamson, D.W.; Brignall, M.S. *Alter. Med. Rev.: J. Clin. Therap.*, **2000**, *5*, 196-208.

<sup>91</sup> Lu, Z.; Nie, G.; Belton, P.S.; Tang, H.; Zhao, B. *Neurochem. Int.*, **2006**, *48*, 263-274.

## 2.2 The help of antioxidants in several human disorders

### 2.2.1 Antioxidants in neurodegenerative diseases

Antioxidants are also able to prevent oxidative stress in neurons and prevent apoptosis and neurological damage.

For these reasons are also investigated as potential resources for the treatments of neurodegenerative diseases, such as Alzheimer's and Parkinson's diseases. Certain diseases of the brain and nervous system are thought to involve free radical processes and oxidative damage, either as a primary cause or as a consequence of disease progression<sup>92</sup>.

A significant amount of unsaturated fatty acids characterizes the nervous systems, as well as the brain, spinal cord and peripheral nerves.

The high lipid content of nervous tissue, coupled with its high aerobic metabolic activity, makes it particularly susceptible to oxidative damage<sup>93</sup>. Endogenous and dietary antioxidants molecules are able to protect nervous tissue from damage by oxidative stress, as documented from several in vitro studies<sup>94</sup>.

### 2.2.2 The role of antioxidants against Alzheimer's disease

Alzheimer's disease is a severe disease that leads to progressively worsening mental decline and ultimately death. This disease is manifested by impairment of memory and by disturbances in reasoning, planning, language, and perception.

Different hypotheses can explain the causes of the Alzheimer's disease; one of these is represents by an increase in the production of a  $\beta$ -amyloid protein in the brain that leads to nerve cell death. Moreover, the reduction of cholinergic neurotransmission, caused by acetylcholinesterase (AChE), which catalyzes the

---

<sup>92</sup> Gilgun-Sherki, Y.; Melamed, E.; Offen, D.; *Neuroph.*, **2001**, *40*, 959-975.

<sup>93</sup> Pratap Singh, R.; Sharad, S.; Kapur, S.; *JIACM*, **2004**, *5*, 218-225.

<sup>94</sup> Contestabile, A. *Curr. Top. Med. Chem.*, **2001**, *1*, 553-68.



cleavage of Acetylcholine in the synaptic cleft after depolarization, is another of the causes of the Alzheimer's disorder.

Several classes of antioxidant agents, such as polyphenols, have proven efficient in reducing or block neuronal death occurring in the pathophysiology of this disorder<sup>95</sup>.

In a study conducted by *Russo, et.al*<sup>96</sup>, it was found that black grape skin extract protected cells in a test tube from oxidative damage and DNA fragmentation when exposed to  $\beta$ -amyloid. Moreover, *Savaskan et.al*<sup>97</sup>, examined the red wine ingredient resveratrol, and found it to be neuroprotective against  $\beta$ -amyloid oxidative stress, again supporting an antioxidant mechanism.

### 2.2.3 The role of antioxidants against Parkinson's disease

Parkinson's disease is a degenerative disorder that involves the central nervous system. Underlying this disease occurs the death of dopamine-generating cells in the substantia nigra, a region of the midbrain; the cause of this cell death is unknown. Rigidity, slowness of movement and difficulty with walking are some of the major symptoms of this disorder. The drug therapy, employed for the Parkinson's disorder, is effective in managing symptoms but does not prevent, cure or slow down the progression of the disease.

It is interesting the role plays by neuroprotective therapies, represented for example by antioxidants molecule, that cause a slow progression of the disease because they can protect the cells that produce dopamine.

Free-radical toxicity may be the underlying cause of nigral cell deterioration in people with parkinson's disease<sup>98</sup>.

Several types of antioxidant are often used to prevent free radical toxicity. For example,  $\alpha$ -tocopherol (vitamin E) is a common free-radical scavenger that has

---

<sup>95</sup>Pasinetti, G.M.; Ho, L. *Nutrit. Diet. Suppl.*, **2010**.

<sup>96</sup> Russo, A.; Palumbo, M.; Aliano, C.; Lempereur, L.; Scoto, G.; Renis, M. *Life Sci.*, **2003**, *72*, 2369-2379.

<sup>97</sup> Savaskan, E.; Olivieri, G.; Meier, F.; Seifritz, E.; Wirz-Justice, A.; Müller-Spahn, F.; *Geront.*, **2003**, *49*, 380-383.

<sup>98</sup> Ciccone, D.C. *J. Amer. Phys. Ther. Assoc.*, **1998**, *78*, 313-319.

been considered a potential agent for delaying the progression of symptoms in people with Parkinson's disease<sup>99</sup>.

Another antioxidant group, known as lazaroids, is being considered for their neuroprotective effects<sup>100</sup>. These compounds appear to interact directly with oxygen-based free radicals and to prevent free-radical-induced damage to lipids and other structures<sup>101</sup>.

#### 2.2.4 The role of antioxidants against diabetes

Diabetes is a metabolic disorder characterized by hyperglycemia and in which the secretion or action of endogenous insulin is not enough.

Oxidative stress is one of the causes involved in the development of complications diabetes. Diabetes is usually accompanied by increased production of free radicals<sup>102</sup> or impaired antioxidant defenses<sup>103</sup>.

Indeed, an increase of amount of free radicals, and then the reduction of antioxidant defense mechanism, promote the development of insulin resistance. Several antioxidants, such as vitamins A, C and E, glutathione and several bioflavonoids, play an important role in countering diabetes. For example, vitamin E suppresses the propagation of lipid peroxidation; Vitamin C, inhibits hydroperoxide formation. Vitamins A and E scavenge free radicals<sup>104</sup>.

---

<sup>99</sup> Ebadi, M.; Srinivasan, S.R.; Baxi, M.D. *Prog Neurobiol.*, **1996**, *48*, 1-19.

<sup>100</sup> Zhao, M.; Richardson, J.S.; Mombourquette, M.J.; L'Veil, J.A. *Free Radic. Biol. Metab.*, **1995**, *19*, 21-30.

<sup>101</sup> Grasbon-Frodl, E.M.; Andersson, A.; Brundin, P.; *J. Neurochem.*, **1996**, *67*, 1653-1660.

<sup>102</sup> Baynes, J.W.; Thorpe, S.R. *Diab.*, **1999**, *48*, 1-9.

<sup>103</sup> Saxena, A.K.; Srivastava, P.; Kale, R.K.; Baquer, N.Z. *Biochem. Pharmacol.*, **1993**, *45*, 539-542.

<sup>104</sup> Laight, D.W.; Carrier, M.J.; Anggard, E.E. *Cardiovasc. Res.*, **2000**, *47*, 457-464.

### 2.3 Polymer-antioxidant conjugates

In recent years, various studies have focused attention on the realization of functionalized polymer products with antioxidant agents, for several applications in the fields of biomedical sciences.

The antioxidant functionalized polymers, for example, can enhance the quality and shelf life of pharmaceutical, cosmetic and nutraceutical products, when used as packaging or as coatings on packaging for oxygen sensitive materials.

The conjugation between antioxidant and polymers, in particular biopolymer, leads to the formation of organic compounds with beneficial health effects and no harmful effects. These interesting systems, indeed, can be used, for example, as preservative agents in food packaging or they could be cosmetic formulations, in order to avoid the oxidation of their component. Moreover, they can be applied in haemodialysis systems, by their introduction in dialysis membranes. Haemodialysis patients, indeed, are exposed to oxidative stress which contributes to cardiovascular disease and accelerated atherosclerosis, the major causes of mortality in these patients<sup>105</sup>.

Several advantages characterized polymer-antioxidant conjugates because from this interaction the resulting systems have the properties of the starting biopolymer (e.g. no toxicity, biocompatibility and biodegradability) and the activity of their conjugated molecules.

Among the many positive aspects:

- the conjugation of a polymeric system with antioxidant agent confers higher stability to the polymeric backbone, which will be less susceptible to degradation reactions;
- covalent bonds between polymer and antioxidant increase the stability of the latter respect the formulation in which the antioxidant is simply mixed with the other ingredients of the preparation;

---

<sup>105</sup>Calo, L.A.; Naso, A.; Pagnin, E.; Davis, P.A.; Castoro, M.; Corradin, R.; Riegler, R.; Cascone, C.; Huber, W.; Piccoli, A. *Clin. Nephrol.* **2004**, *62*, 355.

- synthetic strategies employed for the realization of these conjugates are often easily modulable and allow to operate in non-drastring conditions.

## 2.4 Synthesis of biopolymer-antioxidant by free radical polymerization reaction

In literature, several approaches were explored for the preparation of biopolymers coupled with antioxidant compounds and among these, the possibility to graft antioxidant molecules in a macromolecule by radical reaction<sup>106</sup>, represent an important procedure to realize polymeric matrices characterized by higher stability and slower degradation rate. The resultant conjugates combining the advantages of both the components, show higher stability and slower degradation rate than molecules with low molecular weight, but preserve the unique properties of antioxidant molecules<sup>107</sup>.

By covalent binding of active molecules onto the macromolecular backbone, grafting technique allows the formation of functional systems and is a versatile means to modify polymers.

Grafting reaction is generally carried out by chemical means and the initiators systems were often redox systems. There are different redox reagents in which radicals can be generated and relayed to the polymer so that the grafting reaction occurs<sup>108</sup>, such as: - Fenton's reagent ( $\text{Fe}^{2+}/\text{H}_2\text{O}_2$ ); -  $\text{Fe}^{2+}$ /persulphate ; - Persulfate and Reducing Agent (such as, sodium bisulphite, thiosulphate, or  $\text{Ag}^+$ ) ; -  $\text{Fe}^{2+}$ /Hydroperoxides ; - Direct oxidation by transition metal ions (e.g.  $\text{Ce}^{4+}$ ,  $\text{Cr}^{6+}$ ,  $\text{V}^{5+}$  and  $\text{Co}^{3+}$ ).

Ascorbic acid/hydrogen peroxide ( $\text{AA}/\text{H}_2\text{O}_2$ ) redox pair, as a biocompatible and water soluble radical initiator, was selected, to promote the free-radical

---

<sup>106</sup> Spizzirri, U.G.; Parisi, O.I.; Iemma, F.; Cirillo, G.; Puoci, F.; Curcio, M.; Picci, N. *Carbohydr. Polym.*, **2010**, *79*, 333–40.

<sup>107</sup> Puoci, F.; Iemma, F.; Curcio, M.; Parisi, O.I.; Cirillo, G.; Spizzirri, U.G.; Picci, N. *J. Agric. Food Chem.*, **2008**, *56*, 10646–50.

<sup>108</sup> Bhattacharya, A.; Rawlins, J.W, Ray, A. *Pol. Graf. Crosslink.*, **2009**.

polymerization reaction for the realization of three different antioxidant-biopolymer conjugates, which will be described in the subsequent chapters. The mechanism of reaction considered, which is the same for all conjugates synthesized, is very advantageous to preserving the antioxidant by degradation processes, because it does not occur the formation of toxic reaction by-product and since the reaction takes place at room temperature, avoiding the degradation of the antioxidant. In particular, the hydroxyl radicals, generated by the interaction between redox pair components (Figure 2), are able to attack the sensible residues in the side chains of biopolymer employed, producing radical species on the polymer structure and inducing an antioxidant-biopolymer covalent bond.

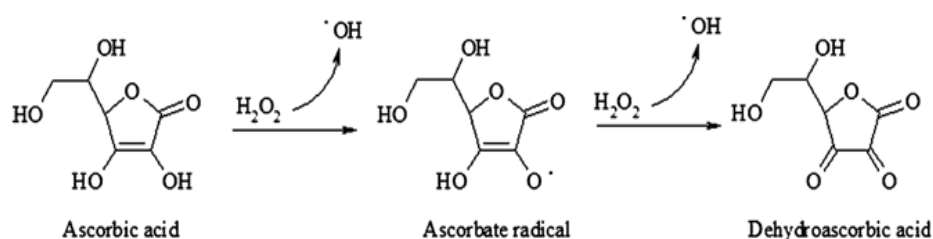


**Figure 2.** Schematic representation of ascorbic acid/hydrogen peroxide redox pair's radical initiator system

Therefore, the interaction between AA/H<sub>2</sub>O<sub>2</sub> redox pair, promotes the formation of the radical species on the biopolymer backbone and thus the covalent conjugation between the biopolymer and the antioxidant molecules employed (Figure 3).

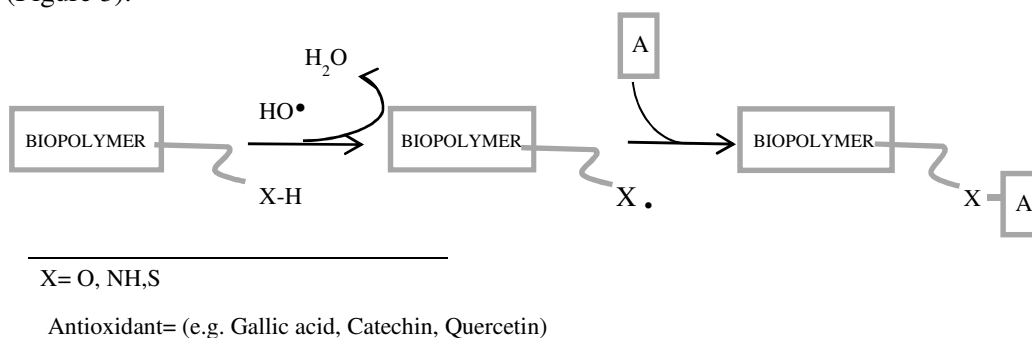


**Figure 3.** Schematic representation of biopolymer-antioxidant conjugate

On the basis of this interesting mechanism of grafting reaction, three different antioxidant bioconjugates were realized as potential "health functional products", with prospective application in pathologic conditions (e.g Alzheimer's, Parkinson's disease and diabetes) or , when used in pharmaceutical formulations, to prevent the degradation of a drug. In literature is confirmed that in all these pathological conditions, the inhibition of specific enzymatic pathways by plants polyphenols play a positive role in overcoming the disease<sup>109</sup>. For this reason, several enzymatic tests were performed, such as, cholinesterase inhibitory assay and  $\alpha$ -amylase inhibitory activity, to test the action of the bioconjugates realized against, respectively, Alzheimer and diabetes diseases. Moreover, antioxidant assays, such as the determination of scavenging effect on the DPPH radical or the  $\beta$ -Carotene-linoleic acid test, were verified, in order to confirm the antioxidant activity of the systems realized. Synthesis, characterizations and biological studies of these functional antioxidant conjugates will be described in detail in the following chapters.

---

<sup>109</sup> Morell, M.K.; Myers, A.M. *Curr. Opin. Plant Biol.*, **2005**, 8, 204–10.

## Chapter 5

### INNOVATIVE ANTIOXIDANT THERMO-RESPONSIVE HYDROGELS BY RADICAL GRAFTING OF CATECHIN ON INULIN CHAIN

#### 1. Introduction

Polymeric-antioxidant systems represent a useful reality in biomedical field, because they can play an important role when are applied as packaging or as coatings on packaging for oxygen sensitive formulations. Pharmaceutical and cosmetic formulations and foodstuffs may be exposed to tough conditions during processing, including chemical and physical causes.

In the foodstuffs, for example, oxidative reactions cause damage to lipids and proteins thereby influencing food quality.

To improve food preservation and to realize new food products and packaging, a useful aid derives from polymeric-antioxidant systems.

The use of antioxidants, indeed, is the most common approach to increase the oxidative stability of foods<sup>110</sup>.

It is even more interesting the possibility to promote the conjugation between natural polymer and antioxidant molecules, because the resulting system have the properties of the starting biopolymer (e.g. biocompatibility, biodegradability and no-toxicity) and the activity of their conjugated molecules.

In literature, several approaches were explored for the preparation of biopolymers coupled with antioxidant compounds and among these, the possibility to graft antioxidant molecules in a macromolecule by radical reaction<sup>111</sup>, represent an important procedure to realize polymeric matrices characterized by higher stability and slower degradation rate.

---

<sup>110</sup>Decker, E.A. *Trends Food Sci. Technol.* **1998**, *9*, 241–248.

<sup>111</sup>Spizzirri, U.G.; Parisi, O.I.; Iemma, F.; Cirillo, G.; Puoci, F.; Curcio, M.; Picci, N. *Carbohydr.Polym.*, **2010**, *79*, 333–40.

The possibility to graft antioxidant moieties in a polysaccharide structure, by radical procedure, represents an interesting innovation that significantly improves the performance of the biomacromolecules, opening new applications in the biomedical and pharmaceutical fields.

The possibility of imparting some of the attractive properties of the molecule used for grafting to a selected macromolecule is the main goal of graft copolymerization.

With the aim to realize a novel material useful in the optimization of food preservation, in this study a new polysaccharide-based hydrogel, with thermo-responsive and antioxidant properties, has been developed with the possible application, in addition, in all the field in which a consistent reduction of oxidative stress is required, to prevent thermal degradation of formulation, minimizing the oxidative damage depending of the temperature of the surrounding medium.

In particular, the inulin backbone, selected as natural polymer, which has a multitude of characteristics beneficial to functional foods, has been functionalized with the antioxidant molecules catechin and the thermo-responsive monomer NIPAAm, by free-radical polymerization reaction, employing AA/H<sub>2</sub>O<sub>2</sub> redox pair, to promote the free-radical polymerization reaction. Thermo-responsive antioxidant hydrogels were characterized by FT-IR spectroscopy, swelling behaviour, DSC, UV-Vis and fluorescence analyses. Furthermore, the analysis of the antioxidant activity of the hydrogels, in relation to the temperature of the surrounding medium, was verified by the determination of scavenging activity on DPPH radicals and the evaluation of total flavonoid content.

## **2 Experimental Section**

### *2.1 Materials*

Inulin from Dahlia tubers (MW ~5.000), N-isopropylacrylamide (NIPAAm), N,N'-ethylenebis(acrylamide) (EBA), (+)-catechin hydrate (CA), hydrogen



peroxide ( $\text{H}_2\text{O}_2$ ), ascorbic acid (AA), 2,2'-diphenyl-1-picrylhydrazyl radical (DPPH), sodium nitrite, aluminium chloride hexahydrate, sodium hydroxide and orthophosphoric acid were obtained from Sigma-Aldrich (Sigma Chemical Co., St Louis, MO, USA). Ethanol, methanol and water were reagent grade or HPLC-grade and provided by Carlo Erba reagents (Milan, Italy).

## 2.2. Instrumentation

The absorption spectra were measured on Jasco V-530 UV-Vis spectrophotometer and for measurement of the absorption spectra of the solid state samples, the diffuse reflectance spectra were recorded on the same instrument equipped with an integrating sphere accessory (Jasco ISN-470). The solid samples were placed between quartz plates ( $200\text{ mm}^2$ ). The corrected emission spectra, all confirmed by excitation ones, were recorded with a Perkin Elmer LS-55 Luminescence spectrometer, equipped with Hamamatsu R928 photomultiplier tube. The fluorescence spectra in the solid state were recorded by using the front face accessory. The solid sample were placed between quartz plate ( $200\text{ mm}^2$ ) on the sample holder. The liquid chromatography consisted of an Jasco BIP-I pump and Jasco UVDEC-100-V detector set at 210 nm. A 250mm $\times$ 4mm C-18 Hibar<sup>®</sup> Column, particle size 5 $\mu\text{m}$  (Merck, Darmstadt, Germany) was employed. As reported in literature the adopted mobile phase was methanol/water/orthophosphoric acid (20/79.9/0.1) and run isocratically at a flow rate of 1.0 mL min<sup>-1</sup>. The column was operated at 30°C. The sample injection volume was 20  $\mu\text{L}$ . Freeze drier Micro Modulyo, Edwards was employed. Calorimetric analyses were performed employing a Netzsch DSC200 PC. The Scanning electron microscopy (SEM) photographs were obtained with a Jeol JSMT 300 A; the surface of the samples was made conductive by deposition of a gold layer on the samples in a vacuum chamber.

### 2.3. Synthesis of antioxidant thermo-responsive hydrogels

The synthesis of antioxidant thermo-responsive hydrogels, by employing ascorbic acid/hydrogen peroxide redox pair as initiator system, was carried out as follows: in a 25 ml glass flask, inulin (Figure 5.1a) was dissolved in 6 mL of distilled water and then NIPAAm (Figure 5.1b), EBA (Figure 5.1c) and CA (Figure 1d) were added (Table I). Finally, 1 mL of 1.0 M H<sub>2</sub>O<sub>2</sub> and 0.054 g of ascorbic acid were introduced into the reaction flask and the mixture was maintained at 25°C for 24 h under atmospheric air. The obtained hydrogels were washed with distilled water, frozen and dried with “freezing-drying apparatus” to afford vaporous solids. Hydrogels were checked to be free of unreacted antioxidant and any other compounds by HPLC analysis after purification step. Blank thermo-responsive hydrogels, that act as control, were prepared in the same reaction conditions but in the absence of antioxidant agent.

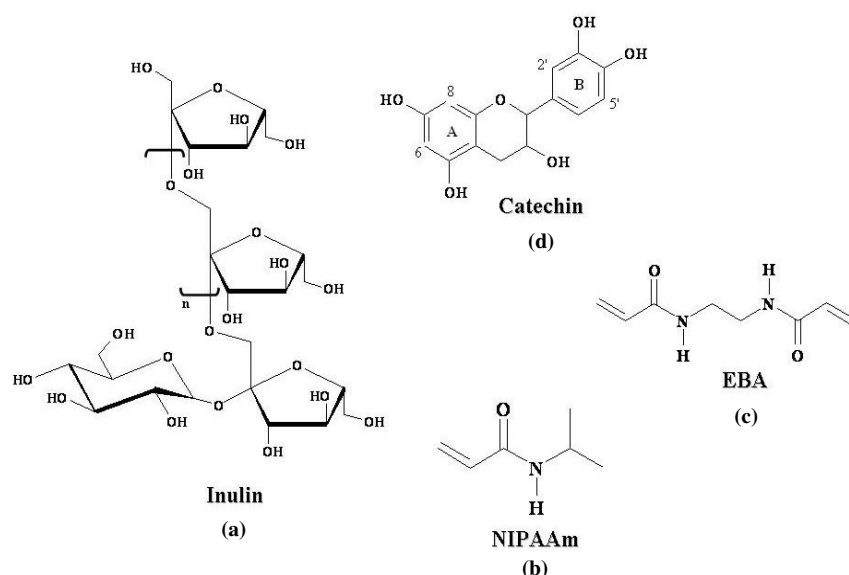


**Figure 5.1.** Chemical structure of (a) Inulin; (b) NIPAAm; (c) EBA; (d) Catechin

**Table I.** Polymerization feed composition of thermo-responsive antioxidant hydrogels

Hydrogel Code	Inulin (mg)	NIPAAm (mg/mmol)	EBA (mg/mmol)	CA (mg/mmol)
I-B	250	500/4.42	100/0.88	-
I-CA	250	500/4.42	100/0.88	50/0.17
II-B	500	500/4.42	100/0.88	-
II-CA	500	500/4.42	100/0.88	50/0.17

Initiator system: H<sub>2</sub>O<sub>2</sub> (1 mL 1.0 M); ascorbic acid (0.054 g/0.03 mmol)

## 2.4 Characterization of antioxidant thermo-responsive hydrogels

### 2.4.1 Calorimetric analysis

In a standard procedure for the determination of the transition temperature of antioxidant thermo-responsive hydrogels (Table II), the sample was immersed in distilled water at room temperature for at least 2 days and allowed to reach the equilibrium state. Then, about 10 mg of the swollen sample were placed inside a hermetic aluminum pan and sealed tightly by a hermetic aluminum lid. The thermal analyses were performed in the range of temperature from 25 to 55°C with a heating rate of 3°C min<sup>-1</sup> on the swollen hydrogel samples under a dry nitrogen atmosphere with a flow rate of 25 mL min<sup>-1</sup>. In order to verify the covalent insertion of CA, about 6.0 mg of dry sample was placed in a hermetic aluminum pan and then sealed. In this case, the thermal analyses were performed from 25°C to 400°C under a dry nitrogen atmosphere with a flow rate of 25 mL min<sup>-1</sup> and a heating rate of 5°C min<sup>-1</sup>.

### 2.4.2 Water content measurement

Aliquots (40–50 mg) of the polymeric particles dried to constant weight were placed in a tared 5-mL sintered glass filter (Ø10 mm; porosity, G3), weighted, and left to swell by immersing the filter plus support in a beaker containing the swelling media (PBS solution, pH 7.0, at 25°C and 45°C). After 24 h, the excess water was removed by percolation at atmospheric pressure. Then, the filter was placed in a properly sized centrifuge test tube by fixing it with the help of a bored silicone stopper, then centrifuged at 3500 rpm for 15 min and weighted. The filter tare was determined after centrifugation with only water. The weights recorded were averaged and used to give the water content percentage (WR %) by the following equation (1):

$$WR\% = \frac{W_s - W_d}{W_d} \times 100 \quad (1)$$

where  $W_s$  and  $W_d$  are weights of swollen and dried polymeric particles, respectively. Each experiment was carried out in triplicate.

## 2.5 Evaluation of the antioxidant activity

### 2.5.1 Scavenging activity on DPPH radicals

Synthesized thermo-responsive antioxidant-inulin conjugate was allowed to react with a stable free radical, 2,2'-diphenyl-1-picrylhydrazyl radical (DPPH), with the aim of evaluating the free radical scavenging properties of these materials. For this purpose, 25 mg of each polymer were dispersed in 1 mL of distilled water in a volumetric flask (25 mL). The samples were incubated in a water bath at 25°C and 45°C respectively and allowed to stand for 16 h. Then, maintaining these temperature conditions, 4 mL of ethanol and 5 mL of ethanol solution of DPPH (200 µM) were added obtaining a solution of DPPH with a final concentration of 100 µM. After 10 min, the absorbance of the remaining DPPH was determined colorimetrically at 517 nm. The same reaction conditions

were applied on the blank hydrogels in order to evaluate the interference of polymeric material on DPPH assay. The scavenging activity of the tested materials was measured as the decrease in absorbance of the DPPH and it was expressed as percent inhibition of DPPH radicals calculated according the following equation (2):

$$\text{inhibition \%} = \frac{A_0 - A_1}{A_0} \times 100 \quad (2)$$

where  $A_0$  is the absorbance of a standard that was prepared in the same conditions, but without any polymers, and  $A_1$  is the absorbance of polymeric samples. The antioxidant activity was expressed as a percentage of scavenging activity on hydroxyl radical, according to equation (2). Each measurement was carried out in quintuplicate, and data were expressed as means ( $\pm$ SEM) and analyzed using ANOVA.

#### 2.5.2 Determination of total flavonoid content

A slightly modified version of the spectrophotometric method was used to determine the flavonoid contents of samples. Briefly, in a test tube 20 mg of each polymer were dispersed in 2 mL of distilled water and allowed to stand for 16 h, respectively at 25°C and 45°C. Then, maintaining these temperature conditions, 150  $\mu$ L of a 5% NaNO<sub>2</sub> solution were added followed, after 6 min, by addition of 300  $\mu$ L of a 6% AlCl<sub>3</sub> · 6H<sub>2</sub>O solution. After another 5 min 1 mL of 1 M NaOH was added, the mixture was brought to 5 mL with distilled water and mixed well. The absorbance was measured immediately at 510 nm against a control prepared using the blank polymers under the same reaction conditions. The amount of total flavonoids in the hydrogels was expressed as mean (micrograms of catechin equivalents per gram of polymer)  $\pm$  SD for five replications, by using the equation obtained from the calibration curve of the antioxidant. This one was recorded by employing five different catechin

standard solutions with the same procedure. The final concentrations of catechin in the test tubes were 10, 25, 50, 75, 100  $\mu\text{M}$ , respectively.

### 3 Results and Discussion

#### 3.1 Synthesis of antioxidant thermo-sensitive network

Inulin, because of its biodegradability and biocompatibility properties, was chosen as polymer backbone to be functionalized with CA, to obtain macromolecular system showing raised antioxidant properties for food and food packaging applications. In addition, the presence in the polymerization feed of NIPAAm and EBA, as stimuli-responsive monomer and crosslinker respectively, allows to synthesize a polymeric network able to modulate their antioxidant properties in response to the temperature of the surrounding environment. The employed synthetic strategy involved the use of the ascorbic acid/hydrogen peroxide redox pair, a biocompatible and water soluble system, as radical initiators. Comparing to conventional initiator systems, like azo compounds, which require relatively high reaction temperature to ensure their rapid decomposition, the aforementioned redox pair shows several advantages. First of all, this kind of system does not generate toxic reaction products; moreover, it is possible to perform the reaction processes at room temperatures, to avoid antioxidant degradation<sup>112</sup>. On the other hand, to activate inulin toward radical reactions and, thus, to promote the insertion of antioxidant molecules (avoiding self-reactions), radical initiators should preferably react with the macromolecule before adding CA. A possible mechanism to synthesize antioxidant thermo-sensitive hydrogels is proposed in Figure 5.2. The hydroxyl radicals, generated by the interaction between redox pair components, attack the sensible residues in the side chains of polysaccharide chain, producing radical species on the sugar structure. These ones react with the antioxidant molecules

---

<sup>112</sup> Kitagawa, M.; Tokiwa, Y. *Carbohydr. Polym.*, **2006**, *64*, 218–223.

inducing an antioxidant-inulin covalent bond. Literature data suggests that on the phenolic ring free radical species attack at the ortho- and para-positions relative to the hydroxyl group<sup>113</sup>. This findings support the hypothesis that the binding sites involved in the antioxidant-sugar conjugation are the positions 2' and 5' (B ring) and 6 and 8 (A ring) for CA (Figure 5.1d). The heteroatom-centered radicals in the side chains of inulin preferentially react in some of the above-mentioned positions.

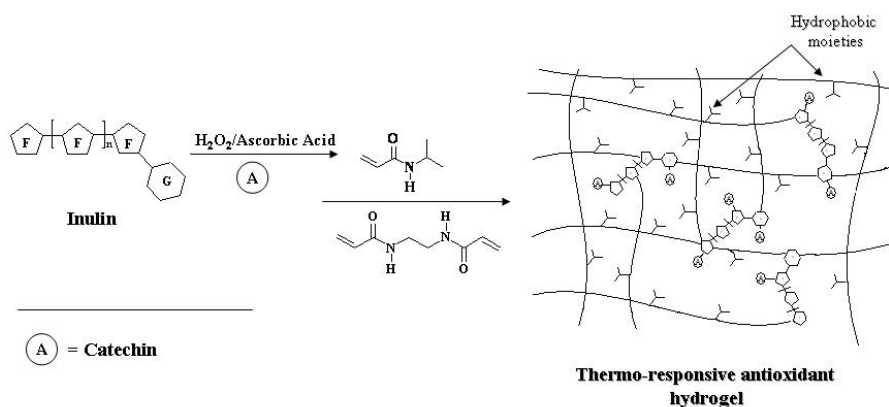


**Figure 5.2.** Schematic representation of the synthesis thermo-responsive antioxidant-inulin conjugate

The proposed synthetic strategy permits to prepare two biomacromolecular networks with antioxidant activity labelled I-CA and II-CA, respectively, as reported in Table I. The inulin was functionalized with CA by introducing in the reaction feed 0.68 mmol antioxidant per grams of carbohydrate for hydrogel I-CA and 0.34 mmol per grams of inulin for II-CA and the macromolecular moieties were chemically inserted in a polymeric structure built using a molar ratio NIPAAm/EBA equal to 5.0 for all formulations. To remove unreacted antioxidant and monomers, physically incorporated in the carbohydrate structure, the hydrogels were extensively washed with water and washing media were analyzed by HPLC. Finally the hydrogels were frozen and dried with freez-

<sup>113</sup> Kobayashi, S.; Higashimura, H. *Prog. Polym. Sci.*, **2003**, 28, 1015–1048.

drier to obtain a porous and vaporous solid extensively characterized. Blank thermo-responsive hydrogels, that act as control, were prepared in the same reaction conditions but in the absence of antioxidant agent.

### **3.2 Characterization of antioxidant thermo-responsive hydrogel**

The materials the respective control polymers were characterized by Fourier Transform IR spectrophotometry, UV-Vis, thermal analyses, morphological analyses and fluorescence analyses.

#### *3.2.1 FT-IR Spectroscopy*

The FT-IR spectra of both I-CA and II-CA conjugates shown the appearance of new peaks at 1557 and at 1525  $\text{cm}^{-1}$ , respectively, awardable to carbon to carbon stretching within the aromatic ring of catechin. The incorporation of the monomers in the hydrogels was confirmed by Fourier transform infrared spectroscopy. The FT-IR spectra of thermo-responsive hydrogels show the disappearance of bands at 990-918 and 980-954  $\text{cm}^{-1}$ , awardable to C-C double bounds of NIPAAm and EBA confirming the absence of unreacted monomers in the polymeric networks. In addition, the characteristic absorption bands of all the reagents in the polymerization feed are evident: 3280 (stretching vibrations of NH of amidic comonomers); 2940 (C-H stretching of  $\text{CH}_3$ ,  $\text{CH}_2$  and CH groups); 1647  $\text{cm}^{-1}$  (C=O stretching amidic groups of NIPAAm and EBA).

#### *3.2.2 UV-vis analyses*

UV-vis spectra of antioxidants and conjugate hydrogels show covalent bond formation between antioxidant moieties and polymeric backbone. In the spectrum of conjugates, the presence of two absorption peak at 278 and 327 nm in the aromatic region is related to the presence of CA covalently bonded to the polymeric network. In addition, in the free antioxidant the wavelength of the



aromatic peaks appear at 229 and 275 nm, lower than grafted hydrogels, as depicted in Figure 5.3.

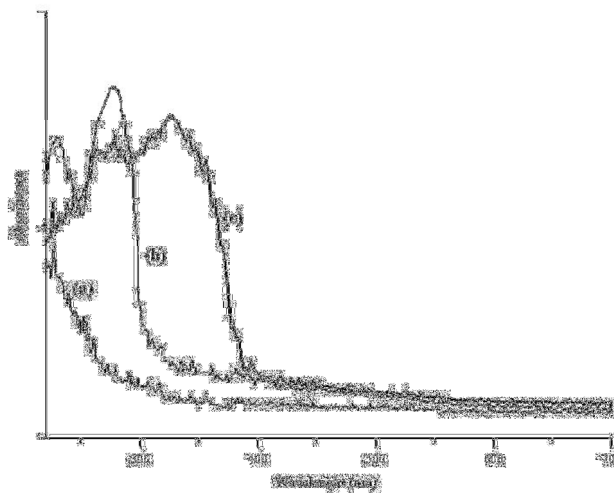


**Figure 5.3.** UV-Vis spectra of II-B (a), CA (b) and II-CA (c)

### 3.2.3 Thermal analyses

Thermal characterization of prepared conjugates was performed by recording of DSC thermograms of dried antioxidant hydrogel (I-CA and II-CA)), blank hydrogel (I-B and II-B), and pure antioxidants (CA), as depicted in Figure 5.4. As far as DSC of I-B and II-B is concerned, a broad endothermic peak, located around 50–140°C, was recorded;  $\Delta H_f$  associated to this transition was respectively 191.4 and 295.2 J per grams of blank hydrogel. The calorimetric analysis of pure CA shows a melting endotherm at 155.8°C. Since the grafting of CA produces structural modification onto the polysaccharide chains, in the DSC thermogram of antioxidant hydrogels marked differences appear.

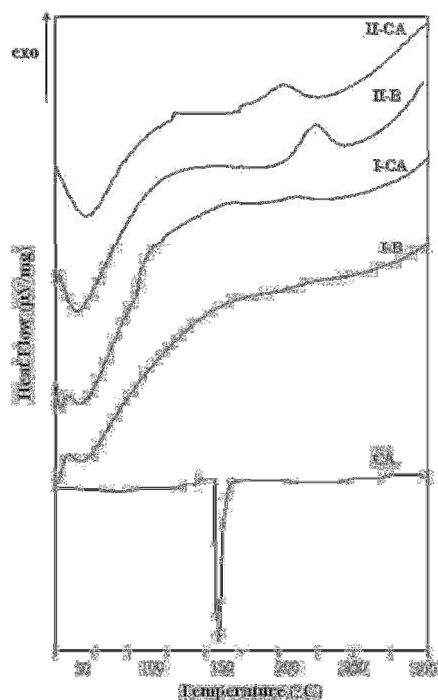


**Figure 5.4.** Calorimetric analyses of and thermo-responsive antioxidant hydrogels (I-CA, II-CA), pure antioxidant (CA) and blank hydrogels (I-B, II-B)

The calorimetric analysis displays the absence of melting endotherm of CA, while, the  $\Delta H_t$  value associated to the glass transition in the conjugate was 399.3 and 570.3 J per grams of grafted hydrogel for I-CA and II-CA, respectively, probably as consequence of more rigidity of polymeric chains. This discrepancy suggests that the glass transition of hydrogel I-CA needs 109% more heat respect to unmodified polysaccharide, while the transition of hydrogel II-CA needs 94% more heat respect to II-B. Thermal analyses were performed on the swollen samples from 25°C to 55°C and the LCST values were collected on Table II. These values were strictly dependent on the hydrophobic/hydrophilic balance in the polymerization feed and on the chemical and structural properties of hydrophilic monomer/crosslinker. The data indicate that all the copolymers are characterized by a LCST higher than the pure PNIPAAm hydrogel<sup>114</sup> as

<sup>114</sup> Geever, L.M.; Devine, D.M.; Nugent, M.J.D.; Kennedy, J.E.; Lyons, J.G.; Hanley, A. Higginbotham, C.L. *Eur. Polym. J.*, **2006**, *42*, 2540.

consequence of the increased hydrophilic/hydrophobic balance in the polymeric structure (Figure 5.5). Thermo-responsive behaviour of PNIPAAm hydrogel is strongly influenced by polymer-water affinity; at temperature below its LCST, the hydrophilic groups (amide groups) in the side chains of the PNIPAAm hydrogel interact with water molecules by hydrogen bonds. However, as the external temperature increases, the copolymer-water hydrogen bonds are broken and the water molecules, rigidly structured around the polymer chains, gain more freedom degrees and can rapidly diffuse across the bulk phase. As a result, hydrogen bonds between solvent molecules in the continuous phase are formed; while, inside the polymeric network, hydrophobic interactions among the isopropyl groups become dominant.

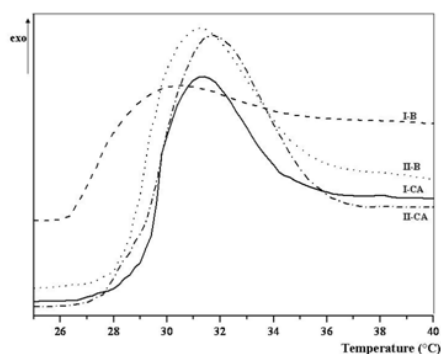


**Figure 5.5.** DSC thermograms at a heating rate of 3°C/min of the blank hydrogels (I-B, II-B), and conjugates (I-CA, II-CA)

When in the polymeric chains hydrophilic groups are randomly inserted, polymer-water interactions significantly increase and more energy is required to destroy hydrogen bond, allowing solvent diffusion. The transition temperatures of the thermoresponsive hydrogels ranged from 30.5 and 33.1°C. The insertion of antioxidant moieties in the polymeric backbone, by modification of hydrophilic/hydrophobic balance of the network, produces an increase of the

transition temperature in respect to the blank polymer of 0.8°C for hydrogel I-CA and 1.9°C for II-CA.

**Table II.** Transition temperature and swelling behaviour of thermo-responsive antioxidant hydrogels

Sample	LCST (°C)	WR (%)		
		25°C	45°C	S <sub>r</sub>
<b>I-B</b>	30.5±0.1	592±5	359±4	1.1
<b>I-CA</b>	31.3±0.2	558±4	450±2	1.3
<b>II-B</b>	31.2±0.2	656±3	380±3	1.8
<b>II-CA</b>	33.1±0.1	818±6	377±3	2.2

### 3.2.4 Surface Morphology

Using scanning electron microscopy, information about the surface properties of the microparticles were obtained. Figure 5.6 clearly depicts the outside surface of the antioxidant thermo-responsive hydrogels I-CA and II-CA, characterized by a high porosity suitable for a rapid swelling/deswelling associated with temperature changes.

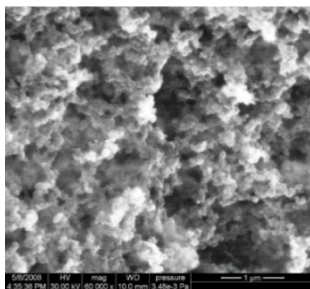


**Figure 5.6.** SEM micrograph of outside surface of conjugate I-CA

### 3.2.5 *Water content measurement*

Investigation of the water affinity of the hydrogels was carried out by studying their swelling behaviour in media (PBS solution  $10^{-3}$  M) at 25 and 45°C and the results are reported in Table II. The data illustrate the water uptake, in grams per gram of dry copolymer, for each studied composition, and the ratio between the swelling at 25°C and 45°C at fixed pH values ( $S_r$ ) was reported for all samples. The materials showed different water affinity at 25 and 45°C due to the pendant hydrophobic groups in the polymeric chains. In particular, at 45°C, there is a considerable lowering of the water content, due to solvent diffusion outside the polymeric network and to resultant hydrophobic interactions between hydrocarbon moieties on the polymeric chains as illustrated in the Figure 5.2. When the temperature decreases to 25°C, below the transition temperature of the hydrogels, the water content is greater than that found at 45°C for all copolymers and the  $S_r$  values ranged from 1.1 to 1.8 for I-B and II-B and from 1.3 to 2.2 for I-CA and II-CA.

## 3.3 Evaluation of the antioxidant activity

### 3.3.1 *Scavenging activity on DPPH radicals*

The DPPH radical is a stable organic free radical with an absorption maximum band around 515–528 nm and thus, it is a useful reagent for evaluation of antioxidant properties of compounds. In the DPPH assay, the antioxidant reduce the DPPH radical to a yellow-colored compound, diphenylpicrylhydrazine, and the extent of the reaction will depend on the hydrogen donating ability of the antioxidant. Conjugates scavenger ability were evaluated in term of DPPH reduction using catechin as reference compound and data are expressed as inhibition (%). As reported in Table III, in experimental conditions, antioxidant polymers showed a scavenging activity strictly correlated to the experimental temperature and to the crosslinking degree of the hydrogels. In particular, DPPH

reductions of 74% was recorded for conjugate I-CA in the swollen state at 25°C, while the same hydrogel produce in the shrunken state at 45°C a DPPH reduction of 55%.

**Table III.** Inhibition (%) of DPPH radical and total flavonoid content of thermo-responsive antioxidant hydrogels

Sample	Inhibition of DPPH Radical (%)		Total Flavonoid Content (mg/g)	
	25°C	45°C	25°C	45°C
I-B	22±2	12±1	0	0
I-CA	74±3	55±2	3.73±0.05	1.63±0.02
II-B	32±2	21±1	0	0
II-CA	80±3	25±1	4.85±0.07	3.67±0.03

Increasing the amount of inulin in the polymerization feed (hydrogel II-CA) remarkable differences of DPPH reduction between the swollen (80%) and the shrunken (25%) states were recorded.

### 3.3.2 Determination of total flavonoid content

It has frequently been reported that both phenolic and flavonoids compounds are closely associated with antioxidant activity<sup>115</sup>. Thus, AlCl<sub>3</sub> assay was employed to have a direct determination of the total flavonoid content, expressed as mg of CA per g of hydrogel. By comparing the obtained data with the CA calibration curve, the amount of catechin equivalent at different temperatures around the transition temperature was determined. In particular, for the conjugates I-CA and II-CA these values in the swollen state were 3.73 mg/g and 4.85 mg/g of

<sup>115</sup> Dewanto, V.; Wu, X.; Adom, K.K.; Liu, R.H. *J. Agric. Food Chem.*, **2002**, *50*, 3010–3014.

hydrogels, while the recorded total flavonoid content in the shranked state were 1.63 mg/g and 3.86 mg/g for I-CA and II-CA, respectively (Table III).

#### **4 Conclusions**

The synthetic procedure proposed in this paper involves one pot reaction consisting of direct polymerization of the inulin with an antioxidant molecule in the presence of a thermo-responsive comonomer and a crosslinking agent to obtain hydrogels with modulable antioxidant properties depending of the external temperature. In particular, CA was chosen as antioxidant agent and the insertion of the reactive species onto the networks was confirmed by FT-IR. In addition, the covalent bond between the carbohydrate chain and the antioxidant was confirmed by calorimetric, UV-vis and fluorescence analyses. The thermal analyses of the hydrogels showed their negative thermo-responsive behaviour with LCST values in the range 31.3-33.1°C as confirmed by water affinity measurements determined at temperatures around swelling-shrinking transition temperatures. The antioxidant activity of the thermo-responsive conjugates were evaluated by different assays and compared to a control, treated in the absence of antioxidant molecule. In particular, the scavenging activity on DPPH radicals and available phenolic groups determinations in polymeric matrices were performed at different temperatures. The results confirmed the modulable antioxidant properties of the hydrogels in response to the thermo-sensitive water affinity of the network. The planned synthetic strategy is a very simple approach to prepare macromolecular systems with high antioxidant power, which could be successfully applied in all the fields in which a consistent reduction of oxidative stress is required.

## *Chapter 6*

### **STARCH-QUERCETIN CONJUGATE BY RADICAL GRAFTING: SYNTHESIS AND BIOLOGICAL CHARACTERIZATION**

#### **1. Introduction**

Several studies indicate that antioxidant molecules, such as flavonoids and phenolic acids, have interesting properties, such as antibacterials, antivirals, antineoplastics, anti-inflammatory features. These molecules show, moreover, a therapeutic efficacy in numerous disorders, for examples, in diabetes, hypertension, neurodegenerative diseases. These pharmacological effects are mostly associated with their antioxidant activity<sup>116</sup>. The possibility to exploit all these important antioxidant properties, in the realization of medical products, such as delivery systems and devices or in the coating process of pharmaceutical formulations, is an evolving topic in biomedical fields. In particular, functional materials, based on polymeric-antioxidant conjugates, may be exploited to protect the “architecture” of biomedical formulations and to prevent their deterioration (e.g. to avoid the oxidation of their components) and also, to take advantages of the known beneficial health effects of the antioxidants molecules against several human disorders. The interest of the polymeric-antioxidant conjugates arises from the need to create functional systems useful in biomedical field, with pronounced physical and chemical efficiency, deriving from the use of the synthetic polymers and interesting pharmacological and biological properties, deriving from the antioxidants molecules. Covalent bonds between polymer and antioxidant increase the stability of the latter respect the formulation in which the antioxidant is simply mixed with the other ingredients of the preparation. A broad range of synthetic strategies of reaction have been

---

<sup>116</sup> Havsteen, B. *Biochem. Pharmacol.*, **1983**, 7, 1141–8.



considered for the realization of this kind of materials, and in particular three main strategies, involving several different steps, are used. One of these concerns the functionalization of antioxidant molecule by the insertion of polymerizable groups and its subsequent polymerization or copolymerization<sup>117</sup>. Another strategy involves the derivatization of a preformed polymeric structure with an antioxidant<sup>118</sup>. Finally, further approach is the grafting of a synthesized monomeric antioxidant onto a polymeric chain via melt processing with free radical initiators<sup>119</sup>. These strategies show some limitations. The synthesis of a monomeric antioxidant requires the purification of reaction products, whereas in the derivatization process, especially if the macromolecular system consists of a cross-linked polymer, a difficult optimization of the reaction conditions is often needed. The aim of this study was the realization of covalent insertion of antioxidant agent (the quercetin molecule) onto macromolecular systems (the starch backbone) by grafting polymerization process, employing a simple mechanism of reaction, which consists in a single-step reaction, using redox initiator systems (*Topic II, Paragraph 2.4*). This approach is very useful to synthesize protein- or polysaccharide- antioxidant conjugates without the generation of toxic reaction by-products and at room temperatures, preserving the antioxidant by degradation processes. The resultant conjugates were analyzed especially in terms of biological properties, to confirm their potential effects on health, against several human disorders, such as in Alzheimer and diabetes disorders. The covalent insertion of quercetin in the biopolymeric backbone was confirmed by several characterizations, such as FT-IR, DSC and fluorescence analyses, while a crude estimation of the amount of quercetin bound per g of polymer was obtained by performing the Folin-Ciocalteu assay. Antioxidant activity was, also, verified in terms of scavenging activity towards free radicals (DPPH, peroxy nitrite) and in terms of inhibition of free radical formation (peroxidation of linoleic acid) and finally the evaluation of total

---

<sup>117</sup> Ortiz, C.; Vazquez, B.; Roman, J.S. *J. Biomed. Mater. Res.*, **1999**, *45*, 184–191.

<sup>118</sup> Atkinson, D.; Lehrle, R. *Eur. Polym. J.*, **1992**, *28*, 1569–1575.

<sup>119</sup> Al-Malaika, S.; Suharty, N.; *Polym. Degrad. Stab.*, **1995**, *49*, 77–89.

antioxidant activity by molybdate assay was verified. Moreover, since usually antioxidants are often loaded to the formulation to prevent degradation of the active pharmaceutical ingredient, the ability of the proposed starch-antioxidant conjugate to prevent drug degradation was tested by performing specific degradation experiments. The conjugate was loaded with a model drug and the stability of the drug under thermal, light and oxidative stresses was evaluated.

## 2 Experimental Section

### 2.1 Materials and Instruments

Starch from corn (S), quercetin (Q), gallic acid (GA), hydrogen peroxide (H<sub>2</sub>O<sub>2</sub>), ascorbic acid (AA), 2,2'-diphenyl-1-picrylhydrazyl radical (DPPH), Folin-Ciocalteu reagent (FCR),  $\beta$ -carotene, linoleic acid, fluorescein, ammonium molybdate, acetylcholinesterase from *Electrophorus electricus* (AChE Type-VI-S, EC 3.1.1.7),  $\alpha$ -amylase (EC 3.2.1.1), tyrosinase from mushroom (E.C. 1.14.18.1), acetylthiocholine iodide (ATCI), physostigmine, 5,5'-dithiobis (2-nitrobenzoic-acid) (DTNB), 3,5-dinitrosalicylic (DNS), L-tyrosine, Kojic acid, Tween 20, sodium nitrite, sodium carbonate, disodium hydrogen phosphate, sodium dihydrogen phosphate, trisodium phosphate, manganese oxide (MnO<sub>2</sub>), sulphuric acid (96%w/w), hydrochloric acid (37% w/w), sodium potassium tartrate, sodium hydroxide, were obtained from Sigma-Aldrich (Sigma Chemical Co., St Louis, MO, USA). Water and ethanol were HPLC-grade and provided by Carlo Erba reagents (Milan, Italy).

The liquid chromatography consisted of a Jasco PU-2089 Plus liquid chromatography apparatus equipped with a Rheodyne 7725i injector (fitted with a 20  $\mu$ L loop), a Jasco UV-2075 HPLC detector and Jasco-Borwin integrator. A reverse-phase C18 Hibar column, 250 mm x 4  $\mu$ m, particle size = 5 $\mu$ m, pore size = 120 $\text{\AA}$  (Merck, Darmstadt, Germany), was employed. According to literature data, the mobile phase adopted for the detection of gallic acid<sup>120</sup> was

---

<sup>120</sup> Wang, H.; Helliwell, K.; You, X. *Food Chem.*, **2000**, *68*, 115–21.

methanol/water/orthophosphoric acid (20:79.9:0.1) at a flow rate of 1.0 mL min<sup>-1</sup>, while a 1% (v/v) formic acid aqueous solution-acetonitrile-2-propanol (70:22:8) at a flow rate of 0.2 mL min<sup>-1</sup> was used for quercetin<sup>121</sup>. Chromatograms were recorded at 210 and 370 nm for gallic acid and quercetin, respectively. IR spectra were recorded as KBr pellets on a Jasco FT-IR 4200. The dialysis membranes of 6-27/32" Medicell International LTD (MWCO: 12–14000 Da) were employed. Freeze drier Micro Modulyo, Edwards was employed. Calorimetric analyses were performed using a Netzsch DSC200 PC. In a standard procedure about 5.0 mg of samples were placed inside a hermetic aluminum pan, and the pan was then sealed tightly by a hermetic aluminum lid. Thermal analyses were performed from 50 to 350 °C under a dry nitrogen atmosphere with a flow rate of 25mL min<sup>-1</sup> and a heating rate of 5 °C min<sup>-1</sup>. A Perkin Elmer Lambda 900 spectrophotometer was employed to obtain the absorption spectra, while the corrected emission spectra, all confirmed by excitation ones, were recorded with a Perkin Elmer LS-55 Luminescence spectrometer, equipped with Hamamatsu R928 photomultiplier tube. The fluorescence spectra in the solid state were recorded by using the front face accessory. The solid sample were placed between the quartz plate (200 mm<sup>2</sup>) on the sample holder.

## 2.2 *Synthesis of Starch Conjugate*

The synthesis of starch-quercetin conjugate was performed as follows: in a 25 mL glass tube, starch (1.0 g) was dissolved in 13 mL of a water/ethanol (5/5, v/v) mixture. Then, 1.5 mL of H<sub>2</sub>O<sub>2</sub> 1.0 M containing 0.081 g of ascorbic acid were added. Finally, after 30 min., 50 mg amount of antioxidant molecule was introduced in the reaction flask and the mixture was maintained at 25°C for 24 h under atmospheric air. The obtained polymer solution was introduced into

---

<sup>121</sup>Careri, M.; Corradini, C.; Elviri, L.; Nicoletti, I.; Zagnoni, I. *J. Agric. Food Chem.*, **2003**, *51*, 5226–31.

dialysis tubes and dipped into a glass vessel containing a PBS solution (0.01M, pH 8.0) at 20°C for 48 h with eight changes of water. The copolymer was checked to be free of unreacted antioxidants and any other compounds by HPLC analysis after purification step. The resulting solution was filtered, frozen and dried with a freeze-drying apparatus to afford a vaporous solid. Blank starch, that acts as a control, was prepared in the same conditions but in the absence of antioxidant agent.

### 2.3 Characterization of Starch Conjugate

#### 2.3.1 Evaluation of Disposable Phenolic Groups by Folin-Ciocalteu Procedure

Amount of total phenolic equivalents was determined using the Folin-Ciocalteu reagent procedure, according to the literature with some modifications<sup>122</sup>. Briefly, 15 mg amount of Starch-Quercetin conjugate was dispersed in distilled water (6 mL) in a volumetric flask. The Folin-Ciocalteu reagent (1 mL) was added and the contents of flask were mixed thoroughly. After 3 min, 3 mL of Na<sub>2</sub>CO<sub>3</sub> (2%) were added, and then the mixture was allowed to stand for 2 h with intermittent shaking. The absorbance was measured at 760 nm against a control prepared using the blank polymer under the same reaction conditions. The amount of total phenolic groups in the polymeric material was expressed as quercetin equivalent (mg) by using the equation obtained from the calibration curve of the free antioxidant, recorded by employing five different quercetin standard solutions. 0.5 mL of each solution were added to the Folin-Ciocalteu system to raise the final concentration of 8.0, 16.0, 24.0, 32.0, and 40.0 × 10<sup>-6</sup> mol L<sup>-1</sup>, respectively. After 2 h, the absorbance of the solutions was measured to record the calibration curve and the correlation coefficient ( $R^2$ ), slope and intercept of the regression equation obtained were calculated by the method of least squares.

---

<sup>122</sup> Pan, Y.; Zhu, J.; Wang, H.; Zhang, X.; Zhang, Y.; He, C.; Ji, X.; Li, H. *Food Chem.*, **2007**, *103*, 913–8.

### 2.3.2 Determination of Scavenging Effect on the DPPH Radical

In order to evaluate the free radical scavenging properties of starch-antioxidant conjugate, its reactivity towards a stable free radical, 2,2'-diphenyl-1-picrylhydrazyl radical (DPPH), was evaluated<sup>123</sup>. For this purpose, in each seven test tubes, 12.5; 25.0; 37.5; 50.0; 62.5; 75.0, 87.5 mg amounts of starch-quercetin conjugate were dispersed in 6 mL of ethanol and then 4 mL of ethanol solution of the DPPH ( $600 \times 10^{-6} \text{ mol L}^{-1}$ ) were added, obtaining a solution of the DPPH with a final concentration of  $240 \times 10^{-6} \text{ mol L}^{-1}$ . The sample was incubated in a water bath at 25 °C and, after 30 min, the absorbance of the remaining DPPH was determined colorimetrically at 517 nm. The same reaction conditions were applied on the blank starch in order to evaluate the interference of polymeric material on DPPH assay. The scavenging activity of the tested polymeric materials was measured as the decrease in the absorbance of the DPPH and it was expressed as percent inhibition of the DPPH radical calculated according the following equation 1:

$$\text{Inhibition}\% = \frac{A_0 - A_i}{A_0} \times 100 \quad (1)$$

where  $A_0$  is the absorbance of a standard prepared in the same conditions, but without any polymers, and  $A_i$  is the absorbance of polymeric samples.

### 2.3.3 Determination of Total Antioxidant Activity

The total antioxidant activity of polymeric materials was evaluated according to the method reported in literature<sup>124</sup>. Briefly, 30 mg of starch-antioxidant conjugate were mixed with 2.4 mL of reagent solution ( $0.6 \text{ mol L}^{-1}$  sulphuric acid,  $28 \text{ mol L}^{-1}$  trisodium phosphate and  $4 \text{ mol L}^{-1}$  ammonium molybdate) and

<sup>123</sup> Ardestani, A.; Yazdanparast, R. *Food Chem.*, **2007**, *104*, 21–9.

<sup>124</sup> Prieto, P.; Pineda, M.; Aguilar, M. *Anal. Biochem.*, **1999**, *269*, 337–41.

0.6 mL of methanol, then the reaction mixture was incubated at 95 °C for 150 min. After cooling to room temperature, the absorbance of the mixture was measured at 695 nm against a control prepared using blank polymer in the same reaction condition. The total antioxidant activity was expressed as quercetin equivalent (mg). By using five different quercetin standard solutions, a calibration curve was recorded. 0.3 mL of each solution were mixed with 1.2 mL of reagent solution to obtain the final concentration of 8.0, 16.0, 24.0, 32.0, and  $40.0 \times 10^{-6} \text{ mol L}^{-1}$ , respectively. After 150 min incubation, the solutions were analyzed by UV-Vis spectrophotometer and the correlation coefficient ( $R^2$ ), slope and intercept of the regression equation obtained by the method of least squares were calculated.

#### 2.3.4 $\beta$ -Carotene-Linoleic Acid Assay

The antioxidant properties of synthesized functional polymer were evaluated through measurement of percent inhibition of peroxidation in linoleic acid system by using the  $\beta$ -carotene bleaching test<sup>125</sup>. Briefly, 1 mL of the  $\beta$ -carotene solution ( $0.2 \text{ mg mL}^{-1}$  in chloroform) was added to 0.02 mL of linoleic acid and 0.2 mL of Tween 20. The mixture was then evaporated at 40° C for 10 min in a rotary evaporator to remove chloroform. After evaporation, the mixture was immediately diluted with 100 mL of distilled water. The water was added slowly to the mixture and agitated vigorously to form an emulsion. The emulsion (5 mL) was transferred to different test tubes containing 1.5; 3.0; 4.5; 6.0; 7.5; 9.0;  $\text{mg mL}^{-1}$  concentration of starch-quercetin conjugate. The tubes were then gently shaken and placed in a water bath at 45 °C for 60 min. The absorbance of the filtered samples and control was measured at 470 nm against a blank, consisting of an emulsion without the  $\beta$ -carotene. The measurement was carried out at the initial time ( $t = 0$ ) and successively at 60 min. The same reaction conditions were applied on the blank starch in order to evaluate the interference of polymeric material on the  $\beta$ -carotene bleaching assay. The antioxidant activity

---

<sup>125</sup> Amin, I.; Zamaliah, M.M.; Chin, W.F.; *Food Chem.*, **2004**, 87, 581–6.

( $A_{ox}A$ ) was measured in terms of successful bleaching of the  $\beta$ -carotene using the following equation (2):

$$A_{ox}A = \left(1 - \frac{A_0 - A_{60}}{A_0^0 - A_{60}^0}\right) \quad (2)$$

where  $A_0$  and  $A_0^0$  are the absorbance values measured at the initial incubation time for samples and control, respectively, while  $A_{60}$  and  $A_{60}^0$  are the absorbance values measured in the samples and in control, respectively, at  $t = 60$  min.

### 2.3.5 Determination of Scavenging properties on peroxynitrite anion

Peroxynitrite was synthesized from sodium nitrite/ $H_2O_2$  acidified with HCl and the residual  $H_2O_2$  was removed by passing the solution through granular  $MnO_2$ . The yellowish stock solution was stored at  $-80^\circ C$  and its concentration was evaluated immediately before its use by measuring the absorbance at 302 nm<sup>126</sup>. The measurements of relative antioxidant capacity were determined by using fluorescein as detecting molecule. Briefly, Fluorescein (to obtain  $2 \times 10^{-6}$  mol  $L^{-1}$  final) in 100mM phosphate buffer, pH 7.4, was mixed in the presence or absence of antioxidant with  $100 \times 10^{-6}$  mol  $L^{-1}$   $ONOO^-$  to the final volume of 2 ml. The tested concentrations of starch-quercetin conjugate were 1.0; 2.0; 3.0; 4.0; 5.0; 6.0 mg  $mL^{-1}$ . As reported in literature, the immediate mixing of the sample with the oxidant added is critical for the reproducibility of the assay<sup>127</sup>. After incubation at room temperature for 15 min, the fluorescence of the samples was measured (excitation: 485 nm, emission: 538 nm). The same reaction conditions were applied on the blank starch in order to evaluate the interference of polymeric material on peroxynitrite assay.

<sup>126</sup> Schinella, G.; Fantinelli, J.C.; Tournier, H.; Prieto, J.M.; Spegazzini, E.; Debenedetti, S.; Mosca, S.M. *Res. Int.*, **2009**, *42*, 1403–9.

<sup>127</sup> Robaszkiewicz, A.; Bartosz, G. *Talanta*. **2010**, *80*, 2196–8.

### 2.3.6 Starch conjugate stability

The weight of the polymers before and after UV irradiation treatment was measured on a Sartorius balance<sup>128</sup>. The percent weight loss was calculated according to the following equation (3):

$$\text{Weight loss} = \frac{m_0 - m_i}{m_0} \quad (3)$$

Where  $m_0$  is the weight of the untreated polymer and  $m_i$  is the weight of the polymer after 15 days UV irradiation.

### 2.3.7 Cholinesterase Inhibitory Assay

Inhibition of AChE were assessed by a modified colorimetric Ellman's method<sup>129</sup>, which is based on the reaction of released thiocholine to give a coloured product with a chromogenic reagent. *Torpedo californica* (electric eel) AChE (Type-VI-S, EC 3.1.1.7, Sigma) was used, while ATCI was used as the substrate of the reaction. 40  $\mu\text{L}$  of AChE (0.36 U  $\text{mL}^{-1}$  in buffer pH 8) and different starchquercetin conjugate amounts were added to 2 ml of buffer pH 8 (0.1 mM) to raise the final concentrations to 5.0; 10.0; 15.0; 20.0; 25.0; 30.0 mg  $\text{mL}^{-1}$  and pre-incubated in an ice bath at 4  $^{\circ}\text{C}$  for 30 min. Duplicate tubes were also treated this way with 20  $\mu\text{L}$  of physostigmine ( $0.1 \times 10^{-3}$  mol  $\text{L}^{-1}$ ) to allow interference of the test substances in the assay to be assessed, and to control any hydrolysis of acetylcholine not due to enzyme activity. The reaction was started by adding DTNB solution (20  $\mu\text{L}$  of  $0.05 \times 10^{-3}$  mol  $\text{L}^{-1}$  in buffer pH 7) and ATCI (20  $\mu\text{L}$   $0.018 \times 10^{-3}$  mol  $\text{L}^{-1}$  in buffer pH 7) and tubes were allowed to stand in a water bath for 20 min at 37  $^{\circ}\text{C}$ . The reaction was halted by placing the

---

<sup>128</sup> Zhao, Y.; Dan, Y. *Eur Polym J.*, **2007**, *43*, 4541–51.

<sup>129</sup> Park, M.; Jung, M. *Molecul.*, **2007**, *12*, 2130–9.



assay solution tubes in an ice bath and adding physostigmine (20  $\mu\text{L}$   $0.018 \times 10^{-3} \text{ mol L}^{-1}$  in buffer pH7). The hydrolysis of acetylthiocholine was monitored by the formation of the yellow 5-thio-2-nitrobenzoate, immediately recorded on a spectrophotometer at 405 nm and the percentage inhibition (%) was calculated by the equation (4)

$$\text{inhibition (\%)} = \frac{(A_b - A_{bc}) - (A_s - A_{cs})}{(A_b - A_{bc})} \times 100 \quad (4)$$

Where  $A_b$  and  $A_{bc}$  are the absorbances of blank and blank positive control, respectively, while  $A_s$  and  $A_{cs}$  are the absorbance of sample and sample positive control, respectively. The same reaction conditions were applied on the blank starch in order to evaluate the interference of polymeric material on cholinesterase assay.

#### 2.3.8 $\alpha$ -amylase inhibitory activity determination

The  $\alpha$ -amylase inhibition assay method was performed according to the literature<sup>130</sup>. Two separate experiments were performed by using starch and starch quercetin conjugate as a substrates. 1 mL amount of S and S-Q dispersions in PBS (0.5% w/v) buffer ( $20 \times 10^{-3} \text{ mol L}^{-1}$ , pH 7.4) were incubated with 1 mL of  $\alpha$ -amylase solution (0.0253 g of  $\alpha$ -amylase in 100 mL of cold distilled water). The colorimetric reagent was prepared mixing a sodium potassium tartrate solution (12.0 g of sodium potassium tartrate, tetrahydrate in 8.0 mL of  $2 \text{ mol L}^{-1} \text{ NaOH}$ ) and  $96 \times 10^{-3} \text{ mol L}^{-1}$  DNS solution. The reaction was measured over 3 min. The generation of maltose was quantified by the reduction of 3,5-dinitrosalicylic acid to 3-amino-5-nitrosalicylic acid, the product being detectable at 540 nm. In the presence of an  $\alpha$ -amylase inhibitor less maltose will be produced and the absorbance value would decrease. The  $\alpha$ -

<sup>130</sup> Fred-Jaiyesimi, A.; Kio, A.; Richard, W. *Food Chem.*, **2009**, *116*, 285–8.

amylase inhibition was expressed as percentage of inhibition and calculated by the following equation (5):

$$\text{Inhibition (\%)} = \frac{A_S - A_{S-Q}}{A_S} \times 100 \quad (5)$$

Where  $A_S$  is the absorbance of starch solution and  $A_{S-Q}$  the absorbance of starch-quercetin solution.

### 2.3.9 Inhibition of tyrosinase activity determination

Tyrosinase-inhibition activity was determined by using L-tyrosine as a substrate<sup>131</sup>. Forty microliters of 200 units mL<sup>-1</sup> of mushroom tyrosinase solution, 1.0 mL of phosphate buffer (pH 6.8), and different amounts of starch-quercetin conjugate (final concentration of 5.0; 10.0; 15.0; 20.0; 25.0; 30.0 mg mL<sup>-1</sup>) were mixed. The assay mixture was pre-incubated at 37 °C for 10 min and then 40 µL of  $10 \times 10^{-3}$  mol L<sup>-1</sup> L-tyrosine was added. The reaction was then further incubated at 37 °C for 15 min. The amount of dopachrome was measured at 475 nm in a microplate reader. The data were expressed as a percentage of inhibition of tyrosinase activity after comparison with a control tube prepared in the same way but in absence of starch. Kojic acid was used as a standard tyrosinase inhibitor control. The same reaction conditions were applied on the blank starch in order to evaluate the interference of polymeric material on tyrosinase assay.

### 2.4 Gallic acid loading by the soaking procedure

1.0 g amount of blank starch and starch-quercetin conjugate were immersed in 30 mL of a gallic acid solution ( $5.00 \times 10^{-3}$  mol L<sup>-1</sup>) in distilled water and soaked for 3 days at room temperature<sup>132</sup>. During this time, the mixture was

<sup>131</sup> Rangkadilok, N.; Sitthimonchai, S.; Worasuttayangkurn, L.; Mahidol, C.; Ruchirawat, M.; Satayavivad, J. *Food Chem. Toxicol.*, **2007**, *45*, 328–36.

<sup>132</sup> Cirillo, G.; Parisi, O.I.; Curcio, M.; Puoci, F.; Iemma, F.; Spizzirri, U.G.; Picci, N. *J. Pharm. Pharmacol.*, **2010**, *62*, 577–582.

continuously stirred and then the solvent was removed under reduced pressure and the powder dried under vacuum overnight.

## 2.5 Stability studies

### 2.5.1 Freeze–thaw stability

Tubes containing  $1.5 \times 10^{-6}$  mol of GA were kept at 2–8 °C for 2 days, and then heated at 40 °C for 2 days per cycle; three cycles of freeze-thaw were conducted<sup>133</sup>. After this time, 10 mL of ethanol were added to the samples and the solutions were analyzed by the HPLC method. The freeze–thaw stability was evaluated by comparing the results after each cycle to the results before freeze–thaw studies. In order to investigate the preservative properties of starch-quercetin conjugate, in separate test tubes 10 mg of conjugate and blank starch, loaded with the same GA amount, were treated under the same conditions. Before HPLC analysis, 10 mL of ethanol were added to the samples to evaluate the amount of unchanged GA.

### 2.5.2 Photo-stability

Gallic acid ( $1.5 \times 10^{-6}$  mol) was treated under strong light (4500 Lx  $\pm$  500 Lx) at room temperature. After 5 days, 10 mL ethanol were added to the sample and the solution was analyzed by the HPLC method. 10 mg of blank starch and starch-quercetin conjugate, previously loaded with the same GA amount, were treated under the same conditions. At day 5, 10 mL of ethanol were added to the sample for HPLC analysis. Photo-stability was evaluated by the recovery of the polyphenol compound and comparing the results obtained in the three cases. The treatment was performed until the complete degradation of the free GA control solution which occurs in 15 days.

---

<sup>133</sup> Waterman, K.C.; Adami, R.C.; Alsante, K.M.; Hong, J.; Landis, M.S.; Lombardo, F.; Roberts, C.J. *Pharm. Dev. Technol.*, **2002**, 7,1–32.

### 2.5.3 Oxidative-stability

10 mg of blank starch and starch-quercetin conjugate loaded with Gallic acid ( $1.5 \times 10^{-6}$  mol) was treated with 10 mL of 30% aqueous hydrogen peroxide solution at 25 °C for 24 h. The sample was transferred to a 25 mL volumetric flask which was then filled to mark with ethanol for HPLC analysis. GA solution (1 mL) was directly treated with 10 mL of 30% aqueous hydrogen peroxide solution at 25 °C for 24 h. The sample was diluted to 25 mL with ethanol and analyzed by the HPLC methods<sup>134</sup>. The treatment was performed until the complete degradation of the free GA control solution which occurs in 25 days.

## 3. Results and Discussion

### 3.1 Synthesis and characterization of starch-quercetin conjugate

In this work, free radical grafting was applied in the synthesis of the starch-quercetin derivative with enhanced stability, to obtain a product with improved biological activities and, when used in pharmaceutical formulations, capability to prevent the degradation of a drug. The synthesis of the conjugate was carried by employing the ascorbic acid/hydrogen peroxide redox pair, a biocompatible and water-soluble radical initiator system. The reported molar ratio of flavonoid to polysaccharide corresponds to the highest amount of quercetin which can be dissolved in the reaction medium: a lower amount of Q in the reaction mixture, indeed, carried out to less effective conjugates. In the proposed reaction mechanism the macroradical formed on the starch backbone and the phenolic ring of the antioxidant react with the formation of a covalent bond. Literature data suggest that the insertion of aromatic antioxidants on the polymeric backbone occurs in the ortho- and para-positions relative to the hydroxyl group<sup>135</sup>. To remove un-reacted antioxidant, physically incorporated in the polysaccharidic structure, the conjugates underwent dialysis process and

---

<sup>134</sup>Ortiz, C.; Vazquez, B.; Roman, J.S. *J. Biomed. Mat. Res.*, **1999**, *45*, 184–191.

<sup>135</sup>Kitagawa, M.; Tokiwa, Y. *Carbohydr. Polym.*, **2006**, *64*, 218–23.

washing media were analyzed by HPLC. Finally, the suspension of grafted starch was lyophilized to obtain a porous material.

### 3.2 Characterization of starch-quercetin conjugate

The covalent incorporation of quercetin in the final conjugate was confirmed by performing fluorescence and thermal analyses, while a crude quantitative determination of the amount of quercetin bound per g of polymeric material was obtained by the Folin-Ciocalteu assay.

#### 3.2.1 Fluorescence analyses

A confirmation of antioxidant insertion in the biopolymer was obtained by comparing the emission spectra of free and bound antioxidant in the solid state (Figure 6.1). A bathochromic shift of the emission peak of Q was observed from 537 nm in the free form to 578 nm in the starch conjugate, and this red shift was used as a confirmation of the covalent linkage between the antioxidant and the polysaccharide because no emission peak was detected in the same wavelength range for blank starch.

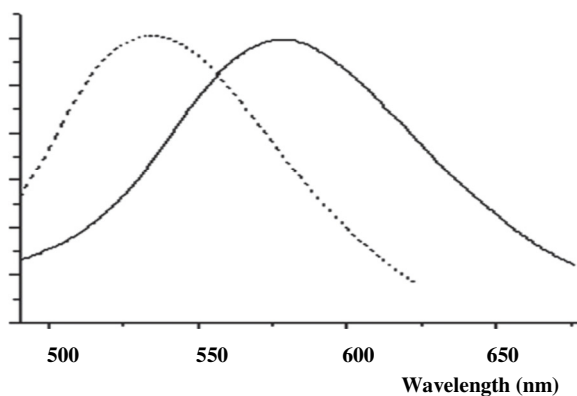


**Figure 6.1.** Emission spectra of free quercetin (- - -) and starch quercetin conjugate (\_\_\_\_\_)

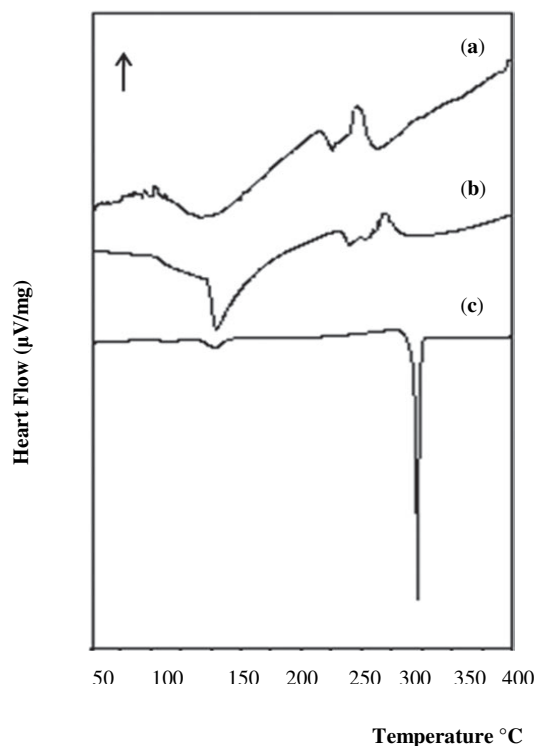


**Figure 6.2.** DSC of free quercetin (c), blank starch (b) and starch quercetin conjugate (a)

### 3.2.2 Thermal analyses

For a further characterization of functional material synthesized DSC analyses was also performed (Figure 6.2). The calorimetric analysis of pure quercetin (Figure 6.2 c) shows a sharp melting endotherm at 322.0 °C, corresponding to the melting point of the antioxidant molecule, while in the DSC thermogram of blank starch (Figure 6.2 b) a broad endotherm, located around 150.5 °C, is clearly visible and has been assigned to the glass transition of the polysaccharidic chain; the  $\Delta H_t$  associated with this transition was  $-202 \text{ J g}^{-1}$ .

The DSC thermogram of starch-quercetin conjugate (Figure 6.2 a) displays the disappearance of the melting endotherm of quercetin and a  $\Delta H_t$  value ( $-254 \text{ J g}^{-1}$ ), associated with the polysaccharidic gel transition, higher than that observed in blank starch, and these different thermal behaviors between the free and

conjugated system were observed and can be ascribed to the covalent doping of the polysaccharide with the flavonoid.

### 3.2.3 Evaluation of Disposable Phenolic Groups by Folin-Ciocalteu Procedure

The amount of quercetin bound per g of polymeric conjugate was calculated by the determination of the disposable phenolic content by the Folin-Ciocalteu assay. Folin-Ciocalteu reagent (FCR) is believed to contain heteropolyphosphotungstates-molybdates. In essence, the molybdenum is easier to be reduced in the complex and electron-transfer reaction occurs between reductants and Mo(VI) with the formation of Mo(V) blue species, possibly  $(\text{PMoW}_{11}\text{O}_{40})^{4-}$  spectrophotometrically detectable. Phenolic compounds react with FCR under basic conditions (adjusted by a sodium carbonate solution): dissociation of a phenolic proton leads to a phenolate anion, which is capable of reducing FCR<sup>136</sup>. This assay was used as a crude determination of the amount of quercetin in the conjugate, and this value, calculated by comparing the data obtained with a quercetin calibration curve, was found to be  $13.1 \pm 0.7$  mg of quercetin per unit of mass (g) of polymer.

## 3.3 Determination of the antioxidant properties

### 3.3.1 Determination of Total Antioxidant Activity

The total antioxidant activity was evaluated by the molybdate assay<sup>137</sup>. The assay is based on the reduction of Mo(VI) to Mo(V) by the flavonoid conjugate with the subsequent formation of a green phosphate/Mo (V) complex at acid pH. The total antioxidant activity was measured by comparison with the free antioxidant and the control starch, which contained no antioxidant component. The high absorbance values indicated that the sample possessed significant

<sup>136</sup>Huang, D.; Ou, B.; Prior, R.L. *J. Agric. Food Chem.*, **2005**, *53*, 1841–56.

<sup>137</sup>Ardestani, A.; Yazdanparast, R. *Food Chem.*, **2007**, *104*, 21–9.

antioxidant activity, which was expressed as mg equivalent of quercetin per g of dry starch conjugate, and this value was found to be  $9.9 \pm 0.4$  mg.

### 3.3.2 Determination of Scavenging Effect on the DPPH Radical

DPPH• is one of the few stable and commercially available organic nitrogen radicals with an absorption maximum band around 515–528 nm. Recently, the DPPH assay has become quite popular in antioxidant studies. One of the reasons is that this method is simple and highly sensitive. DPPH• accepts an electron or hydrogen radical to become a stable diamagnetic molecule, and thus the antioxidant effect is proportional to the disappearance of DPPH• in test samples<sup>138</sup>. From the DPPH• inhibitory profile (Figure 6.3) of starch and starch-quercetin conjugate, it is clear the high antioxidant power of the conjugate, with an  $IC_{50}$  value of  $2.52 \pm 0.3$  mg mL<sup>-1</sup>, while the control sample showed no relevant scavenging activity.

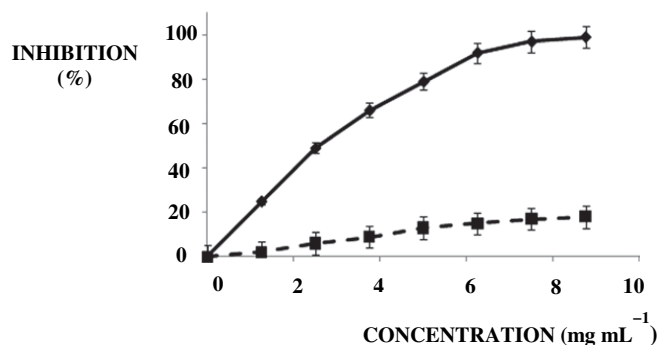


**Figure 6.3.** Inhibition profile on DPPH radical by blank starch (---■---) and starch-quercetin conjugate (—◆—). Data are expressed as means ( $\pm$  SD) of five independent experiments

### 3.3.3 Determination of Scavenging properties on peroxynitrite anion

Peroxynitrite radical was synthesized according to the literature<sup>139</sup>, and fluorescein was used as ONOO<sup>-</sup> detecting agent because it is bleached by hydroxyl, peroxy radicals and by peroxynitrite and hypochlorite. In all cases,

<sup>138</sup> Moon, J-K.; Shibamoto, T.; *J. Agric. Food Chem.*, **2009** ;57, 1655–66.

<sup>139</sup> Schinella, G.; Fantinelli J.C.; Tournier, H.; Prieto, J.M.; *Food Res. Int.*, 2009, 42, 1403–9.



the bleaching can be prevented by antioxidants, so the degree of protection may be a measure of the antioxidant activity of a sample <sup>140</sup>. Starch-queracetin conjugate was found to be a good protecting agent because of the ONOO<sup>-</sup> scavenging and the IC<sub>50</sub> was found to be 1.15 ± 0.2 mg mL<sup>-1</sup> (Figure 6.4). The inhibitory profile is reported as a function of polymers concentration, and the scavenging effect can be ascribed to the presence of queracetin into the polymeric chain (blank starch was not effective).

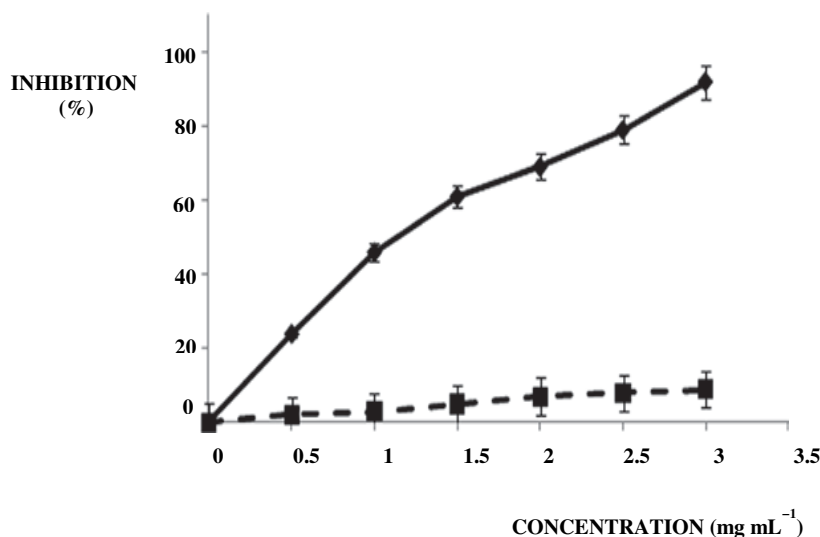


**Figure 6.4.** Inhibition profile on peroxynitrite anion by blank starch (---■---) and starch-queracetin conjugate (---◆---). Data are expressed as means (±) SD of five independent experiments

### 3.3.4 $\beta$ -Carotene-Linoleic Acid Assay

A further characterization of the antioxidant properties was performed in terms of lipid peroxidation inhibition (Figure 6.5). Linoleic acid was used as a substrate and  $\beta$ -carotene as detecting agent. In the  $\beta$ -carotene-linoleate model system, one hydrogen atom of linoleic acid is withdrawn, leaving a free radical ready to attack  $\beta$ -carotene molecules. In this reaction,  $\beta$ -carotene molecules lose the double bond and their characteristic orange color fades, and this oxidative

<sup>140</sup> Robaszkiewicz, A.; Bartosz, G.; *Talanta*, **2010**, *80*, 2196–8.

degradation of  $\beta$ -carotenes by radicals on linoleic acid is measured by the decrease in absorbance at 470 nm <sup>141</sup>.

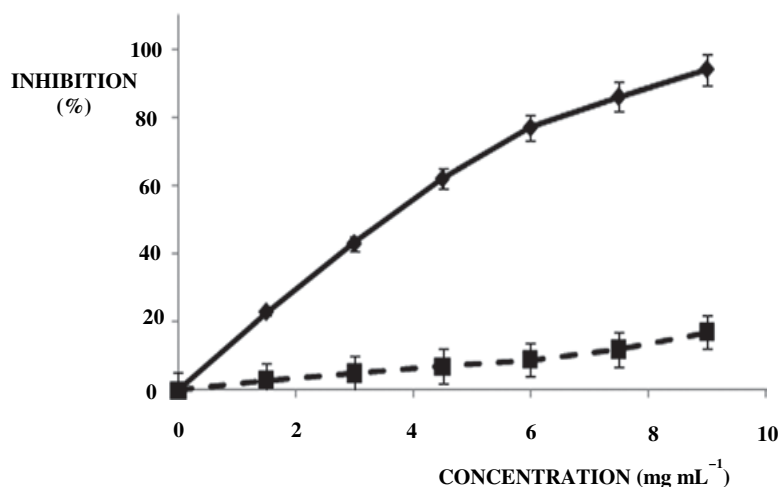


**Figure 6.5.** Inhibition profile on peroxy radical by blank starch (---■---) and starch-querceetin conjugate (---◆---). Data are expressed as means ( $\pm$  SD) of five independent experiments

The inhibition of the lipid peroxidation by different concentrations of the conjugate is reported in Figure 6.5. The high antioxidant properties of the conjugate is clearly understandable, with an  $IC_{50}$  value of  $4.31 \pm 0.7$  mg mL<sup>-1</sup>. Also in this case, the blank polysaccharide was ineffective.

### 3.4 Drug stabilization

The ability of the proposed starch-antioxidant conjugate to prevent drug degradation was tested by performing specific degradation experiments. The conjugate was loaded with a model drug and the stability of the drug under thermal, light and oxidative stresses was evaluated. Gallic acid was chosen as model drug because it may indeed be considered as one of simplest models for

<sup>141</sup> Kodali, V.P.; Sen, R.; *Biotechnol J.*, **2008**, *3*, 245–51.

natural organic matter<sup>142</sup>. This phenolic compound, indeed, is known to undergo rapid degradation processes when exposed to several different environmental stimuli<sup>143</sup>. A specific evaluation of the S-Q conjugate to prevent the degradation of this molecule is thus useful to show the general applicability of the conjugate in the prevention of the active pharmaceutical ingredient degradation. The results show an enhanced ability of starch conjugate in preventing the gallic acid degradation. In particular, amount of preserved GA by the antioxidant macromolecular system was almost  $95 \pm 1.2 \%$  in all the environment tested, while blank starch was not effective, with preserved GA of about  $30 \pm 1.5 \%$  under light stress,  $43 \pm 1.7 \%$  under thermal treatment and  $52 \pm 1.2 \%$  under oxidative stress. Free GA was used as control to evaluate the degradation rate, and the stresses were maintained until the complete degradation of this model drug.

### 3.5. Enzymatic activities

#### 3.5.1 Cholinesterase Inhibitory Assay

AChE is one of the fastest known enzymes which catalyzes the cleavage of acetylcholine in the synaptic cleft after depolarisation. Inhibitors of AChE, such as galanthamine, are used frequently in the pharmacotherapy of Alzheimer Disease: AChE is, indeed, dramatically down-regulated in patients suffering from this disease. Since it has been demonstrated that oxidative stress is intimately involved in age-related neurodegenerative diseases, there have been a great number of studies which have examined the positive benefits of antioxidants in the pathophysiology of these disorders<sup>144</sup>. The starch conjugate was tested as AChE inhibiting agent and good activity was found with an IC<sub>50</sub>

---

<sup>142</sup>Quici, N.; Litter, M.I.; *Photochem Photobiol Sci.*, **2009**, *8*, 975–84.

<sup>143</sup>Melo, R.; Leal, J.P.; Takacs, E.; Wojnarovits, L. *J. Hazard Mat.*, **2009**, *172*, 1185–92.

<sup>144</sup>Ramassamy, C; *Eur. J. Pharmacol.*, **2006**, *545*, 51–64.

value of  $12.1 \pm 1.8 \text{ mg mL}^{-1}$ , confirming this macromolecule could be of particular relevance in nutraceutical supplementation.

### 3.5.2 $\alpha$ -amylase inhibitory activity determination

Another tested enzyme was  $\alpha$ -amylase, which is involved in carbohydrate digestion by mammals. This enzyme hydrolyzes R (1,4)-glucosidic linkages with retention of configuration at the sugar anomeric center. Rapidly digested and absorbed dietary carbohydrates result in a sharp increase in the postprandial blood glucose level. For diabetic patients, the elevated blood glucose level after a meal presents a challenge for managing meal-associated hyperglycemia. Therefore, the inhibition of  $\alpha$ -amylase by pharmaceutical agents is an accepted clinical strategy for managing postprandial glycemia in diabetic patients. Molecules present in plants, and flavonoid in particular, have been shown to inhibit amylase<sup>145</sup>. Based on this consideration, the ability of the conjugate to act as  $\alpha$ -amylase inhibitor was evaluated. In our condition, two different experiments were performed by using, as substrate, blank starch and starch-quercetin conjugate, respectively. The obtained results show that the presence of quercetin covalently bonded to the sugar carried out to a considerable reduction of the enzymatic activity, with an inhibition of  $44 \pm 2.1 \%$  in the tested concentration.

### 3.5.3 Inhibition of tyrosinase activity determination

Tyrosinase is an enzyme involved in the natural development of skin, hair and eye coloring and is also of particular relevance in the initial step in melanin synthesis<sup>146</sup>. The effects of the synthesized conjugate on the enzymatic activity of this enzyme was tested, and the results showed an effective inhibition with an  $IC_{50}$  of  $15.7 \pm 2.0 \text{ mg mL}^{-1}$ , confirming the beneficial effects of the proposed

---

<sup>145</sup> Hou, W.; Li, Y.; Zhang, Q.; Wei, X.; Peng, A.; Chen, L.; Wei, Y. *Phytother. Res.*, **2009**, *23*, 614–8.

<sup>146</sup> Rangkadilok, N.; Sitthimonchai, S.; Worasuttayangkurn, L.; Mahidol, C.; Ruchirawat, M.; Satayavivad, J. *Food Chem. Toxicol.*, **2007**, *45*, 328–36.

antioxidant system on human health. The blank starch was ineffective in all the performed experiments.

#### **4. Conclusion**

A new polysaccharide-flavonoid derivative was successfully synthesized by free radical grafting of quercetin on starch. The obtained macromolecular system was characterized by spectroscopic technique and quantitative analyses to prove the effective covalent linkage of the antioxidant on the polymeric backbone. The beneficial effects of the conjugate on human health were proved by performing specific antioxidant and enzymatic tests in which the conjugate show high activity in comparison with blank starch. Furthermore, the ability of starch derivative to stabilize a model drug was evaluated to show the wide applications of the antioxidant macromolecular system. These results show the novelties of the conjugate proposed in this paper compared to the known antioxidant bioconjuates. For the first time, indeed, the ability of an insoluble macromolecular system to inhibit specific enzymes involved in several pathologic states, is shown.

## Chapter 7

### BIOLOGICAL ACTIVITY OF A GALLIC ACID-GELATIN CONJUGATE

#### 1. Introduction

Polymer therapeutics have become promising tools, in biotechnology field, to improve therapeutic strategies<sup>147</sup>, e.g. in cancer therapy. In particular, polymer therapeutics includes several type of systems, such as polymer drugs<sup>148</sup>, polymer-drug conjugates<sup>149</sup>, polymer-protein-conjugates<sup>150</sup>. The efficacy of small molecule antitumor agents used clinically may be limited by poor pharmacokinetics, undesired toxicity, and side effects.

Water-soluble polymers offer the potential to increase drug circulation time, improve drug solubility, prolong drug residence time in a tumor, and reduce toxicity. The conjugation of these drugs with water-soluble polymers shows an improvement of therapeutic efficacy than the drugs alone, because occurs an increase of their aqueous solubility and occurs a more simple administration, and further, are reduced side effects<sup>151</sup>. In recent years, antioxidants have gained importance due to their potential as prophylactic and therapeutic agents in many diseases. Antioxidants reduce or retard free radical generation and prevent the oxidation of cellular oxidizable substrates. In particular, the considerable interest for the antioxidant molecules is linked to their role against the harmful free radicals which play an important part in the onset of various diseases, such as cancer, diabetes, cardiovascular diseases, autoimmune diseases and neurodegenerative disorders. Moreover, several research studies, indicate that

<sup>147</sup> Duncan, R. *Nat. Rev. Cancer*, **2007**, *6*, 688–701.

<sup>148</sup> Donaruma, L.G. *Prog. Polym. Sci.*, **1974**, *4*, 1-25.

<sup>149</sup> Duncan, R. *Nat. Rev. Drug Discov.*, **2003**, *2*, 347-360.

<sup>150</sup> Harris, J.M.; Chess, R.B. *Nature Rev. Drug Discov.* **2003**, *2*, 214-221.

<sup>151</sup> Chen, X.; McRae, S.; Parelkar, S.; Emrick, T. *Bioconjugate Chem.* **2009**, *20*, 2331–2341.

antioxidants may slow or possibly prevent the development of cancer and gallic acid is one of these.

Anti-cancer properties of this phenolic compound have been demonstrated<sup>152</sup>. Numerous scientific studies have documented that this agent, indeed, induces cell death in several human cancer cell lines, such as in human prostate cancer cells<sup>153</sup>. Moreover, gallic acid is characterized from many other important positive properties, e.g. antioxidant, anti-allergic, anti-inflammatory activities<sup>154,155</sup>.

In this study, with the objective of creating a novel polymer therapeutic, taking advantage of interesting activity of the gallic acid compound, a novel biopolymer-antioxidant conjugate was realized. In particular, a gelatin-gallic acid conjugate was developed and proposed as potential useful macromolecular systems in medicine. The conjugate was synthesized by free radical grafting reaction, triggered by biocompatible and water soluble radical initiator systems, (*Topic II, Paragraph 2.4*) between a natural polymer, represented by the gelatin backbone, and the gallic acid agent. A biological characterization was performed analyzing different properties of the obtained conjugate. First, the scavenging properties toward peroxynitrite anion were tested. Second, the antioxidant functionality of the conjugate for various diseases was explored by testing its activity on selected enzymes<sup>156</sup>. Specifically, acetyl cholinesterase and  $\alpha$ -amylase were tested to investigate presumed beneficial effects of the synthesized biopolymer in the treatment of Alzheimer disease and diabetes. Furthermore, the anticancer activity of Gel-GA was determined in prostate carcinoma and renal cell carcinoma cell lines.

---

<sup>152</sup> Inoue, M.; Sakaguchi, N.; Isuzugawa, K.; Tani, H.; Ogihara, Y. *Boil. Pharm. Bull.*, **2000**, *23*, 1153-1157.

<sup>153</sup> Chen, H.M.; Wu, Y.C.; Chia, Y.C.; Chang, F.R.; Hsu, H.K.; Hsieh, Y.C.; Chen, C.C.; Yuan, S.S. *Cancer Lett.*, **2009**, *286*, 61-71.

<sup>154</sup> Hseu, Y.C.; Chang, W.H.; Chen, C.S.; Liao, J.W.; Huang, C.J.; Lu, F.J.; Chia, Y.C.; Hsu, H.K.; Wu, J.J.; Yang, H.L. *Food Chem. Toxicol.*, **2008**, *46*, 105-114.

<sup>155</sup> Gali, H.U.; Perchellet, E.M.; Klish, D.S.; Johnson, J.M.; Perchellet, J.P. *Carcinogenesis*, **1992**, *13*, 715-718.

<sup>156</sup> Kwon, Y.-I.; Apostolidis, E.; Shetty, K. *Bioresour. Technol.*, **2008**, *99*, 2981-2988.

## 2 Experimental Section

### 2.1 Materials

Gelatin (Ph Eur, Bloom 160) (GL), gallic acid (GA), hydrogen peroxide (H<sub>2</sub>O<sub>2</sub>), ascorbic acid, sodium nitrite, hydrochloridric acid (37% w/w), manganese dioxide (MnO<sub>2</sub>), fluorescein, disodium hydrogen phosphate, sodium dihydrogen phosphate, acetylcholinesterase from *Electrophorus electricus* (AChE Type-VI-S, EC 3.1.1.7),  $\alpha$ -amylase (EC 3.2.1.1), acetylthiocholine iodide (ATCI), physostigmine, 5,5'- dithiobis (2-nitrobenzoic-acid) (DTNB), 3,5-dinitrosalicylic (DNS), phosphate buffered saline (PBS) were obtained from Sigma-Aldrich (Sigma Chemical Co., St. Louis, MO). Dulbecco's modified Eagle medium (DMEM), fetal bovine serum (FBS), penicillin-streptomycin, HEPES buffer solution 1 M, nonessential amino acid solution (NEAA), and trypsin, 0.05% (1 $\times$ ) with EDTA were purchased from Invitrogen (Karlsruhe, Germany). Cell proliferation reagent WST-1 was purchased from Roche (Mannheim, Germany). Gel-GA conjugate was synthesized according to the literature<sup>157</sup>.

### 2.2 Instrumentation

The dialysis membranes of 6-27/32" Medicell International LTD (MWCO: 12-14000 Da) were employed. Freeze drier Micro Modulyo, Edwards, was employed. Spectrofluorimetric grade solvents was used for the photophysical investigations in solution at room temperature. A Perkin-Elmer Lambda 900 spectrophotometer was employed to obtain the absorption spectra, while the corrected emission spectra, all confirmed by excitation ones, were recorded with a Perkin-Elmer LS 50B spectrofluorimeter, equipped with Hamamatsu R928 photomultiplier tube. The high-pressure liquid chromatography (HPLC) analyses were carried out using a Jasco PU-2089 Plus liquid chromatography equipped with a Rheodyne 7725i injector (fitted with a 20  $\mu$ L loop), a Jasco UV-2075

---

<sup>157</sup> Spizzirri, U. G.; Iemma, F.; Puoci, F.; Cirillo, G.; Curcio, M.; Parisi, O. I.; Picci, N. *Biomacrom.*, **2009**, *10*, 1923–1930.



HPLC detector, and Jasco-Borwin integrator. A reversed-phase C18 column ( $\mu$ Bondapak, 10  $\mu$ m of 250  $\times$  4.6 mm internal diameter obtained from Waters) was used. As reported in literature <sup>158</sup>, the mobile phase was methanol/water/orthophosphoric acid (20/79.9/0.1) at a flow rate of 1.0 mL min<sup>-1</sup>, while the detector was set at 260 nm.

### 2.3 Synthesis of Gel-GA Conjugate

The Gel-GA conjugate was synthesized as follows: in a 50 mL glass flask, 0.5 g of gelatin were dissolved in 50 mL of H<sub>2</sub>O, then 1.0 mL H<sub>2</sub>O<sub>2</sub> 5.0 M (5.0 mmol) and 0.25 g of ascorbic acid (1.4 mmol) were added and the mixture was maintained at 25 °C under atmospheric air. After 2 h, 0.35 mmol of GA were added to solution. The solution of gelatin and antioxidant, after 24 h, was introduced into dialysis tubes and dipped into a glass vessel containing distilled water at 20 °C for 48 h with eight changes of water. The resulting solution was frozen and dried with a freeze drier to afford a vaporous solid. The purified conjugate was checked to be free of unreacted antioxidant and any other compounds by HPLC analysis after the purification step. Blank gelatin (Gel), that acts as a control, was prepared when grafting process was carried out in the absence of GA.

### 2.4 Characterization of Gel-GA Conjugate

#### 2.4.1 Determination of Scavenging Properties on Peroxynitrite Anion

Peroxynitrite was synthesized from sodium nitrite/H<sub>2</sub>O<sub>2</sub> acidified with HCl and the residual H<sub>2</sub>O<sub>2</sub> was removed by passing the solution through granular MnO<sub>2</sub> <sup>159</sup>. The yellowish stock solution was stored at -80 °C and its concentration was evaluated immediately before its use by measuring the absorbance at 302 nm. The measurements of relative antioxidant capacity were determined by using

---

<sup>158</sup> Wang, H.; Helliwell, K.; You, X. *Food Chem.* **2000**, *68*, 115–121.

<sup>159</sup> Schinella, G.; Fantinelli, J. C.; Tournier, H.; Prieto, J. M.; Spegazzini, E.; Debenedetti, S.; Mosca, S. M. *Food Res. Int.* **2009**, *42*, 1403– 1409.

Fluorescein as detecting molecule. Briefly, Fluorescein (to obtain  $2 \times 10^{-6}$  mol L<sup>-1</sup> final) in 100 mM phosphate buffer, pH 7.4, was mixed in the presence or absence of antioxidant with  $100 \times 10^{-6}$  mol L<sup>-1</sup> ONOO<sup>-</sup> to the final volume of 2 mL. The tested concentrations of Gel-GA conjugate were 1.5, 3.0, 4.5, 6.0, 7.5, and 9.0 mg mL<sup>-1</sup>. As reported in literature, the immediate mixing of the sample with the oxidant added is critical for the reproducibility of the assay<sup>160</sup>. After incubation at room temperature for 15 min, the fluorescence of the samples was measured (excitation: 485 nm, emission: 538 nm). The same reaction conditions were applied on the blank gelatin to evaluate the interference of polymeric material on peroxy nitrite assay. Each measurement was carried out in five independent experiments and data were expressed as means ( $\pm$ SD) and analyzed using one-way analysis of variance (ANOVA).

#### 2.4.2 Cholinesterase Inhibitory Assay

Inhibition of AChE was assessed by a modified colorimetric Ellman's method<sup>161</sup> that is based on the reaction of released thiocoline to give a colored product with chromogenic reagent. *Torpedo californica* (electric eel) AChE (Type-VIS, EC 3.1.1.7, Sigma) was used, while ATCI was used as the substrate of the reaction. A total of 40  $\mu$ L of AChE (0.36  $\mu$ U/mL in buffer pH 8.0) and different Gel-GA amounts were added to 2 mL of buffer, pH 8 (0.1 mM), to raise the final concentrations of 4.0, 6.0, 8.0, 10.0, 12.0, 14.0, and 16.0 mg mL<sup>-1</sup> and preincubated in an ice bath at 4 °C for 30 min. Duplicate tubes were also treated this way with 20  $\mu$ L of physostigmine ( $0.1 \times 10^{-3}$  mol L<sup>-1</sup>) to allow interference of the test substances in the assay to be assessed and to control any hydrolysis of acetylcholine not due to enzyme activity. The reaction was started by adding DTNB solution (20  $\mu$ L of  $0.05 \times 10^{-3}$  mol L<sup>-1</sup> in buffer pH 7.0) and ATCI (20  $\mu$ L  $0.018 \times 10^{-3}$  mol L<sup>-1</sup> in buffer pH 7) and tubes were allowed to stand in a water bath for 20 min at 37 °C. The reaction was halted by placing the assay solution tubes in an ice bath and adding physostigmine (20  $\mu$ L  $0.018 \times 10^{-3}$  mol

<sup>160</sup> Robaszkiewicz, A.; Bartosz, G. *Talanta*, **2010**, *80*, 2196–2198.

<sup>161</sup> Park, M.; Jung, M. *Molecul.*, **2007**, *12*, 2130–2139.

L<sup>-1</sup> in buffer pH 7.0). The hydrolysis of acetylthiocholine was monitored by the formation of the yellow 5-thio-2-nitrobenzoate, immediately recorded on a spectrophotometer at 405 nm and the percentage inhibition (%) was calculated by the eq 4.

$$Inhibition (\%) = \frac{(A_b - A_{bc})(A_s - A_{cs})}{(A_b - A_{bc})} \times 100 \quad (4)$$

Ab and Abc are the absorbance of blank and blank positive control, respectively, while As and Asc are the absorbance of sample and sample positive control, respectively. The same reaction conditions were applied on the blank gelatin to evaluate the interference of polymeric material on cholinesterase assay and on GA standard solutions. Each measurement was carried out in five independent experiments and data were expressed as means ( $\pm$ SD) and analyzed using one-way analysis of variance (ANOVA).

#### 2.4.3 $\alpha$ -Amylase Inhibitory Activity Determination

The  $\alpha$ -amylase inhibition assay method was performed according to the literature<sup>38</sup> using starch as a substrate. A total of 1 mL of starch dispersed in PBS (0.5% w/v) buffer ( $20 \times 10^{-3}$  mol L<sup>-1</sup>, pH 7.4) was incubated with 1 mL of  $\alpha$ -amylase solution (0.0253 mg of  $\alpha$ -amylase in 100 mL of cold distilled water) and Gel-GA conjugate at different concentration (4.0, 6.0, 8.0, 10.0, 12.0, 14.0, and 16.0 mg mL<sup>-1</sup>). The colorimetric reagent was prepared by mixing a sodium potassium tartrate solution (12.0 g of sodium potassium tartrate, tetrahydrate in 8.0 mL of 2 mol L<sup>-1</sup> NaOH) and  $96 \times 10^{-3}$  mol L<sup>-1</sup> DNS solution. The reaction was measured over 3 min. The generation of maltose was quantified by the reduction of 3,5-dinitrosalicylic acid to 3-amino-5-nitrosalicylic acid, the product being detectable at 540 nm. In the presence of a R-amylase inhibitor less maltose will be produced and the absorbance would decrease. The  $\alpha$ -amylase inhibition (%) was calculated by the following eq 5.

$$Inhibition (\%) = \frac{A_0 - A_1}{A_0} \times 100 \quad (5)$$

where  $A_0$  is the absorbance of the starch control solution and  $A_1$  is the absorbance of the sample. The same reaction conditions were applied on the blank gelatin in order to evaluate the interference of polymeric material on cholinesterase assay on GA standard solutions. Each measurement was carried out in five independent experiments, data were expressed as means ( $\pm$ SD), and analyzed using one-way analysis of variance (ANOVA).

## **2.5 Anticancer Activity**

### *2.5.1 Cell Culture*

Prostate cancer cell lines DU145 and PC-3 as well as renal cell carcinoma cells A498 were cultured in DMEM containing 10% FBS, 1% HEPES buffer, 1% nonessential amino acids, and 1% streptomycin/penicillin (all from Invitrogen, Karlsruhe, Germany) at 37 °C in a humidified atmosphere containing 5% CO<sub>2</sub>. The cells were harvested by trypsin/EDTA treatment. Gelatin and Gel-GA stock solutions were prepared freshly before each experiment in PBS by shaking overnight at room temperature. Dilutions were made in culture medium.

### *2.5.2 Viability*

The cellular viability was quantified using WST-1 in 96- well culture plates. Cells were seeded in 96-well plates using 7.500 DU145 cells/well, 10.000 PC-3 cells/well, and 6.000 A498 cells/well. After 24 h at a growth density of 50-60%, cells were incubated with pure GA, pure gelatin, or Gel-GA for 72 h. The treatment was stopped by washing the cells with PBS followed by incubation with 10  $\mu$ L of WST-1 in 100  $\mu$ L of fresh medium per well for 1-4 h. The mean viability of cells from five wells was measured relative to the untreated control (100%) by measuring the absorbance at 450 nm. Reference wavelength was 620 nm. The absorbance of medium only (blank) was subtracted from each value.

### 2.5.3 Proliferation

A total of 40,000 DU145 cells were seeded in duplicates in six-well plates. After 72 h at 60% growth density, cells were incubated with pure GA, pure gelatin, or Gel-GA for 96 h. Proliferation was measured by harvesting the cells using trypsin/EDTA and counting them using a Z2 Coulter counter (Beckman Coulter, Fullerton, U.S.A.). The mean results of duplicates with mean absolute deviations were expressed relative to the untreated control.

## 3 Results and Discussion

### 3.1 Synthesis and Antioxidant Function of the Gel-GA Conjugate

The Gel-GA conjugate was synthesized as described previously<sup>20</sup> by employing the optimized reaction condition, which allows to obtain the higher functionalization degree of the final conjugate. The employed synthetic strategy involved the use of the ascorbic acid/hydrogen peroxide redox pair, a biocompatible and water-soluble system, as radical initiators (Figure 7.1).

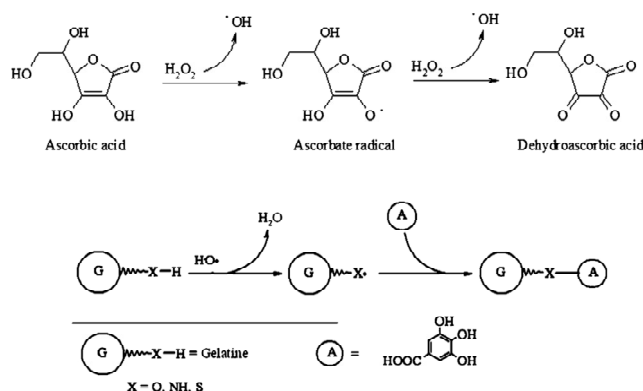


Figure 7.1. Synthesis of Gel-GA conjugate

The formation of a covalent bond between the antioxidant polyphenol and the protein was investigated by UV-vis analyses. The spectrum of free GA (10  $\mu$ M) is characterized by two absorption peak in the aromatic region at 211 and 258 nm. In the spectrum of Gel-GA conjugate (1.5 mg/mL), the presence of two

absorption peaks in the aromatic region at 227 and 272 nm is related to the presence of GA covalently bonded to the aminoacidic chains. The higher wavelength detected in the conjugate is ascribable to the formation of the covalent bonds between heteroatom in the protein side chains and antioxidant aromatic ring with a subsequent extension of the conjugation.

As a further confirmation of the covalent functionalization of the protein, the spectra of Gel-GA were recorded. Also, in this case, a bathochromic shift of the emission peaks of GA from 354 to 416 nm is detected and this spectral red shift is due to the covalent conjugation because no emission peak is detected in the same wavelength range for blank gelatin.

### 3.2 Characterization of starch-quercetin conjugate

#### 3.2.1 Determination of Scavenging Properties on Peroxynitrite Anion

It is known that the peroxynitrite anion is an oxidant relevant in many pathological situations because it can attack a wide range of biological molecules. Thus, it is important to know how the damage by these species can be counteracted by components of the body, especially blood plasma and other extracellular fluids<sup>162</sup>. In the employed experimental protocol, peroxynitrite anion was synthesized according to the literature<sup>163</sup> and fluorescein was used as ONOO<sup>-</sup> detecting agent because it is bleached by hydroxyl, peroxy radicals, and by peroxynitrite and hypochlorite. In all cases, the bleaching can be prevented by antioxidants. Thus, the degree of protection is a measure of the antioxidant activity of a sample. Gel-GA conjugate was found to be effective in protecting because of the ONOO<sup>-</sup> scavenging. The IC<sub>50</sub> was found to be 2.17 (0.4 mg mL<sup>-1</sup>). Gel-GA inhibited bleaching in a concentration-dependent manner (Figure 7.2). The scavenging effect can be ascribed to the presence of GA in the polymeric chain because blank Gel was found to be ineffective.

<sup>162</sup> Robaszkiewicz, A.; Bartosz, G. *Biochem. Biophys. Res. Commun.*, **2009**, *390*, 659–661.

<sup>163</sup> Schinella, G.; Fantinelli, J. C.; Tournier, H.; Prieto, J. M.; Spegazzini, E.; Debenedetti, S.; Mosca, S. M. *Food Res. Int.*, **2009**, *42*, 1403–1409.

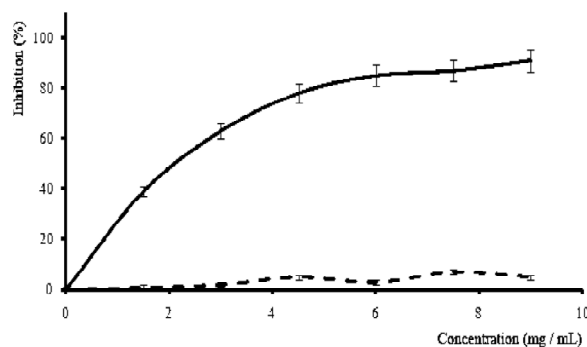


**Figure 7.2.** Scavenging activity toward peroxynitrite anion as a function of the concentration by Gel-GA (-) and Gel (- - -)

### 3.2.2 Cholinesterase Inhibitory Assay

AChE is one of the fastest known enzymes, which catalyzes the cleavage of acetylcholine in the synaptic cleft after depolarisation. In spite of the multifactorial nature of Alzheimer's disease, most current agents follow one therapeutic approach, based on the so-called cholinergic hypothesis of cognitive dysfunction. This hypothesis postulates that at least some of the cognitive decline experienced in this pathology from a deficiency in neurotransmitter acetylcholine and, thus, in cholinergic neurotransmission, which seems to play a fundamental role in memory<sup>164</sup>. Furthermore, inhibitors of AChE, such as galanthamine, are used frequently in the pharmacotherapy of Alzheimer's disease. Because there is evidence demonstrating that oxidative stress is intimately involved in age-related neurodegenerative diseases, there have been a large number of studies which have examined the positive benefits of antioxidants in the pathophysiology of these disorders<sup>165</sup>. In the present study, the Gel-GA conjugate as a new proteic inhibitor of AChE was tested with a modified Ellman method<sup>166</sup>. The pure carrier served as control. Gelatin was found to not interfere with the enzyme activity. In contrast, Gel-GA showed an

<sup>164</sup> Ballard, C. G.; Greig, N. H.; Guillozet-Bongaarts, A. L.; Enz, A.; Darvesh, S. *Curr. Alzheimer Res.*, **2005**, 2, 307–318.

<sup>165</sup> Ramassamy, C. *Eur. J. Pharmacol.*, **2006**, 545, 51–64.

<sup>166</sup> Park, M.; Jung, M. *Molecul.*, **2007**, 12, 2130–2139.

inhibitory profile, which depended on the conjugate concentration (Figure 7.3A). The inhibitory properties on AChE were expressed as percentage and the  $IC_{50}$  value was found to be  $7.1 \pm 1.3 \text{ mg mL}^{-1}$ . From these results there is increasing evidence of the potential beneficial effect of the Gel-GA conjugate against the damaging effects of neurodegenerative disorders. The cholinesterase inhibitory activity and the stronger radical scavenging property of the proposed macromolecular system suggest how the use of this material in medicine could be useful in the chemoprevention of Alzheimer's disease. The recorded  $IC_{50}$  value corresponds to  $5.1 \mu\text{g mL}^{-1}$  GA equivalent concentration, which is similar to that of free GA ( $3.2 \pm 0.6 \mu\text{g mL}^{-1}$ ), confirming that the conjugation process does not negatively interfere with the GA properties.

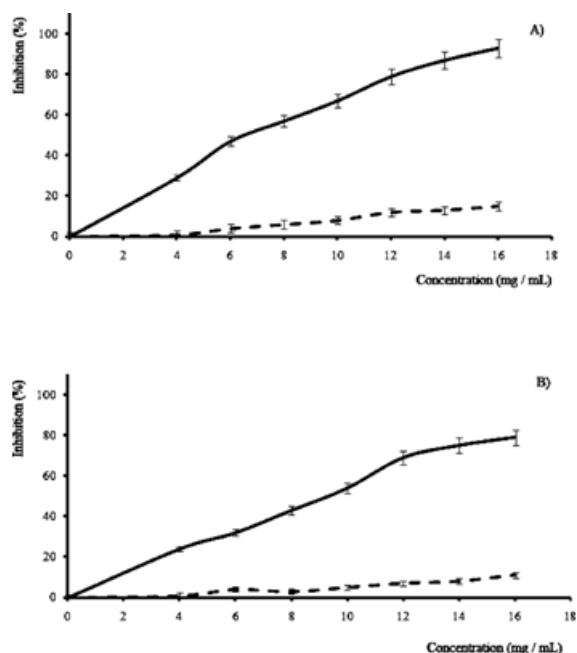


**Figure 7.3.** Inhibition of enzymatic activity by Gel-GA (-) and Gel (- -) as a function of the concentration. (A) AChE; (B)  $\alpha$ -amylase. Error bars represent the SD of quintuplicate of a representative experiment



### 3.2.3 $\alpha$ -Amylase Inhibitory Activity Determination

The second tested enzyme was  $\alpha$ -amylase, which is involved in carbohydrate digestion by mammals. This enzyme hydrolyzes R(1,4)-glucosidic linkages with maintenance of configuration at the sugar anomeric center. This allows the intestinal absorption of the dietary carbohydrates with a subsequent sharp increase in the postprandial blood glucose level. For diabetic patients, the elevated blood glucose level after a meal represents a challenge for managing meal-associated hyperglycemia. Therefore, the inhibition of  $\alpha$ -amylase by pharmaceutical agents is an accepted clinical strategy for managing postprandial hyperglycemia in diabetic patients. There are reports of established  $\alpha$ -amylase inhibitors and their effects on blood glucose levels after food uptake<sup>167</sup>. Plant phenolic compounds modulate the enzymatic breakdown of carbohydrates by inhibiting amylases<sup>168</sup>. Various biological and health-beneficial effects have been demonstrated by phenolic compounds in plants<sup>169</sup>.

Based on this consideration, the inhibitory activity of the synthesized proteic conjugate was evaluated pure Gel did not influence the enzymatic activity of  $\alpha$ -amylase. Gel-GA, however, was found to efficiently impair  $\alpha$ -amylase function. The presence of GA covalently bound to the protein carried out to a considerable reduction of the enzymatic activity, with an  $IC_{50}$  value of  $9.8 \pm 1.1 \text{ mg mL}^{-1}$  (Figure 7.3B). The results of this investigation suggest that the phenolic compound present in the Gel-GA conjugate may regulate the glucose uptake from the intestinal lumen by inhibiting carbohydrate digestion and absorption, leading to normal glucose homeostasis. Gel-GA interferes with or delays the absorption of dietary carbohydrates in the small intestine, leading to suppression of postprandial blood glucose surges and, therefore, may be a preferred alternative for inhibition of carbohydrate breakdown and control of glycemic index of food products. As reported in the AChE case, the conjugation process

<sup>167</sup> Shobana, S.; Sreerama, Y. N.; Malleshi, N. G. *Food Chem.*, **2009**, *115*, 1268–1273.

<sup>168</sup> McDougall, G. J.; Shpiro, F.; Dobson, P.; Smith, P.; Blake, A.; Stewart, D. *J. Agric. Food Chem.* **2005**, *53*, 2760–2766.

<sup>169</sup> Hou, W.; Li, Y.; Zhang, Q.; Wei, X.; Peng, A.; Chen, L.; Wei, Y. *Phytother. Res.*, **2009**, *23*, 614–618.

did not significantly reduce the GA inhibitory activities: the recorded IC<sub>50</sub> value, indeed, corresponds to 6.8  $\mu\text{g mL}^{-1}$  GA equivalent concentration and it is very similar to that of free GA (5.9 (0.8  $\mu\text{g mL}^{-1}$ )).

### 3.3 Anticancer Activity

Gallic acid, identified as an active component of grape seed extract, was shown to exhibit anticarcinogenic activity in various tumor models in vitro and in vivo, including lung and prostate cancer<sup>170,171</sup>. To include effects on tumor cells in the characterization of Gel-GA presented herein, we evaluated the viability of prostate cancer and renal cell carcinoma cells following incubation with the conjugate. DU145 cells are known to be sensitive to GA<sup>172, 173</sup>. This was confirmed herein in a concentration-dependent manner. In all tumor cell lines tested, pure GA at 40  $\mu\text{g mL}^{-1}$  efficiently reduced the relative viability to <10% of the control (Figure 7.4).

---

<sup>170</sup> Ji, B. C.; Hsu, W. H.; Yang, J. S.; Hsia, T. C.; Lu, C. C.; Chiang, J. H.; Yang, J. L.; Lin, C. H.; Lin, J. J.; Suen, L. J.; Wood, W. G.; Chung, J. G. *J. Agric. Food Chem.*, **2009**, *57*, 7596–7604.

<sup>171</sup> Kaur, M.; Velmurugan, B.; Rajamanickam, S.; Agarwal, R.; Agarwal, C. *Pharm. Res.*, **2009**, *26*, 2133–2140.

<sup>172</sup> Agarwal, C.; Tyagi, A.; Agarwal, R. *Mol Cancer Ther.*, **2006**, *5*, 3294–3302.

<sup>173</sup> Veluri, R.; Singh, R. P.; Liu, Z.; Thompson, J. A.; Agarwal, R.; Agarwal, C. *Carcinogen.*, **2006**, *27*, 1445–1453.

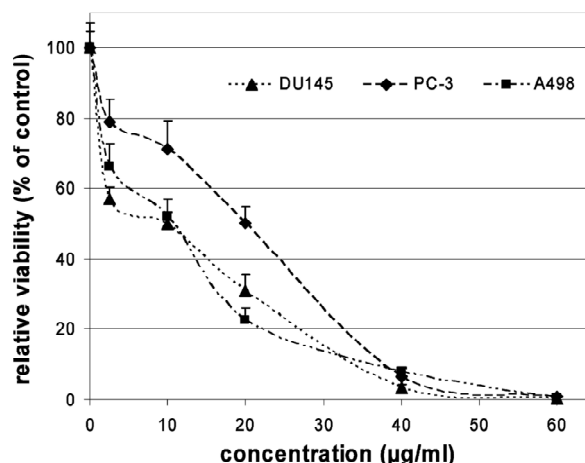


**Figure 7.4.** Viability of prostate cancer and renal cell carcinoma cells was decreased by pure gallic acid in a concentration-dependent manner in three different tumor cell lines. The viability is shown relative to the untreated control (100%)

Similar results were presented by Veluri et al. who used  $50 \mu\text{g mL}^{-1}$  GA and found an inhibition of DU145 growth by  $>90\%$ <sup>174</sup>.

The anticancer activity of the Gel-GA conjugate was evaluated by comparing its effect on cancer cell viability with pure gelatin. Gel-GA reduced the viability of all three cancer cell lines considerably stronger than the pure carrier. For example, whereas  $800 \mu\text{g mL}^{-1}$  of pure gelatin reduced the viability of A498 renal cell cancer cells to 64% in comparison to untreated cells, Gel-GA decreased the viability to 27% at the same concentration (Figure 7.5).

<sup>174</sup> Agarwal, C.; Tyagi, A.; Agarwal, R. *Mol Cancer Ther.*, **2006**, *5*, 3294– 3302.

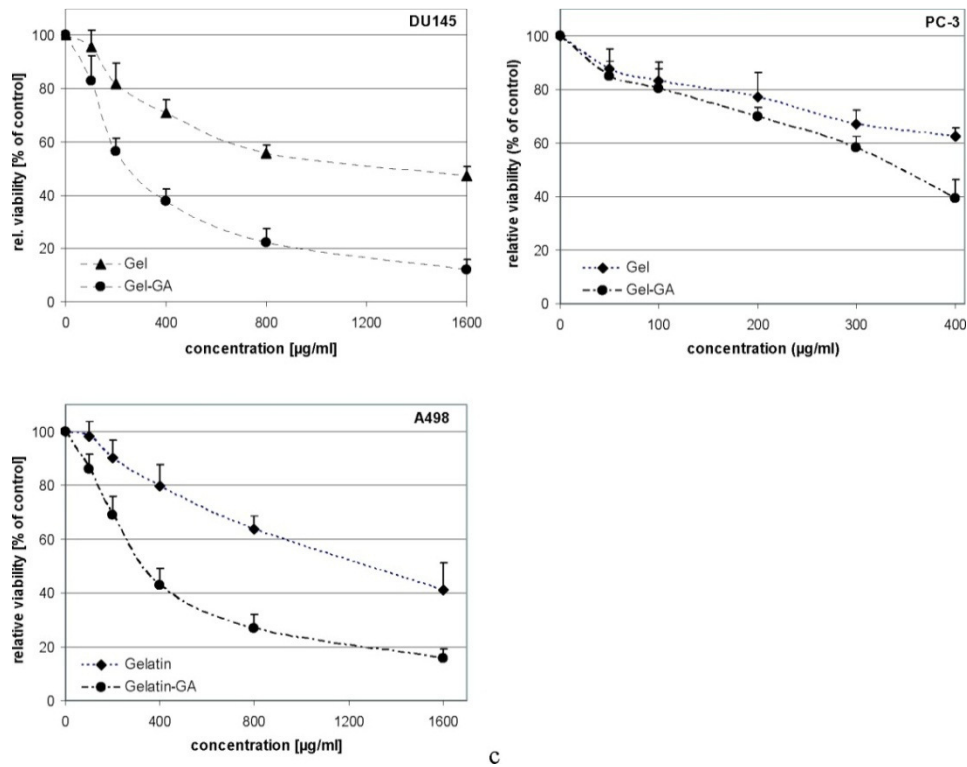


**Figure 7.5.** Viability of prostate cancer (DU145, PC-3) and renal cell carcinoma cells (A498) after treatment with the Gel-GA conjugate and pure gelatin for 72 h. Mean values of five replicates were normalized to untreated cells (control) and shown as relative viability

Moreover, the antitumor action of Gel- GA was confirmed on proliferation of DU145 prostate cancer cells. Whereas pure gelatin moderately impaired proliferation, the Gel-GA conjugate caused a prominent reduction of cell number to 60-70% of pure gelatin (Figure 7.6).

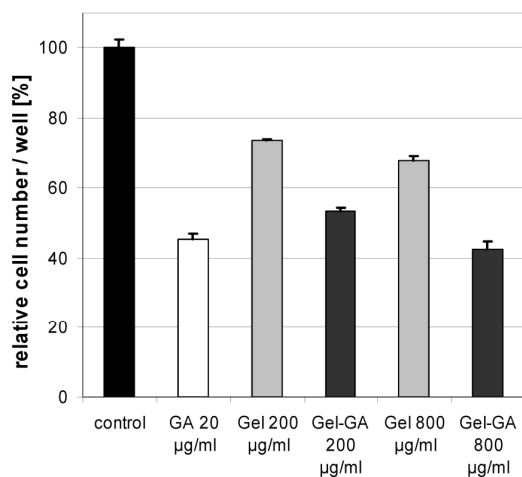


**Figure 7.6.** Reduction in cell number of DU145 prostate carcinoma cells after an incubation for 96 h with gelatin and Gel-GA conjugate at 2 different concentrations. The cell numbers are shown relative to untreated cells (100%). Pure GA served as positive control

#### 4 Conclusions

In conclusion, the present study presents the biological characterization of a new conjugate of GA bound to a gelatin carrier. The enzymatic tests clearly prove that the proposed protein-polyphenol conjugate is able to reduce the enzymatic activity of AChE and  $\alpha$ -amylase, with potential application in pathologic conditions such as Alzheimer's disease and diabetes. In addition, the Gel-GA conjugate maintained the anticancer activity of GA as shown by a reduction in tumor cell viability in comparison to pure gelatin. However, to improve a limitation of the Gel-GA conjugate presented herein, the loading capacity of the carrier for GA should be increased to reach higher GA concentrations without increasing the concentration of the gelatin carrier.

## SECTION III

### MODIFICATION OF BIOMATERIAL FOR THE CELL MICROENCAPSULATION

#### 3.1 Cell Microencapsulation

Cell microencapsulation is an interesting technology that involves immobilization of cells within a polymeric semi-permeable membrane that allows the diffusion of fundamental agents for cell metabolism, such as nutrients, oxygen and growth factors and, at the same time, the leak of metabolic waste. Furthermore, the semi-permeable membrane must ensure the protection of cells, which may be considered as foreign invaders, against the action of immune cells and antibodies (Figure 1).

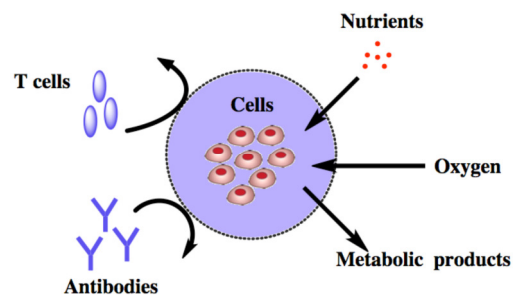


**Figure 1.** Schematic representation of the cell microencapsulation principle

*Bisceglie*<sup>175</sup> made the first attempt encapsulate cells in polymer membranes. He demonstrated that tumor cells in a polymer structure transplanted into pig abdominal cavity remained viable for a long period without being rejected by the immune system<sup>176</sup>.

---

<sup>175</sup> Bisceglie, V. *Zeitschrift für Krebsforschung*, **1993**, 40, 122–140.

The immunoisolation of cells for transplantation, a delivery system for gene therapy and the possibility to synthesizing in vitro proteins and hormones , are just some of the possible applications of the technique of cell microencapsulation. Polymers that are used as semi-permeable membranes, for this technology, must have some important properties such as biocompatibility, ensure the cellular metabolism, immune-protection and a good mechanical stability. Hydrogels exhibit several features that make appealing their use in this context. Hydrogels, indeed, may mimic extracellular matrices and provides a number of advantages for microencapsulation<sup>177</sup>.

But only a limited number of natural and synthetic polymers have been identified for the realization of this type of material and alginate<sup>178</sup>, chitosan<sup>179</sup>, agarose<sup>180</sup>, hyaluronic acid<sup>181</sup>, poly(ethylene glycol) (PEG)<sup>182</sup>, are the most employed systems.

### 3.5 Consideration for the Design of a Cell Microencapsulation Device

#### 3.2.1 Alginate as coating material

Alginate is by far the most frequently used biomaterial in the field of cell microencapsulation<sup>183</sup> due to its abundance, advantageous gelling properties and good biocompatibility. Alginate is an anionic polysaccharide composed of  $\alpha$ -L-guluronic (G -blocks) and  $\beta$ -D-mannuronic (M- blocks) interspersed with region of mixed sequences (Figure 2).

---

<sup>177</sup> Weber, L.M.; Hayda, K.N.; Haskins, K. et al. *Biomater.*, **2007**; 28, 3004-11.

<sup>178</sup> Lim, F.; Sun, A.M.; *Scie.*, **1980**, 210, 908-10.

<sup>179</sup> Zielinski, B.A.; Aebischer, P.; *Biomater.*, **1994**, 15, 1049-56.

<sup>180</sup> Sakai, S.; Kawabata, K.; Ono, T.; et al. *Biomater.*, **2005**, 26, 4786-92.

<sup>181</sup> Khademhosseini, A.; Eng, G.; Yeh, J.; et al. *J. Biomed. Mater. Res. A*, **2006**, 9, 522-32.

<sup>182</sup> Cruise, G.M.; Hegre, O.D.; Lamberti, F.V.; et al. *Cell Transplant.*, **1999**, 8, 293-306.

<sup>183</sup> Santos, E.; Zarate, J.; Orive, J.; Hernández, R.M.; Pedraz, J.L. *Adv. Experim. Med. Biol.*, **2010**, 670, 5-21.

It is possible to form physical gels from the alginate backbone by hydrogen bonding at acid pH, and by ionic interaction with divalent or trivalent ions (e.g.  $\text{Ca}^{2+}$ ,  $\text{Ba}^{2+}$ ,  $\text{Al}^{3+}$ ), that act as cross-linkers between adjacent polymer chains and in particular divalent cations preferably bind the G-blocks.

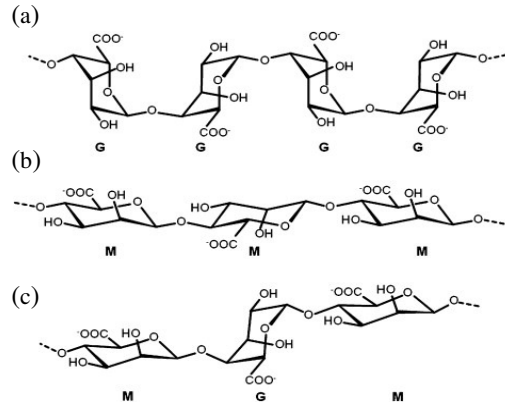


**Figure 2.** Alginate structure (a) G-blocks; (b) M-blocks; (c) mixed sequence of G- and M- blocks

The use of alginate for the realization of semi-permeable gel network, as coating material for the cell encapsulation, is very advantageous due to the ability of this polysaccharide of forming excellent gels in mild and under physiological conditions. Indeed, the encapsulation can be performed in aseptic environment at room temperature, at physiological pH and using isotonic solutions<sup>184</sup>. All these positive aspects, deriving from the use of alginate, promote a high viability of enclosed cells and a low risk of releasing harmful products in vivo derived of the use of toxic components during the formation of the microcapsules.

### 3.2.2 Hydrogel crosslinking method for beads preparation

The main techniques for beads preparation are ionotropic gelation and polyelectrolyte coacervation.

The *ionotropic gelation technique*, is an advantageous method exploits for the realization of the hydrogel beads and is based on the ability of polyelectrolytes

<sup>184</sup> Schmidt, J.J.; Rowley, J.; Kong, H.J. *J. Biomed. Mater. Res. A*, **2008**, *87*, 1113-22.



(e.g. alginate) to cross link in the presence of counter ions (e.g.  $\text{Ca}^{2+}$ ) to form hydrogels.

The gelation process is spontaneous, and the structure of the resulting gel depends on polyelectrolytes structure (molecular weight, architecture, density, nature of the charge) and on the ions crosslinking the polymer. In the case of alginate, gelification occurs in the presence of divalent cations, such as calcium<sup>185</sup>, barium<sup>186</sup>, and strontium<sup>187</sup>. Divalent cations interact with G-blocks of alginate to form bridges between polymer chains in a highly cooperative structure. *Polyelectrolyte Complexes or Complex Coacervation Gels*, indeed, is another method for the realization of hydrogel beads to improve the mechanical strength and permeability barrier of hydrogels. This method involve the addition of oppositely charged another polyelectrolyte to the ionotropically gelled hydrogel beads. This technique requires mild process conditions, allowing cells to retain their ability to grow and divide inside the capsule.

### 3.2.3 Microencapsulation techniques

Several techniques have been developed for the production of microspheres intended for cell microencapsulation. Emulsification, extrusion and co-extrusion are the most employed technique but several new technologies are emerging, such as microfluidic, microlithography and micromolding methods<sup>188</sup>. Emulsification is an advantage technique for industrial purposes because guarantees a large-scale production. But one of the limitations of this method is represent by the use of an organic phase, such as oil, which is mixed with a aqueous solutions, might compromise cell survival during the encapsulation procedure. Another negative aspect of the emulsification is represent, moreover, by the formation of the beads with large diameters, from hundreds of micrometers to millimeters, with large size distribution.

---

<sup>185</sup> Kierstan, M.; Bucke, C. *Biotechnol. Bioeng.*, **1977**, *19*, 387–397.

<sup>186</sup> Zekorn, T.; Siebers, U.; Horcher, A.; Schnettler, R.; Klock, G.; Bretzel, R.G.; Zimmermann, U.; Federlin, K. *Transplant. Proc.*, **1992**, *24*, 937–939.

<sup>187</sup> O'Shea, G.M.; Goosen, M.F.; Sun, A.M. *Biochim. Biophys. Acta*, **1984**, *804*, 133–136.

<sup>188</sup> Rabanel, J.M.; Banquy, X.; Zouaoui, H.; Mokhtar, M.; Hildgen, P.; *Biotechn. Prog.*, 2009, *25*, 946-63.

In extrusion techniques, the polymer solution, containing cell, is extruded through a small needle, permitting to the droplets formed to fall freely into a gelling bath where they are cross-linked by the addition of an appropriate reagent, such as divalent cations. The simplest extrusion method comprises dripping with only gravitational force as driving force. A limitation represent from this technique is the dimension of the spherical hydrogels that is, in presence of a low-viscosity solutions, in the range of 1.5 to 3 mm. But one of the challenge of this technologies is to obtain microspheres with diameter in the range of 100 to 500  $\mu\text{m}$  because microspheres with these dimension have several positive aspect, such as good stability, an higher surface-to-volume ratio and finally, show a good transport of nutrients<sup>189</sup>.

Is possible obtain microspheres with ideal dimension by reducing the time required for the droplet formation, employing an useful device, the air-syringe pump droplet generator ,in which exploits the use of air-flow to blow droplets from a needle tip into a gelling bath before they fall due to gravity, as illustrated in Figure 3. The basis of operation of this coaxial air-flow droplet generator, there is a syringe pump that is used to force the suspension of cells in polymer solution through the needle. The obtained droplets are usually in the range of 400-600  $\mu\text{m}$  and show a good uniformity.

---

<sup>189</sup> De Vos et al.,1996

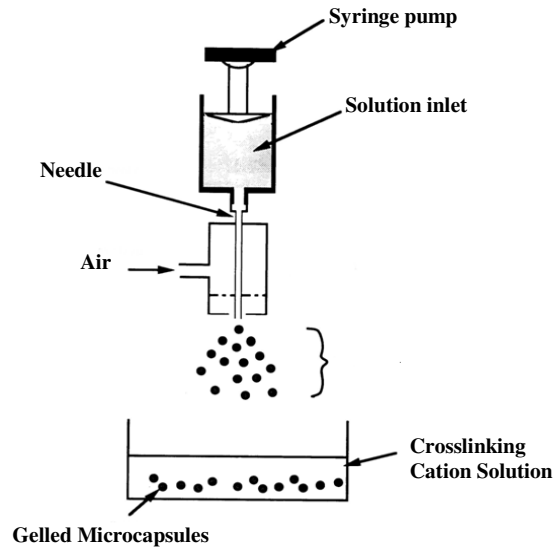


**Figure 3.** Principle of coaxial air-flow droplet generator

#### 3.2.4 Mechanical stability of microcapsule

The mechanical stability is an important requirement for the material employed for protecting transplanted cells, to ensure, above all, effective protection during delivery (e.g. by injection).

Indeed, the breakage of the capsules allows for the exposure of the entrapped cells to the immune system leading to the graft failure<sup>190</sup>.

Coating material deriving from  $\text{Ca}^{2+}$ -alginate interactions, however, show any problems related to the propensity to suffer osmotic swelling with the consequence increase of permeability and thus, destabilization and finally the breakage of the matrix. To avoid these problems and to improve the permeability and the resistance to the matrix, resulting materials for encapsulation are generally coated with an additional polycation layer, such as poly-*l*-lysine (PLL). However, poly-*l*-lysine is considered cytotoxic and, for this reason, it is well known the biocompatibility problems arisen by the use of

<sup>190</sup> Santos, E.; Zarate, J.; Orive, J.; Hernández, R.M.; Pedraz, J.L. *Adv. Experim. Med. Biol.*, **2010**, 670, 5-21.

alginate-poly-*l*-lysine-alginate microcapsules<sup>191</sup> which limits its application in cell encapsulation technology.

It was demonstrated that surface modification with polyethylene glycol (PEG) derivatives can significantly reduce the unwanted host response to any implant by masking the underlying charged surfaces and sterically hindering the approach of protein molecules present in the implant environment, thus avoiding cell attachment and spreading. For the cell immobilization technique, PEG-based hydrogel represent an attractive material for their interesting features, such as hydrophilic character and high water content, properties that make them similar to native tissues. Indeed, PEG molecules with different reactive end groups have been investigated as precursors to form chemically cross-linked hydrogels with a good mechanical stability. There are several approaches employed for the realization of PEG hydrogels, such as the photopolymerization, in which PEG solution is converted in hydrogel, using light, under mild conditions but one disadvantage of this method is represented by the UV light and by the resulting radicals that can prejudice the cell survival.

Michael-type addition reaction can be exploited to prepare another type of PEG-based hydrogel in which occurs the conjugate addition of vinyl sulfone terminated PEG (PEG-VS) with thiol terminated cross-linker. However, the formation of covalently cross-linked PEG-based hydrogels of spherical shape and suitable surface/volume ratio, which is essential for cell nutrition and active delivery, is still a challenge.

In the work that will be described in the next chapter (*Chapter 8*) will be described the synthesis of the modified PEG employing an alternative to the common polymerization method. This method is represented by the asymmetrical functionalization of commercially available symmetrical PEG, as potential candidates for biomaterials modification, in particular intended for cell microencapsulation. This work will include, also, the chemical modification of

---

<sup>191</sup> Juste, S.; Lessard, M.; Henley, N.; et al., *J. Biomed. Mater. Res. A*, **2005**, *72*, 389-98.

sodium alginate with heterobifunctional PEG, macromolecular characterization, preparation and characterization of hydrogel microspheres.

## Chapter 8

### DEVELOPMENT OF HYBRID HYDROGEL BASED ON Na-alg-PEG INTENDED FOR BIOMEDICAL AND BIOTECHNOLOGICAL APPLICATIONS

#### 1. Introduction

Pegylation defines the modification of a biomolecules by the linking of one or more polyethylene glycol (PEG) chains. It is an important process, widely exploited in biomedical fields, to modify macromolecules, biomolecules and surfaces. Poly (ethylene glycol) (PEG) (Figure 8.1) hydrogel is one of the most studied and widely applied hydrogels, for example as matrices for controlled release of biomolecules and scaffolds for regenerative medicine, because they have important properties, such as non-immunogenicity, biocompatibility, good solubility in water and in many organic solvents.

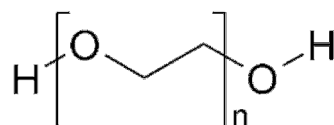


Figure 8.1. Structure of Poly (ethylene glycol)

PEG chains possessing a functional group at only one end are not suitable for subsequent derivatization /modification, which is frequently crucial for the design of biomaterials or for biomedical applications.

For good-performance pegylation, heterotelechelic PEG is required, such as PEG molecules having two different reactive functional end groups.

two main approaches are commonly used for the functionalization of PEG<sup>192</sup>:

- alteration of the terminal hydroxyl group through a series of reaction to a more active functional group;
- reaction of PEG, under controlled conditions, with difunctional compounds so that one of the functional groups reacts with PEG and the other remains active. In most case, several steps are conducted to achieve the expected derivatization.

Several heterobifunctional PEG derivatives are commercially available but at relatively high cost. The most common approach for obtaining heterobifunctional PEG uses anionic ring-opening polymerization of ethylene oxide<sup>193</sup> but this type of polymerization is considered hazardous. An alternative of this polymerization method consist in an alternation of the terminal hydroxyl groups of commercially available PEG. The asymmetric activation of the hydroxyl group at one chain end allows the introduction of a series of functional groups.

This work summarizes the synthesis of a novel heterobifunctional thiol-PEG-amine (SH-PEG-NH<sub>2</sub>), as potential candidates for biomaterials modification, via asymmetric activation of commercially available symmetrical PEG, with molecular weight 300 g/mol. Then, the applicability of this obtained system for pegylation technology was verified by hybrid hydrogels formation with alginate chains. In particular was verified the formation of physical hydrogel by grafting an amine terminated PEG into alginate chain. At the same time, the introduction of the thiol at the end of the PEG chains allowed for the formation of hydrogel via the formation of disulfide bonds. The combination of ionotropic gelation and chemical cross-linking yielded hybrid microspheres.

---

<sup>192</sup> Yokoyama, M; Okano, T.; Sakurai, Y.; Ohsako, N. *Bioconjug. Chem.*, **1992**, 3 , 275-6

<sup>193</sup> Banerjee, S.S.; Aher, N.; Rajesh, P.; Khandare, J. *J. Drug Del.*, **2012**, 17.

## 2. Experimental Section

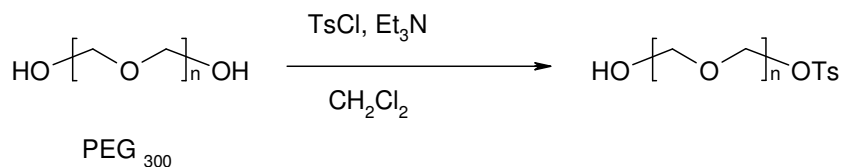
### 2.1 Materials

PEG ( $M_w$  300 g/mol), p-toluenesulfonyl chloride (TsCl), triethylamine ( $Et_3N$ ), sodium azide ( $NaN_3$ ), triphenylphosphine ( $PPh_3$ ), 3-(N-Morpholino)propanesulfonic acid (MOPS), tris(2-carboxyethyl) phosphine hydrochloride (TCEP), N-hydroxysuccinimide (NHS), 2-(N-morpholino)ethanesulfonic acid (MES), N-ethyl-N'-(3-dimethylaminopropyl)carbodiimide hydrochloride (EDC), sodium hydrosulfide hydrate (NaSH) and N,N-dimethylformamide (DMF) were purchased from Sigma-Aldrich (Sigma-Aldrich, Switzerland). Thioacetic acid, potassium bicarbonate, and acetic acid were obtained from Fluka (Fluka, Switzerland). Dichloromethane (DCM), methanol (MeOH) and diethyl ether were obtained from Fisher Scientific, Switzerland. Finally, sodium sulfate anhydrous was purchased from AppliChem, Germany.

### 2.2 Synthesis of heterobifunctional PEG

#### 2.2.1 Synthesis of tosyl-PEG-OH (1)

To a solution of the PEG (300 g/mol; 50 g, 44.4 mL) in 400 mL of dry  $CH_2Cl_2$ , was added TsCl (2.82 gr, 0.1 equiv.) and  $Et_3N$  (8.3 mL, 0.4 equiv.) (Scheme I).



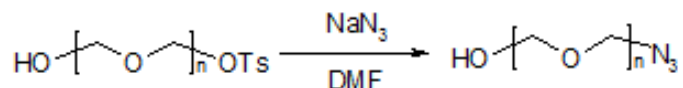
**Scheme I.** Synthesis of Tosyl-PEG-OH

The reaction mixture was stirred at  $0^\circ\text{C}$  for 8 h. The solution was filtered, washed twice with saturated  $NH_4Cl$  solution and twice with water. The organic layer was dried over sodium sulfate, filtered and reduced to small volume by rotary evaporation.



## 2.2.2 Synthesis of Azide-PEG-OH (2)

Monotosylated PEG-OH (18g) and  $\text{NaN}_3$  (12.6 gr, 5 equiv.), were dissolved in 200 mL of dry DMF and the mixture was stirred overnight at  $90^\circ\text{C}$  under argon atmosphere (Scheme II).

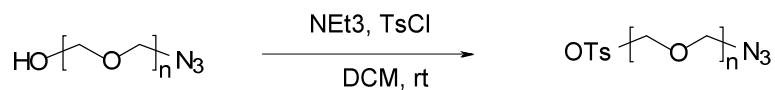


**Scheme II.** Synthesis of Azide-PEG-OH

After cooling, at room temperature (rt), and filtration, DMF was removed under vacuum. The crude product was dissolved in 100 mL of water and extracted three times with DCM. The organic layer was dried over sodium sulfate, filtered, reduced to a small volume by rotary evaporation and used as is for the next step.

## 2.2.3 Synthesis of Azide-PEG-Tosyl (3)

Azide-PEG-OH (13 gr) was dissolved in 200 mL DCM.  $\text{NEt}_3$  (16.5 mL, 3 equiv.) and TsCl (15.25 gr, 2 equiv.) were added (Scheme III).



**Scheme III.** Synthesis of Azide-PEG-Tosyl

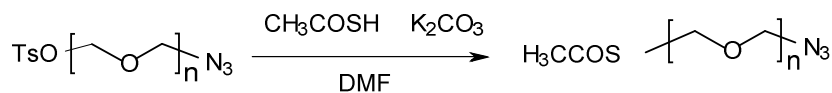
The mixture was stirred overnight at rt.

The solution was stirred filtered, washed twice with saturated  $\text{NH}_4\text{Cl}$  solution and twice with water.

The organic layer was dried over sodium sulfate, filtered and reduced to small volume by rotary evaporation.

## 2.2.4 Synthesis of Thioacetate-PEG-azide (4)

**Protocol I:** TsO-PEG-N<sub>3</sub> (10 gr) was dissolved in 100 mL dry DMF. Potassium carbonate (K<sub>2</sub>CO<sub>3</sub>, 5 equiv.) and thioacetic acid (CH<sub>3</sub>COSH, 5 equiv.) were added and the mixture was stirred overnight at rt under nitrogen (Scheme IV).

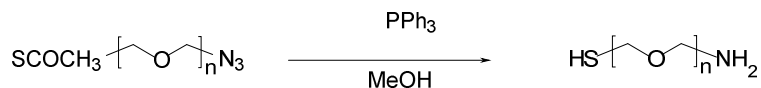


**Scheme IV.** Synthesis of Thioacetate-PEG-azide

DMF was removed by rotary evaporation, and the crude product was dissolved in 100 mL DCM. The solution was filtered, and treated with activated charcoal for 2 h. The organic layer was dried over sodium sulfate, filtered and reduced to small volume by rotary evaporation.

## 2.2.5 Synthesis of Thiol-PEG-amine (5)

Thioacetate-PEG-Tosyl (7 gr) was dissolved in 200 mL dry methanol; PPh<sub>3</sub> was added (25.6 gr, 5 equiv.) and the reaction mixture was heated to reflux overnight under argon (Scheme V).

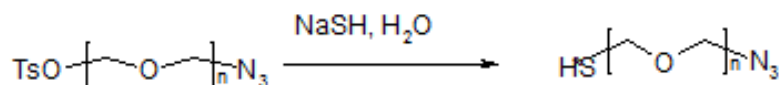


**Scheme V.** Synthesis of Thiol-PEG-amine

The solution was cooled down to rt and the solvent was removed by rotary evaporation.

## 2.2.6 Synthesis of Thiol-PEG-azide (4\*)

Protocol II: TsO-PEG-N<sub>3</sub> (10 gr) was dissolved in 200 mL H<sub>2</sub>O (Scheme IV \*).

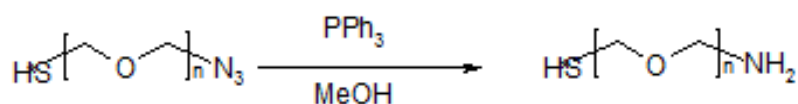


**Scheme IV\***. Synthesis of Thiol-PEG-azide

Neutralization of product was obtained with HCl (until pH 7) Then, 5 gr of NaCl were added and the extraction of the product with DCM (5 times with 50 mL DCM) was performed. The organic layer was dried over sodium sulfate for 1h, filtered and reduced to small volume by rotary evaporation.

## 2.2.7 Synthesis of Thiol-PEG-amide (5\*)

Thiol-PEG-azide (7 gr) was dissolved in 200 mL of dry methanol; PPh<sub>3</sub> was added (25.6 gr, 5 equiv.) and the reaction mixture was heated to reflux overnight under argon (SchemeV\*).



**Scheme V\***. Synthesis of Thiol-PEG-amide

The solution was cooled down to rt and the solvent was removed by rotary evaporation.

## 2.3 Preparation of hydrogels

## 2.3.1 Synthesis of PEG-grafted Na-alginate

The applicability of the obtained heterobifunctional PEG for pegylation technology was demonstrated by grafting of Thiol-PEG-amide with sodium alginate (Na-alg) (PEG-*grafted*-Na-alg) (Figure 8.2).

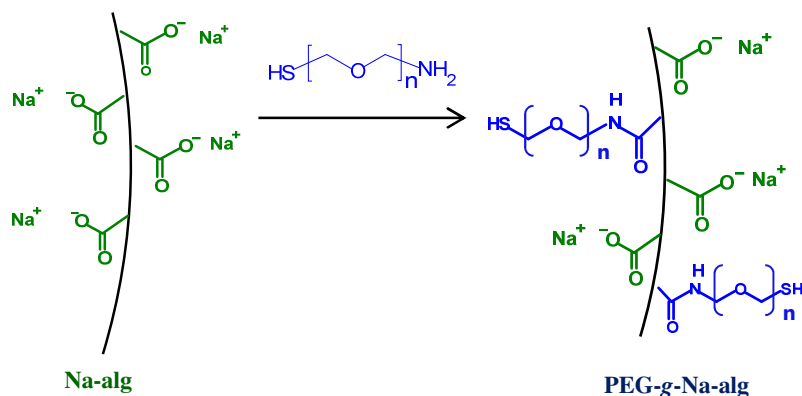


**Figure 8.2.** Conjugation of Thiol-PEG-amine to Na-alg

Na-alg (Kelton HV, 500 mg, 0.5mM) and NHS (100 mg) were dissolved in 50 mL of 50 mL of MES solution (0.1 M, pH 6). A solution of Thiol-PEG-amine was added. After stirring for 15 min at rt, EDC was added (Table I) and the stirring was continued for 3h , followed by the addition of NaOH and 30 min incubation at rt. Varying the amount of EDC, is state can be obtained different PEG-*grafted*-Na-alg, with defined degrees of graft. Purification was achieved by dialysis (4 days) against distilled water, which was changed 3 times a day. During the first 3 days, NaOH (30  $\mu$ L, 6M), NaCl (1 mL, 5M) and TCEP (1mL, 5M) were added twice daily to the Na-alg-PEG solution contained inside the dialysis tube. The purified polymer solution was filtered through a 0.22  $\mu$ m membrane and lyophilized to yield a white, solid material. The grafting reaction between thiol-PEG-amine and Na-alg was obtained via amide bonding. Indeed, carboxylate groups of Na-alg and thiol-PEG-amine reacted in presence of EDC and NHS in aqueous solution.

**Table I.** Experimental conditions for PEG-g-Na-alg hydrogels

Alg-Na (mg)	NHS (mg)	MES (mL)	HS-PEG-NH <sub>2</sub> (gr)	EDC (mg)	Code
500	100	20	1	200	<b>P-1</b>
500	100	20	1	300	<b>P-2</b>
500	100	20	1	500	<b>P-3</b>

The degree of graft, which refers to the percentage of reacted carboxylic groups on Na-alg, was determined by <sup>1</sup>H-NMR and the different results depend on the synthesis condition, especially the EDC amount.

### 2.3.2 Preparation of hydrogel by ionotropic gelation

The capacity of Na-alg-PEG to form hydrogels by ionotropic gelation in presence of calcium ions was analyzed. PEG-g-Na-alg was dissolved in MOPS stock solution (10Mm MOPS + 0.45% NaCl, pH 7.4) with a final concentration of 2 wt%. The gelation bath was prepared with 2.2 wt% CaCl<sub>2</sub> with 1 µl/mL of Tween. All solutions were sterile filtered (0.2 µm). The coaxial air-flow droplet generator was employed as instrument that enables the extrusion of the solution of PEG-g-Na-alg into the based calcium gelation bath. Microspheres were gelled at 37°C for 5 min, collected by filtration, washed twice with MOPS stock solution, and stored in MOPS solution at 4°C.

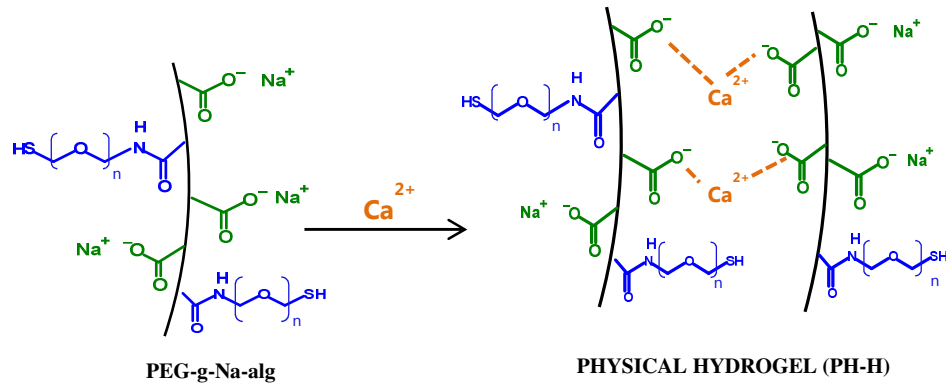


**Figure 8.3.** Physical hydrogel realized by ionotropic gelation of PEG-g-Na-alg

The obtained hydrogel is characterized by electrostatic interaction and for this reason, the resulting microspheres will be denoted as physical hydrogel (PH-H) (Figure 8.3).

#### 2.3.3 Preparation of hydrogel by disulfide bond formation

The preparation of chemically cross-linking hydrogel from Na-alg-PEG was achieved via spontaneous disulfide bonding. In practice, a solution of Na-alg-PEG (5wt % in MOPS) was left at 37°C in a glass vial for 72 h. This hydrogel is designed as chemical hydrogel (CH-H). The disulfide bond formation occurs spontaneously in air and the reaction is reversible, by the addition of TCEP agent.

#### 2.3.4 Preparation of hybrid hydrogel

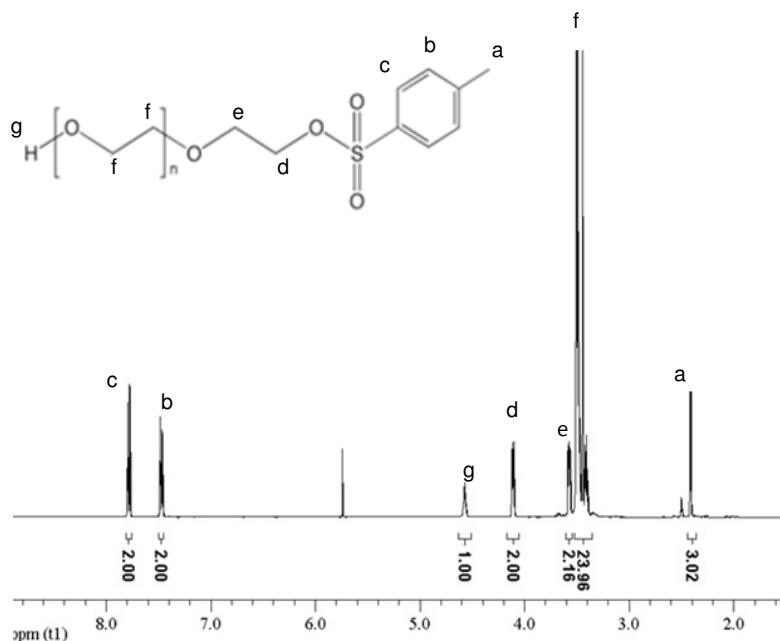
Exploiting the ability of Na-alg-PEG to form physical hydrogels, in presence of calcium ions, and chemical hydrogel, by spontaneous disulfide bond formation, hybrid hydrogels were realized. First, by ionotropic gelation PH-H hydrogel were obtained. Then, the resulting microspheres were collected by filtration, and suspended in MOPS solution. The suspension was left under stirring (40rpm) for 72h at 37°C (CH-H formation). The resulting hybrid hydrogel (HH) were

collected by filtration, washed with MOPS solution, and stored in the washing solution at rt.

### 3. Results and Discussion

#### 3.1 Synthesis of heterobifunctional PEG

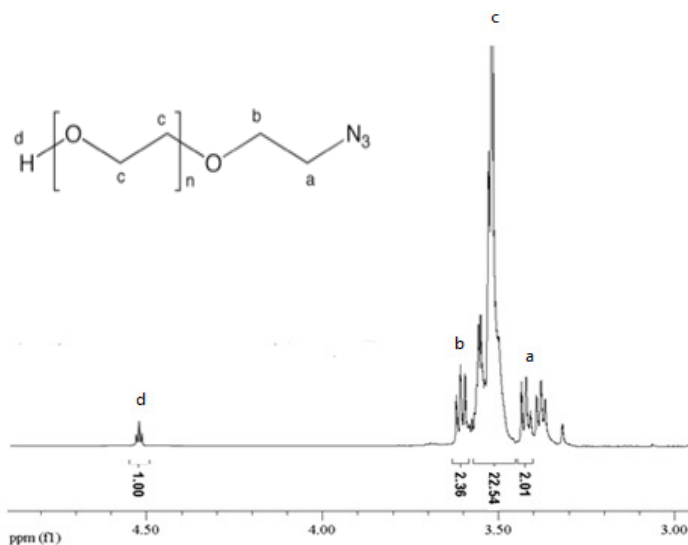
Tosyl-PEG-OH (1) was synthesized as precursor for the realization of heterobifunctional PEG, characterized by thiol and amine ends groups. This first step involved the activation of one of free hydroxyl group of PEG backbone as tosylate form (Spectrum 1). This easy method to monotosylate symmetrical PEG, using a stoichiometric amount of tosyl chloride, was performed in presence of Et<sub>3</sub>N, employed to neutralize the resulting mixture. The product was confirmed by <sup>1</sup>H-NMR spectrum. The <sup>1</sup>H-NMR chromatogram, indeed, shows, in particular, the peaks related to the protons of tosyl group introduced (e.g. 7.79 ppm and 7.49 ppm, ecc..) and the presence of a triplet at 4.56 ppm, corresponding to the proton of remaining of free hydroxyl group of PEG backbone.



**Spectrum 1.** <sup>1</sup>H-NMR of Tosyl-PEG-OH

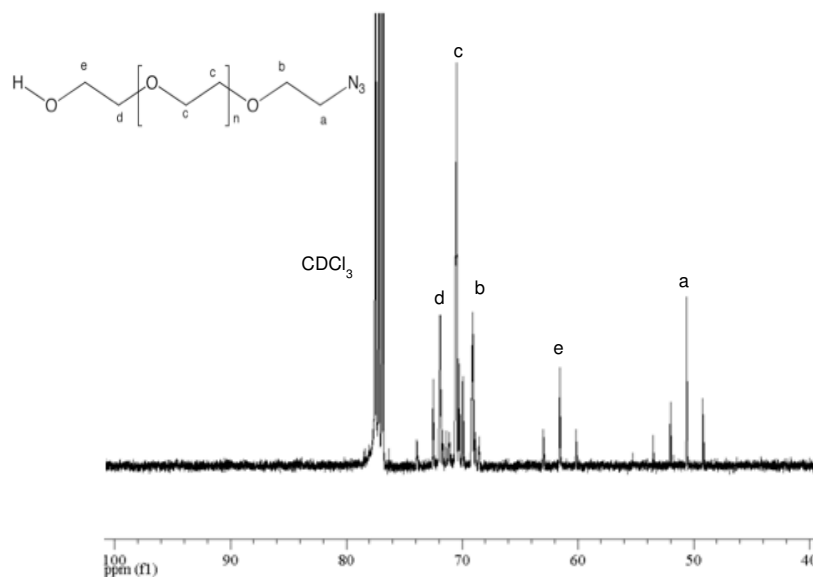
<sup>1</sup>H-NMR (DMSO,  $\delta$  in ppm): 7.79 (2H, d), 7.49 (2H, d), 4.56 (1H, t, OH), 4.11(2H, t, CH<sub>2</sub>-SO<sub>2</sub>), 3.49 (2H, t, PEG backbone), 2.43 (3H, s, CH<sub>3</sub>).

The conversion of the tosylate end group by  $\text{NaN}_3$  yielded Azide-PEG-OH (2). This product was obtained by  $\text{S}_{\text{N}}2$  reaction and causes the displacement of the leaving group with the potent azide nucleophile, in dimethylformamide. The quantitative introduction of the azide function was proved by the absence of tosylate peaks in the  $^1\text{NMR}$  (Spectrum 2a) spectrum while the  $^{13}\text{C-NMR}$  confirmed the introduction of the azide function (Spectrum 2b). Indeed, at 50.64 ppm the displacement of carbon adjacent to azide was observed.



**Spectrum 2a.**  $^1\text{H-NMR}$  of Azide-PEG-OH  
 $^1\text{H-NMR}$  (DMSO,  $\delta$  in ppm): 3.6 (2H, t,  $\text{CH}_2\text{-CH}_2\text{-N}_3$ ),  
3.5 (22H, s, PEG backbone), 3.4 (2H, t,  $\text{CH}_2\text{-N}_3$ )





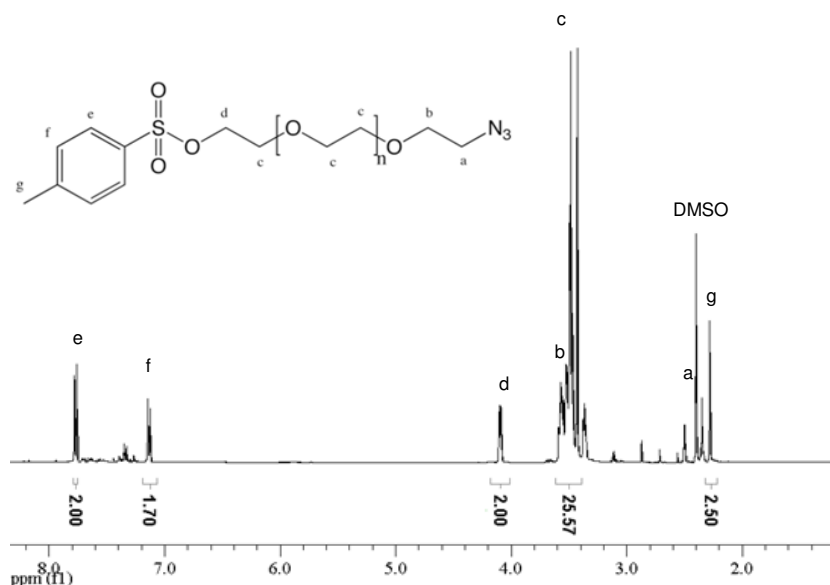
**Spectrum 2b.**  $^{13}\text{C}$ -NMR of Azide-PEG-OH  
 $^{13}\text{C}$ -NMR ( $\text{CDCl}_3$ ,  $\delta$  in ppm): 71.9; 70.5; 69.1; 61.6; 50.6

The other aim of this synthesis it was the realization of the thiolic terminal group of PEG backbone.

PEG with a terminal thiol group was found to be very efficient for the pegylation.

For example, nanoparticles with PEG characterized by a thiol terminal function, are characterized by an increased stability and hydrophilicity, and therefore, less risk of toxicity in biological systems.

The Azide-PEG-OH (2) was considered as precursor for the realization of Azide-PEG-Tosyl (3). The modification of the remaining free hydroxyl group of PEG backbone as tosylate form was obtained employing  $\text{TsCl}$ , as agent able to convert OH group into the corresponding tosyl derivative. The obtained product was confirmed by  $^1\text{NMR}$  in  $\text{DMSO-d}_6$  since the hydroxyl group is not detectable at 4.56 ppm (Spectrum 3).



**Spectrum 3.** <sup>1</sup>H-NMR of Azide- PEG- Tosyl

<sup>1</sup>H-NMR (DMSO,  $\delta$  in ppm): 7.78 (2H, d), 7.4 (2H, d), 4.1 (2H, t,  $\text{CH}_2\text{-SO}_2$ ), 3.5 (25 H, s, PEG backbone), 3.39 (2H, t,  $\text{CH}_2\text{-N}_3$ ), 2.41 (3H, s,  $\text{CH}_3$ )

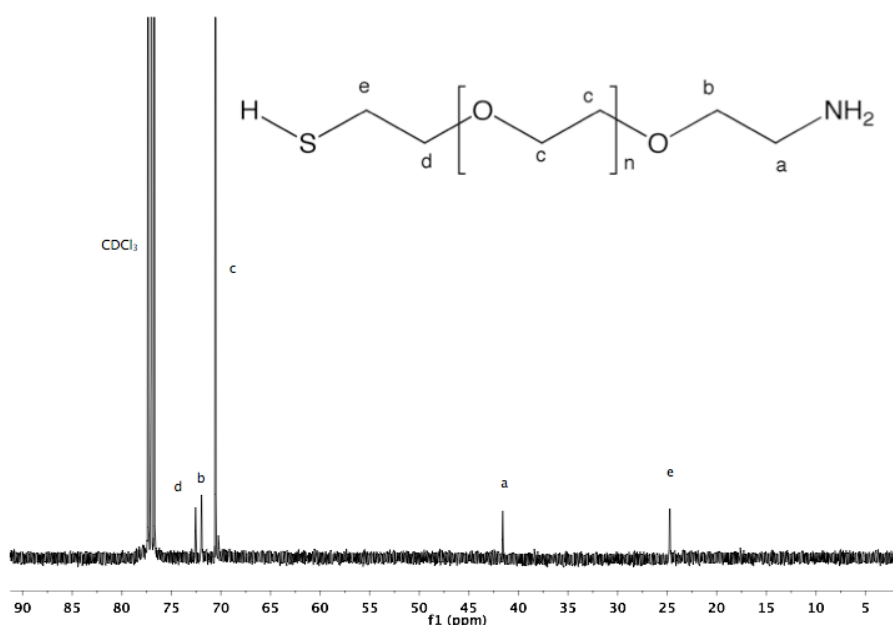
The terminal thiol group was achieved through two different mechanisms synthetic.

In the first protocol, starting from the Azide-PEG-Tosyl (3), the tosylate group was first displaced by reaction with the in situ formed potassium thioacetate in DMF to yield thioacetate-hydroxyl PEG (4). The introduction of the thioester end group was confirmed by <sup>1</sup>H and <sup>13</sup>C-NMR. (These spectra are not show).

In the second protocol, starting from the Azide- PEG- Tosyl (3), with an excess of sodium hydrosulfide hydrate (NaSH) in water, the Thiol-PEG-azide was synthesized (4\*). Also, in this case, the product was confirmed by <sup>1</sup>NMR-chromatogram (The spectra is not show).

This second protocol of reaction is faster than the first , because in a single step of reaction allows the formation of thiol end group, without any intermediate steps as happens, instead, in the first protocol , to obtain thiol end group. In particular, in the first protocol, by the reaction with potassium carbonate/thioacetic acid was obtained a thioacetate end group and, moreover, it was necessary another step for obtaining the cleavage of thioacetate, by

triphenylphosphine, to obtain free thiol end groups, Thiol-PEG-amine(5). Even in the case of Thiol-PEG-azide (4\*) it has been necessary the use of  $\text{PPh}_3$  to promote the reduction of azide group in amine. This complete reduction of azide was achieved following the Staudinger reduction. The reduction mechanism involves the formation of a linear phosphazine intermediate, which yields an iminophosphorane with concomitant loss of  $\text{N}_2$ . Spontaneous hydrolysis of iminophosphorane yields a primary amine and the corresponding phosphine oxide<sup>194</sup>. The completeness of the reaction was confirmed by  $^{13}\text{C}$ -NMR (Spectrum 4). The spectra exhibited peaks at 41.78 and 73.45 ppm corresponding to  $\alpha$ - and  $\beta$ -amine carbons, respectively. No traces of the characteristic peak of azide at 50.64 ppm were detected, that confirming the complete conversion azide in amine function.

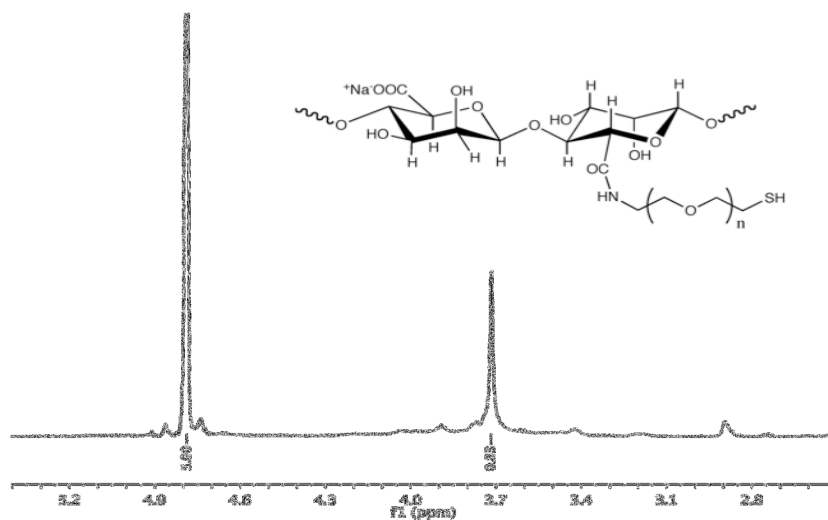


**Spectrum 4.**  $^{13}\text{C}$ -NMR of Thiol-PEG-amine  
 $^{13}\text{C}$ -NMR ( $\text{CDCl}_3$ ,  $\delta$  in ppm): 70.5; 71.7; 73; 41.7; 24.5

<sup>194</sup> Van Berkel, S.S.; Van Eldijl, M.B.; Van Hest, J.C.M. *Angew. Chem. Intern. Edit.*, **2011**, *50*, 8806-8827.

### 3.2 Hydrogel formation

Hybrid microspheres (HH) were obtained by exploiting the ability of Na-alg-PEG to form hydrogels in presence of calcium ions, and the disulfide bond formation. Three different hydrogels (P-1; P-2; P-3) were synthesized employing various amount of EDC, which was used as a carboxyl activating agent for the coupling of primary amines, to yield amide bonds. Were realized three products (Table I), but only the product P-3, with a degree of graft equal to 3.5 %, was considered for the further studies (Spectrum 5). The extrusion of PEG-g-Na-alg into calcium gelation bath yielded PH-H. This result confirms that the covalent interaction of Na-alg with a modified PEG backbone did not affect the ionotropic gelling behavior of these molecules.



**Spectrum 5.** <sup>1</sup>H-NMR of PEG grafted-Na-alg in D<sub>2</sub>O

The extrusion of PEG-g-Na-alg into calcium gelation bath yielded PH-H. This result confirms that the covalent interaction of Na-alg with a modified PEG backbone did not affect the ionotropic gelling behavior of these molecules. However, no spherical microspheres was obtained when using PEG-g-Na-alg having a degree of graft < 1.7 % (P-1 and P-2). The degree of graft equal to 3.5 % (P-3) was found to meet better the requirement of microspheres preparation.

The spherical shape of the resulting hydrogel was confirmed (Figure 8.4), and this degree of graft was enough to form chemically cross-linked hydrogel.

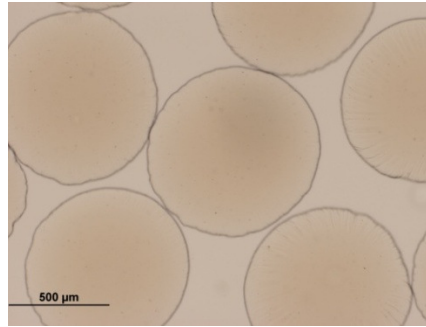


**Figure 8.4.** Hybrid microspheres of PEG-g-Na-alg

The CH-H, instead, was obtained via disulfide bonds because of the spontaneous character of the oxidation reaction, under air atmosphere without adding any extra reagent. Moreover, the reversible behavior of the obtained CH-H was verified employing TCEP, selected for its strong reducing capacity (Figure 8.5).

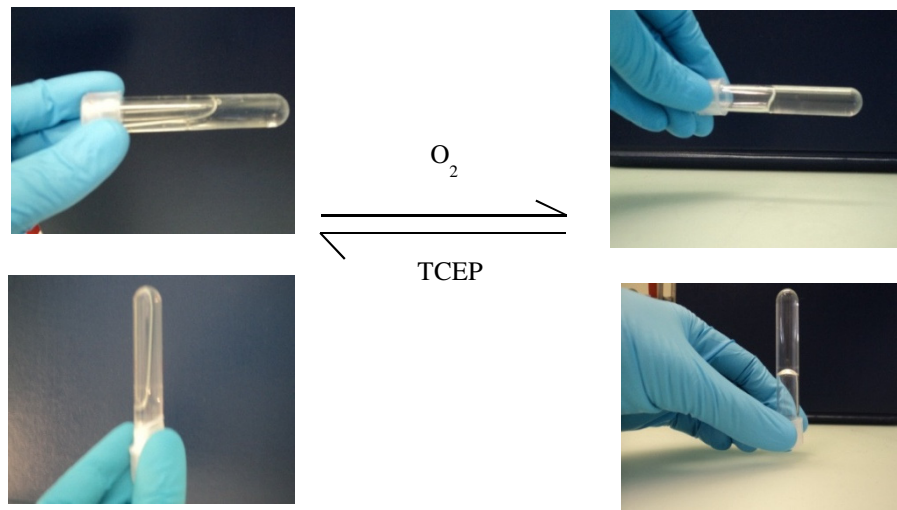


**Figure 8.5.** Chemically cross-linked hydrogel prepared via disulfide bond formation

The stability of the disulfide bond formation was confirmed by subjecting the sample to liquefaction in sodium citrate, selected as calcium chelating agent. The resulting hydrogels, after their incubation at rt in 10 mL of sodium citrate (100 mM in MOPS solution) for 24 h, maintain the integrity of the structure (Figure 8.6). This result confirms the efficiency of the chemical cross-linking.

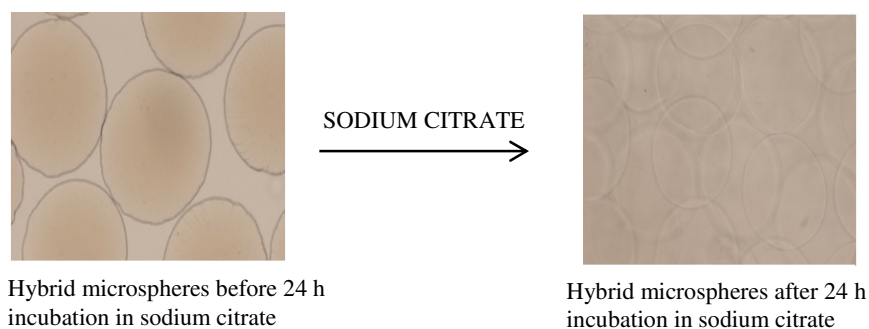


**Figure 8.6.** Hybrid microspheres after 24 h incubation in sodium citrate

The same experimental conditions were performed for the microspheres based on unmodified Na-alg. After only 10 minutes of incubation, in sodium citrate, the microspheres were dissolved.

#### 4. Conclusion

This work describes the synthesis of heterobifunctional thiol-PEG-amine via asymmetric activation of commercially available symmetrical PEG, as potential candidates for biomaterials modification, e.g. cell microencapsulation. The applicability of the synthesized heterobifunctional PEG was demonstrated by covalent conjugation of latter with Na-alg, which is one of the most important biopolymer used in the cell microencapsulation technology. The gel formation of PEG-g-Na-alg following three different approaches was studied. The extrusion of PEG-g-Na-alg into calcium ions yielded physical hydrogels, by

ionotropic gelation. The introduction of the thiol at the end of the PEG chains allowed for the formation of hydrogels via the formation of disulfide bonds (chemical hydrogel). The degree of graft equal to 3.5% seems to be enough to obtain stable networks. The main aspect of the chemical hydrogels formation is related to the spontaneous character of the reaction employed. Indeed, the reaction takes place in air atmospheres and doesn't require additional reagents or initiator, which was an important relevant disadvantage in past approaches.

Finally, the combination of ionotropic gelation and chemical cross-linking yielded hybrid hydrogels. The term "hybrid" refers to the mechanism by which the hydrogels are built, which combines the preparation of alginate-based physical hydrogel and simultaneous covalent cross-linking. The preparation of hybrid hydrogels is emerging as a new and promising approach to prepare engineered hydrogels.